A3G COMPLEXES: A NOVEL ROLE OF A3G IN RESTRICTING THE LATE STEPS OF HIV-1 REPLICATION

By

KENNETH LAMONT MARTIN

Dissertation

Submitted to the Faculty of the

Graduate School of Vanderbilt University

in partial fulfillment of the requirements

for the degree of

DOCTOR OF PHILOSOPHY

In

Microbiology and Immunology

August, 2011

Nashville, Tennessee

Approved:

Professor James Crowe

Professor James Hildreth

Professor Chris Aiken

Professor Terry Dermody

Professor Richard D'Aquila

TABLE OF CONTENTS

ACKNOWLEDGEMENTS

My graduate career has been aided by numerous individuals, too many to mention all. However, I must acknowledge those that have helped along my path to becoming a better scientist and person. First, I would like to thank my research advisor, Dr. Richard D'Aquila. My route to the D'Aquila lab was not direct, to say the least. Dr. D'Aquila allowed me to come into his lab and gave me the freedom to conduct research that I was passionate about. He has guided me along the way and given me countless pieces of advice. I am extremely grateful to have had this opportunity and will use the knowledge and skill I have gained in the D'Aquila lab for the rest of my scientific career. The members of the D'Aquila lab certainly were instrumental also in my growth as a scientist and for that I am thankful.

Secondly, my dissertation committee composed of; Drs. Jim Crowe (Chair), Chris Aiken, Terry Dermody, James Hildreth have been a constant support system. They expected nothing less than the best from my research, presentations, and actions. For this I am grateful and this professional development has definitely aided in me securing a position as a scientist with Procter & Gamble. The years of advice have definitely paid off.

I would also like to thank the Department of Microbiology and Immunology for creating an environment conducive to learning and research. My coursework was taught by very knowledgeable and caring teachers that aided in learning.

The culture created in the department allows one to think and to mature at a fast pace.

Next, I would like to thank my family, especially my father and mother, Mr. and Mr. Leander Martin, Jr. and Mrs. Betty Martin. Your support through these years has been much appreciated. Though I may not express it all the time, this long journey of education could not have been done without you. Not only that, it likely would have never begun. You instilled in me at an early age a love for learning and for that I am truly grateful. Also, I would like to acknowledge my two brothers, Leander and Lavell for your encouraging words and support.

Finally, I would like to thank a whole host of other family and friends. Especially, like to thank my best friend Jeremiah McCluney. These years have brought many discussions and trials, but through it all we have come out better and stronger. I thank you for your daily conversation and encouraging spirit, even in the midst of some very discouraging circumstances. Robert Jones has been a constant source of encouragement and conversation. I will always treasure the friendship of these two for years to come. Then to my Nashville friends, too many to name, thank you for your love and support. Though I will be moving away I know our friendship will remain strong and for this and all things I am thankful.

LIST OF TABLES

TABLE **PAGE**

LIST OF FIGURES

FIGURE **PAGE**

CHAPTER I

Background and Research Objectives

HIV-1 and Intrinsic Immunity

Human immunodeficiency virus or HIV is a retrovirus that infects cells of the immune system. Over time, the immune system becomes weaker; and the host becomes more susceptible to infections. Anti-retroviral drugs have greatly lengthened the time a patient advances to the late stages of the disease and develop AIDS (acquired immunodeficiency syndrome). According to the World Health Organization 34 million people were living with HIV in 2008, with 2.7 million people becoming newly infecting. The devastation and burden on health care caused by this virus is clear.

HIV-1 is the most common strain found in the United States. HIV-1 contains nine genes that encode 15 proteins. In addition to the three major proteins common to all retroviruses, Gag, Pol, and Env, HIV encodes four accessory proteins, Nef, Vpr, Vpu, and Vif. These proteins are so named because they are dispensable for *in vitro* replication. Accessory proteins are required for *in vivo* replication (6). Two of these accessory proteins, Vif and Vpu, have been shown to overcome innate retroviral restriction factors present in mammalian cells (80, 97, 103, 140, 151, 152). Restriction factors can inhibit viral replication at various stages of the lifecycle. It was discovered that these accessory proteins counteract proteins important in intrinsic immunity (5, 6).

The ability of humans to defend themselves from attacks by microorganisms depends mainly on the immune system. An efficient immune response is a very coordinated event. A successful immune response must clear foreign microorganisms while not causing damage to self. The immune system is generally thought of as having two main arms: the innate and adaptive immune responses (139). The innate response is our body's first defense against microbes and does so in a non-specific manner. The adaptive response is composed of highly specialized cells, B and T cells that recognize only specific pathogens. Following an adaptive response, long-lasting immunity is normally developed (157).

Recently, a form of cell-autonomous immunity has been shown to exist, termed intrinsic immunity (14). Intrinsic immunity combines aspects of both the innate and adaptive immune responses. Intrinsic immunity is provided by proteins expressed within cells and serve to protect cells from exogenous viruses and endogenous retroelements. These defense proteins have been termed, restriction factors (44, 67). Several major restriction factors that posses anti-HIV activity are; Trim5α, tetherin, Mov10, and some members of the A3 family (50, 114, 129, 133, 173). A3G (A3G) is the most studied of the A3 family and the most potent restrictor of the family. All of these proteins have significant effects on HIV-1 production.

Vif is a small 23 kDa protein and one of the four accessory gene products of HIV-1. Viral infectivity factor or Vif is associated with the production of infectious viral particles (71). *In vitro* experiments determined that while Vif-

deleted virus can readily infect cells, the progeny virions are 100-1,000 fold less infectious than those of wild-type virus (141). Further experiments determined that cells were either Vif-dependent, termed non-permissive, or Vif-independent, termed permissive (71). The great majority of studied cell lines are permissive, indicating they support a spreading infection of Vif-deleted virus (107). Examples of permissive cells include 293T, SupT1, and CEM-SS (58). Primary T cells, the major target of HIV *in vivo,* are non-permissive. There are a small number of non-permissive cell lines, such as HUT78 and CEM T cell lines (134). These results suggested that either permissive cells express a "Vif-like" factor or non-permissive cells express a restriction factor overcome by Vif. In 1998, experiments using heterokaryons of permissive and non-permissive cells determined that the non-permissive phenotype was dominant over permissive (92). Therefore, non-permissive cells likely expressed a restriction factor that was overcome by viral Vif.

Discovery of A3G Restriction

In 2002, using a subtractive-hybridization approach, the restriction factor overcome by Vif was identified as apolipoprotein B mRNA-editing enzyme, catalytic polypeptide-like 3G or A3G. A3G (A3G) is a 46 kDa protein (133). A3G is one member of a six-member gene family of DNA-editing enzymes (16). The A3 proteins are clustered on human chromosome 22. Most of the A3 proteins have been shown to posses cytidine deaminase activity (143). A3G binds RNA

and ssDNA (174). The binding of A3G to ssDNA leads to enzymatic conversion of cytidine to uridine.

A3G binds to the nucleocapsid domain of the HIV-1 polyprotein Pr55 Gag (90). This interaction is essential for A3G incorporation into progeny virions, in the absence of Vif. A3G is released into the target cell following virus entry. A3G can then catalyze the cytidine deamination of the negative strand or first strand reverse transcripts (17). These C-to-U changes register as G-to-A hypermutations on positive strand DNA. Interestingly, G-to-A hypermutations have been observed in lentiviruses such as HIV-1 and the hepadnavirus, hepatitis B virus (111). These G-to-A hypermutations can either lead to degradation of the viral genome or integration of lethally hypermutated provirus. Vif interacts with an ubiquitin ligase to form a, Vif-cullin5-elonginB-elonginC complex (77). This complex leads to the degradation of A3G in the producer cell.

Evidence is accumulating that in addition to the inhibition of exogenous retrovirus replication, A3G along with A3F and A3B can inhibit the replication of endogenous retrotransposons (40, 165). It is thus conceivable that the A3 proteins evolved as a cellular defense to restrict retrotransposition.

A3G-mediated Restriction

It is believed that A3G and A3F inhibit HIV replication by the same mode of action, I will therefore use the term APOBEC to refer to their collective anti-HIV activity (60). Until now, APOBEC activity had only been described to be effective in the target cell and not the producer cell. Packaging of the APOBEC protein

into virions is thus essential for anti-viral activity (128). Virion packaging of the APOBEC is facilitated by either binding to viral RNA alone or to both nucleocapsid and viral RNA in the producer cell (3). The APOBEC is released into the target cell following virus entry. The APOBEC can then catalyze the cytidine deamination of the negative strand or first strand reverse transcripts (174). These C-to-U changes register as G-to-A hypermutations in the positive strand DNA. A3G causes a specific hypermutation signature in GG dinucleotides and A3F activity is distinguished by mutations only in a GA dinucleotide context (9, 76). However, the virus overcomes APOBECs anti-viral activity via Vif. Anti-HIV-1 restriction by A3G is shown schematically in Fig. 1-1 (36).

Of note, G-to-A hypermutations have been observed in the genomes of lentiviruses such as HIV-1, including predominance of hypermutation in a GG dinucleotide context (an A3G-specific signature) in proviruses from some subjects, while others show GA dinucleotide context predominance (an A3F-

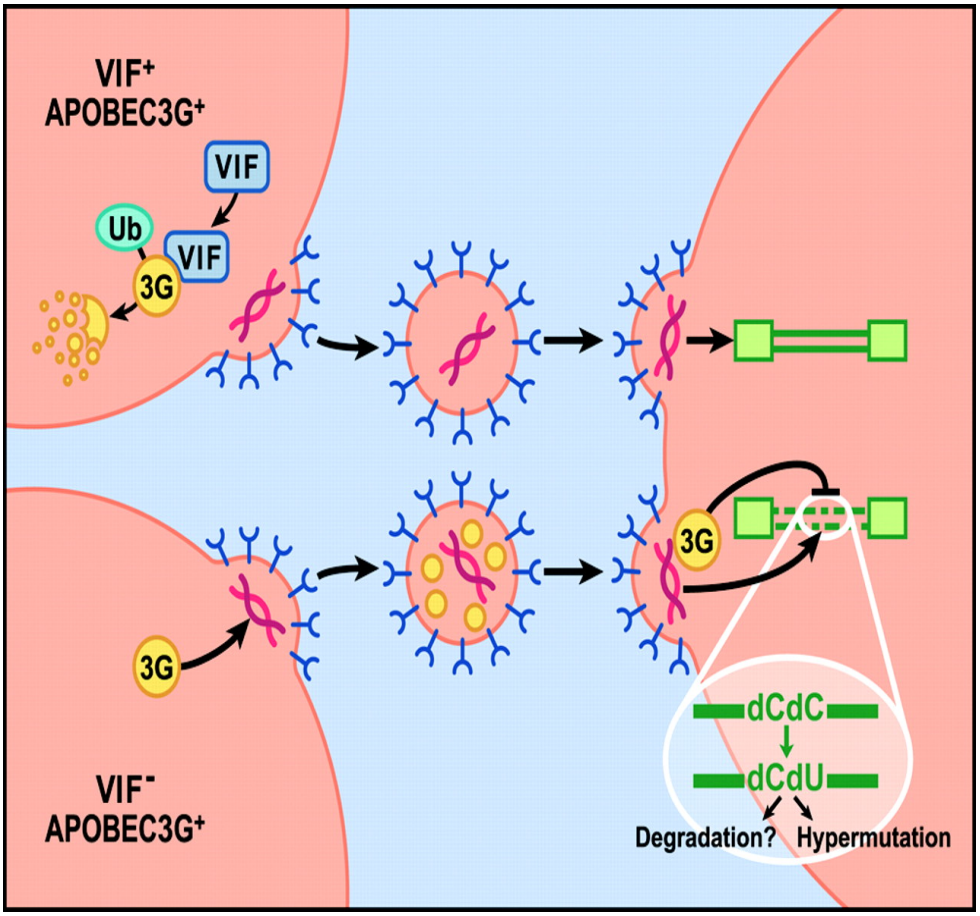

Figure 1-1. Restriction of HIV-1 by A3G. Restriction of HIV-1 and HIV-1 Δ*vif* by A3G is shown in nonpermissive cells. A3G virion packaging results in inhibition of reverse transcription and integration.

Borrowed from: Cullen, B.R. (2006) Role and Mechanism of Action of the A3 Family of Antiretroviral Resistance Factors. Journal of Virology, 80(88): 1067–1076.

specific signature) (9). A gradient of hypermutation in HIV genomes parallels the duration that negative strand HIV DNA remains single stranded (122, 142). The hepadnavirus, hepatitis B virus, also contains G-to-A hypermutations and A3G also restricts the replication of hepatitis B virus (149). It is now clear that APOBECs are responsible for the high amount of G-to-A mutations found in these viruses.

A3G Enzymatic Activity

Chelico *et al.,* in 2006 and Nowarski *et al.,* in 2008 published opposing ideas of how A3G works as an enzyme (28, 106). Chelico and colleagues showed that A3G is a processive 3'-to-5' cytidine deaminase. Processive enzymes slide along their target substrate, but also can exhibit molecular jumping, on the same strand of DNA (28). Biochemical analysis suggests A3G cytidine deamination is accomplished by an A3G dimer. This would allow for easy jumping, since a monomer could disassociate with the ssDNA and re-associate to the twisted DNA at another point and allow the second monomer to "jump" without losing contact with the ssDNA. A3G is able to jump and slide on ssDNA to find cytidines to target for deamination. The binding of A3G to ssDNA is thought to be random. Several studies have shown that G-to-A hypermutation is observed more frequently in the 5' region of minus-strand cDNA. This results in a 5'-to-3' gradient of hypermutation.

Nowarski *et al.,* showed the exact opposite mode of action of A3G, that A3G works by intersegmental transfer (106). This group showed rather than

being processing, A3G works distributively on adjacent cytidines. In intersegmental transfer A3G would make use of both the N-terminal and C-terminal DNA-binding domains. This would ensure that contact with the folded DNA molecule was not lost, but allow A3G to simultaneously bind two distinct regions of the DNA (106). This would cause dispersed deamination. Work still remains to determine exactly which method of enzymatic activity is employed by A3G.

The deamination reaction simply is cytidine + H_2O = uridine + NH_3 (51). In the case of A3G, the zinc finger motif is critical for the coordination of Zn (113, 166). The active site of the enzyme is hydrated by water and catalyzes the conversion of cytidine to uridine. The Landau group back in 2004 established that A3G enzymatic activity is only targeted against ssDNA (174). A3G was found to not deaminate target sites in ssRNA, dsRNA, or ds DNA.

There have been conflicting reports of the necessity of cytidine deaminase activity for target cell restriction. Several studies point to the fact that active site mutation of A3G still shows almost normal levels of HIV-1 and HTLV-1 restriction (15, 104) .

A3G and Vif Interaction

It is believed that the region necessary for A3G interaction are mainly in the N-terminal region of Vif (123). Two groups confirm that residues 40-71 contribute to Vif's ability to bind A3G. This binding site however is believed to be non-linear. In that, not all residues in this region when mutated abolish Vif-A3G

interaction. Though the residues involved in A3G binding may not be linear, they may represent nearby surfaces in the tertiary structure.

The Pathak lab in 2007 showed that residues $Y^{40}RHHY^{44}$ and $D^{14}RMR^{17}$ are important for functional interaction and degradation of A3G (123). Yamashita *et al.,* in 2008, identified several residues in the N-terminal half of Vif necessary for A3G binding (170). These mutants W21A, S32A, W38A, Y40A, and H43A all poorly bound A3G. These results extended the binding site identified previously. Work from Donahue *et al.,* involving our lab showed that the PPLP motif in HIV-1 Vif is essential for binding and degradation of A3G (41). The PPLP motif consists of residues 69-72. It was known prior that this region was critical for Vif-Vif interaction. Also, that the PPLP motif was critical for Vif function and mutations in this motif lead to decreased virus infectivity. These results suggest that Vif may require homo-multimerization prior to A3G binding. Indeed, Miller *et al.,* in 2007 showed that peptides that block Vif-Vif interaction resulting in the production of virions with dramatically increased levels of A3G (99). They proposed that this peptide may provide an effective means of blocking the viral counterstrike against our innate cellular defense against HIV-1.

The binding sites in A3G necessary for Vif binding have been discovered using molecular genetics approaches. Two studies identified a large region of A3G necessary for Vif binding. Conticello *et al.,* in 2003 identified the region as containing residues 54-124 (35). This was modified by Zhang *et al.,* in 2008 showing the binding site to lie between residues 105 and 156 (179). In 2007, Huthoff *et al.,* used alanine scanning to show that residues at positions 128-130

to be most critical (64). D128 had already been known to play a role in the species specificity of the A3G-Vif interaction. Additionally, they found that the proline at position 129 and the aspartic acid at 130 contributed to an overall negative charge that was necessary for Vif binding. These residues are very near residues Y124 and W127 which are known to be vital for A3G packaging. Any pharmacologic agents that target the A3G/Vif interaction would have to do so without preventing the ability of residues 124 and 127 to aid in virion packaging.

In 2009, the Pathak lab extended the A3G binding site, demonstrating that amino acids 126-132 were important for Vif binding (124). However, they found that the A3F binding site for Vif was located between amino acids 283 and 300. This shows two related proteins with very distinct regions necessary for Vif interaction. Indeed, the A3G and A3F binding site interact with different regions of Vif.

Vif-mediated A3G degradation

The mechanism of Vif-induced A3 degradation is well-understood. Vif recruits (Ub)-activating (E1), Ub-conjugating (E2), and Ub-ligating (E3) enzymes (77). The most diverse of these complexes are the E3 Ubiquitin ligase enzymes. Vif recruits an E3 complexes containing Cullin 5 as a core component. Elongin C also binds and recruits the E3-ubiquitin ligase complex poly-ubiquinates A3G leading to A3G's proteasomal degradation. Vif contains a SLQ(Y/F) motif similar to those found in SOCS proteins (13, 96, 97). This consensus sequence in SOCS proteins link proteins for degradation with a multisubunit E3 ubiquitin

ligase. Vif then forms the Vif-cullin5-elonginB-elonginC complex. This complex interacts with A3G and A3F and lead to proteasomal degradation in the producer cell. Intriguingly, A3B also inhibits HIV-1 replication, but in a Vif-independent manner (40). However, A3B expression is restricted and may not normally be expressed in lymphocytes.

The N-terminal region of Vif contains a zinc coordination site, HCCH (between residues 100-142), which binds to cullin 5 in the absence of elongin C (98, 113). Mutations in this region impair zinc coordination, cullin 5 binding, and thus inhibit A3G degradation. Vif is monoubiquitinated in the absence of A3G, this has no impact on its half-life (97). However, when coexpressed with A3G, Vif becomes polyubiquitinated and is degraded. This indicates that Vif protein is also degraded during the process of A3G degradation and so the virus must continually express Vif to pose an effective anti-HIV response. The PPLP motif in Vif has also been shown to be necessary for both A3G binding and degradation (41).

Iwatani *et al.,* in 2009 showed that four lysine residues in the C-terminal half of A3G are the targets of polyubiquitination (65). These residues, Lys-297, 301, 303, and 334 when mutated block Vif-mediated degradation. When all four lysine residues were mutated to arginine A3G was completely resistant to Vif and able to restrict reverse transcription in the target cell.

Low Molecular Mass and High Molecular Mass A3G

A3G exists in two major forms in cells, low molecular mass (LMM) and high molecular mass (HMM) (31, 32). The LMM form is enzymatically active in deaminating cytidines. The size of LMM form ranges from 46 kDa to about 160 kDa in size. The LMM is likely composed of A3G monomers, dimers, trimers, and tetramers. The HMM form is inactive for cytidine deaminase activity. The HMM complex can range in size from 700 kDa to 2 MDa. HMM A3G is found in activated T cells and naïve T cells in tissues, both of which allow incoming Vif-positive HIV genomes to be reverse transcribed and integrated (31). Furthermore, the presence of Vif contributes to production of infectious virions from activated T cells. Both Vif and polyubiquinated forms of A3G were identified as cofractionating with HMM A3G complexes (31).

In 2005, experiments demonstrated that endogenous LMM A3G can restrict incoming virus at the reverse transcription stage (31). Chiu and colleagues in the lab of Warner Greene showed resting T cells possessed mainly LMM A3G, while activated cells had HMM A3G. Following T cell activation, LMM A3G was shown to shift into the HMM complex by high performance liquid chromatography. It was initially thought these experiments answered long-standing questions about why resting and naïve T cells in the blood possess a post-entry block to incoming HIV genome replication. siRNA-mediated knockdown of LMM A3G in resting T cells effectively relieved the early replication block during reverse transcription in these cells and allowed for the production of

significant amounts of virus. However, since the initial report these experiments have not been replicated.

Chen and colleagues repeated the experiments by Chiu using the same siRNA and others, one of which showed 2 fold more reduction in A3G levels compared to the initial Chiu construct (70). They were unable to discern an effect on the infectivity of resting T cells after A3G knockdown. Additionally, Santoni conducted experiments in which T cells were activated by PHA and IL-2 and transduced with various vectors that expressed Vif, siRNA directed against A3G, or control scrambled siRNAs (127). The cells were then maintained in low IL-2 and allowed to return to a resting phenotype. The post-activation cells were then infected with a fluorescent reporter HIV-1. They found that although A3G expression was reduced by Vif and or siRNA directed against A3G, there was no correlation between HIV resistance and the amount of A3G present in the cytoplasm.

These HMM complexes were thought to be aggregated protein in the cytoplasm with no function due to their lack of enzymatic activity. But, Wichroski *et al.,* in 2006 showed that HMM or A3G complexes colocalized with γ-tubulin, but not vimentin (164). Vimentin is known to form cages around aggresomes. They also showed these bodies to be distinct from those cytoplasmic bodies formed by another HIV-1 restriction factor, Trim5α. Multimerization of A3G was found to be RNA-dependent by Opi *et al.,* in 2006 (110).

I call the HMM form, A3G complexes. A3G complexes are the focus of the work presented here. Until now, there was no known role for these

complexes in HIV-1 replication. I show that A3G complexes decrease HIV-1 production, likely by reducing the half-life of HIV-1 Gag.

A3G and RNA Granules

The HMM complex contains on average 100 different proteins (32, 78, 159). These proteins represent many classes from chaperones (Hsp70, Hsc70, Hsp 60), hnRNA (Nucleolin, Ro, and La), dead box proteins (DDX1, DDX5, DDX3), ribosomal (40S S11, 60S S15a, 60S P2, L28, and S6), transcriptional regulators (NFAR), translational regulators (CBP80, PABPC1, eIF4e-G1, Dcp1), molecular motors (kinesin heavy chain, β -tubulin), and RNA processing proteins (staufen, Pur β, TAP RNA transporter, GW182). Rana first showed that these HMM complexes colocalized with structures known as RNA granules using confocal microscopy. Co-immunoprecipitation experiments showed that most of these proteins interaction with A3G were RNA dependent (164).

RNA granules are non-membrane bound structures that are used for RNA storage and degradation or for localized translation (7). RNA granules are highly dynamic in nature. Proteins normally come together to perform a specific function related to RNA metabolism or storage and then disassemble. There are several classes of RNA granules; germ cell granules, neuronal (Staufen) granules, stress granules, and processing bodies (7).

Germ cell granules are so named because they are found in germ cells and function during development (52). These Ribonuceloprotein particles contain maternal mRNA required for germ cell specification. These granules

store RNA until various stages of development are reaches and disassemble to allow the translation of the maternal mRNA at the correct time.

Neuronal granules are also termed Staufen granules. These granules contain translational machinery and allow for localized translation at distant synaptic structures (75). In neurons that can be considerable in size, it would take a long time for information gathered at far synapses to reach the nucleus to initiate translation and then translation. Therefore, neurons store critical mRNA's, such as those for neurotransmitters, in granules in synapses so that incoming information can quickly cause the localized translation of important proteins.

Stress granules are induced during periods of cellular stress (78, 162). It is believed that during stress certain housekeeping mRNAs are shuttled into s tress granules to delay their translation in favor of proteins needed for cellular survival. These include heat shock proteins, such as molecular chaperones. This increases the rate of synthesis of critical proteins.

Processing bodies (P-bodies) are sites of both mRNA storage and decay (22, 52). RNAs can be shuttled into P-bodies for storage, so that they can be later translated at the appropriate time. RNAs in P-bodies can also be destined for degradation, by P-body/late endosome interactions. P-bodies contain many of the mRNA decay factors. It was once believed that P-bodies also contained the RISC complex and were necessary for miRNA- and siRNA-mediated gene silencing. Teixeira *et al.,* in 2005 showed that P-Bodies are sensitive to RNase, reminiscent of the early studies of HMM complexes (146).

However, evidence is accumulating that suggests that a separate structure termed GW-bodies are responsible for miRNA-induced gene silencing (55, 88, 120). These GW-bodies are so named do to their abundance of GW182, while most P-bodies have little to no GW182. GW-bodies have been shown to interact with late endosomes and Multi-vesicular Bodies or MVB's.

The cellular function of A3G may be closely related to RNA granules and it is important to note that others have found that A3G may shuttle between polysomes and stress granules (22). Polysomes are strings of ribosomes joined by a common mRNA. They function to synthesize several polypeptides simultaneously from a common mRNA, as such polysomes are variable in length. These researchers found A3G bound to RNA at polysomes, specifically HIV-1 RNA, and these A3G-mRNA complexes moved from polysomes to stress granules, under experimentally induced stress. Stress granules and P-bodies contain a protein named, Mov10 (24, 50).

Newly Discovered HIV-1 Restriction Factors

Mov10 is a component of RNA granules that restricts HIV-1 replication at multiple-stages of the replication cycle (24, 50). Mov10 is a putative RNA-helicase and part of the DExD superfamily of proteins. The overexpression of Mov10 in the producer cell leads to the reduction of HIV-1 Gag (24). Mov10 is also packaged into the virion and reduced viral infectivity. The reduction in Gag levels leads to reduced virus output.

A3G and Mov10 colocalize in cells. Overexpression of A3G and Mov10 led to significant reductions in the proteolytic cleavage of HIV-1 Gag (24). This inhibition was additive, in that A3G and Mov10 expression alone decreased Gag cleavage. Overexpression however, has no effect on the infectivity of the resulting virions. The mechanism for this inhibition is yet to be established.

MicroRNA's or miRNAs are about 22 nucleotides in length and work in conjunction with the RNA-induced silencing complexes (RISC) to downregulate gene expression. The RISC complex is also known to localize to P-bodies. The exact role of P-bodies in miRNA-mediated gene expression is unclear. Studies have found them to be both necessary and unnecessary for miRNA gene regulation. miR29a has been shown by two groups to restrict HIV-1 production (102).

miR29a is expressed highly in activated T cells. Rana and colleagues found that disruption of P-bodies lead to increased levels of HIV-1 production (102). They showed that miR29a was able to bind to the 3'UTR of HIV-1 RNA and transport the RNA to P-bodies. miR29a action lead to reduced virus output and viral infectivity. One group also found that miR29a can reduce the expression levels of HIV-1 Nef (2).

I present work in this thesis that knockdown of P-body component RCK/p54 leads to increased HIV-1 production. This increase is the result of at least two independent events. RCK/p54 knockdown abrogates P-body formation which allows for HIV-1 RNA that otherwise would be stored in P-bodies to be translated. RCK/p54 knockdown has a second independent effect in cells

containing A3G. A3G complexes are abrogated, which increases HIV-1 Gag half-life and allows for higher virus production.

A3G Structure

Several groups have studied the C-terminal domain of A3G. This has resulting in at least three NMR structures and now two X-ray crystal structures. The two X-ray crystal structures differ, but the latest one supports information provided by the NMR structures. This latest crystal from Shandilya *et al.,* structure posses four large interfaces that they hypothesize may play an important role in A3G homo-oligomerization (132).

A3G contains two consecutive Z motifs. These Z motifs give the enzyme order. The A3G contains 2 zinc coordination sites or zinc fingers that work by way of one histidine and two cysteines (132). The consensus sequence of $Hx_1Ex_{24-28}PCx_{2-4}C$ is present across the entire A3 family. Likewise, like other cytidine deaminases A3G posses a core α-β-α fold. The crystal structure by Holden *et al.,* in 2005 showed conservation of the active site with known structures of other cytidine deaminases (62).

The C-terminal domain consists of a five-stranded β sheet that is surrounded by six α-helices. Four large interfaces are present that others speculate could be potential oligomerization sites (132). However, these sites are not believed to be present in the N-terminus. Oligomerization is thought to be playing a key role in A3G enzymatic activity. Also, the HMM complex of A3G is a large ribonucleoprotein complex and multiple sites for interaction with itself

and with other proteins and RNA would explain the ability of A3G to form these large complexes within the cell.

The N-terminal region of A3G has been modeled by Zhang *et al.,* using structures of APOBEC2 (178). Many mutations that result in the species-specificity of A3G and the ability of A3G to homo-oligomerize and are required for virion-packaging are in this region. This model predicts that these residues are under positive-selection pressure and are on exposed surfaces in the protein, which would confirm their importance. Specifically, D128K is present in an exposed α helix, helix 4. This structural model also suggests a surface hot-spot domain that includes residues R122-W127. These amino acids have been shown by several groups to be important in the packaging of A3G into virions. Also, mutation in this region seems to affect A3G ability to interact with the nucleocapsid region of HIV-1 Gag and non-specific RNA binding. Bennett *et al.,* in 2008 demonstrated that the C-terminal deaminase domains of A3G are necessary for A3G dimerization (12). Specifically, residues 209-336 were found to be necessary and sufficient for homoligomerization.

I make use of the D128K, Y124A, and W127A mutants in my work presented in Chapter II to determine the role of A3G complexes in an anti-HIV effect. These mutations all lie in a region undergoing positive selection and are required for anti-viral activity. The structure of A3G may give clues as to the regions of A3G necessary for A3G complex formation.

A3F and A3B

A3G is the most potent of the A3 family in restricting HIV-1 and thus has been the most studied. However, several other A3 proteins have been shown to possess anti-viral activity. A3F and A3B are such A3 family members (40, 86, 180). A3F not only restricts HIV-1 replication, but posses decreased sensitivity to HIV-1 Vif –mediated degradation (87). A3B has been shown in the lab to have limited ability to restrict HIV-1, but completely resistant to HIV-1 Vif-mediated degradation. In patients, the G-to-A hypermutation preference is mostly of the A3G mutation signature. However, the A3F mutation signature is rather prevalent. A3G deaminates cytosines that are preceded by another cytosine, 5'-CC. A3F preference is for a cytosine that is preceded by a thymidine, 5'-CT.

A3G and A3F are expressed in the peripheral blood lymphocytes, the spleen, ovary, and testes; A3B has not been found in these tissues. A3B has been found expressed in various cancel cell lines (20, 121). As such, most effort has been focused on A3G and A3F being that they are expressed in lymphocytes. A3B is not expressed in any of the natural cellular targets of HIV-1 and likely plays no role in restrictive HIV-1 *in vivo*.

Like A3G, A3F forms HMM complexes (164). A3F can homo-oligomerize and it is believed it can hetero-oligomerize with A3G too. A3F mRNA has been found within HMM complexes. The APOBEC family of proteins is shown in Fig. 1-2 (66).

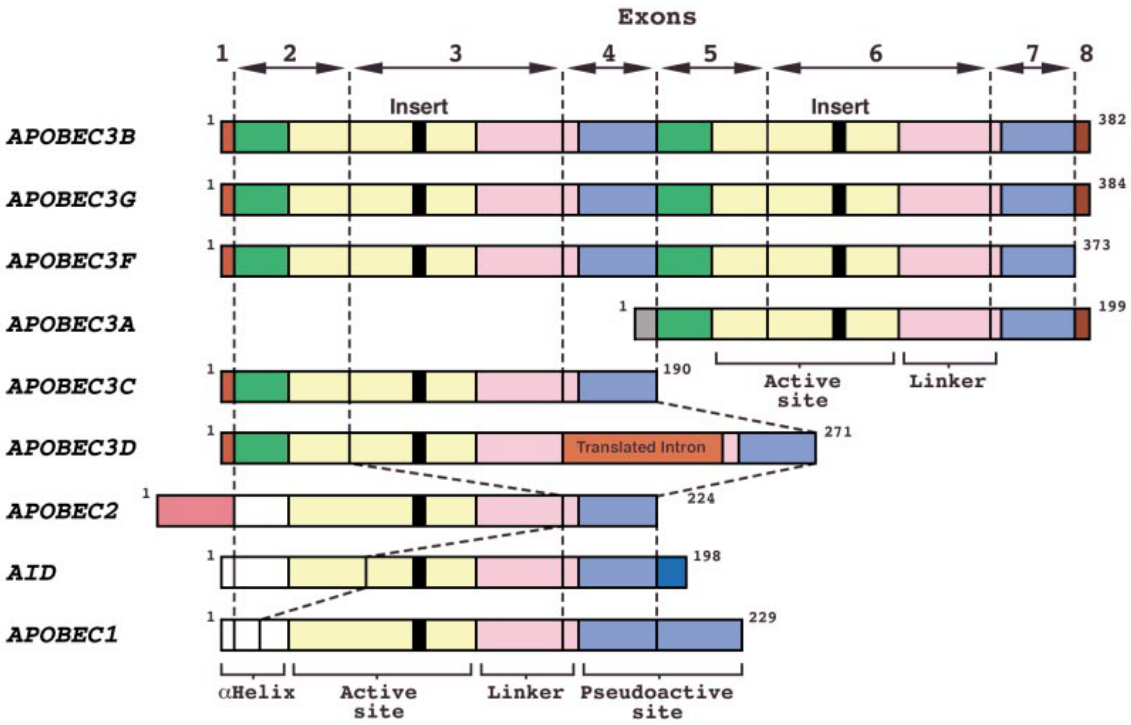

Figure 1-2. The human APOBEC family of proteins. A3B, A3G, A3F, and A3D pc activity. A3B, A3G, A3F, and A3C all restrict the replication of at least one endoge retroelement.

Borrowed from: Jarmuz, A., Chester, A., Bayliss, J., Gisbourne, J., Dunham, I., Scott, J., and Navaratnam, N. (2002) An anthropoid-specific locus of orphan C to U RNA-editing enzymes on chromosome 22. Genomics, 79 (88), 285-96.

A3G Virion Packaging

Approximately 4 to 11 A3G molecules are packed into each virion (115). One molecule of A3G per virion may not be enough for virus neutralization. Paradoxically, it may even improve viral fitness by producing drug resistant mutations, or even mutations that help the virus to invade the immune system.

Though conflicted reports were initially reported in the literature about the necessity of RNA for A3G packaging, it is thought that A3G packaging requires interactions with HIV-1 Gag nucelocapsid and non-specific interactions with RNA (90). Warner Greene's lab showed using pulse-chase experiments that newly synthesized A3G is packaged into budding virions (138). Though their data showed that HMM complexes form within the same time as needed for virion incorporation, they simplest explanation of the data was that LMM A3G was packaged into the virion.

The RNA necessary for A3G packaging is not entirely clear. It is known that NC is responsible for binding of HIV-1 genomic RNA, but a small RNA, 7SL has also emerged as being critical for A3G packaging (10, 158). Burnett *et al.,* showed that multimers of A3G were recruited to the plasma membrane, the site of virus assembly (25). This lent further evidence for the necessity for A3G-A3G interactions in A3G function. Using FRET, these multimers of A3G were shown to colocalize with Gag during viral assembly.

Immunology of A3G

Multiple studies have shown a great variation of A3G and A3F expression from patient to patient. This led researchers to examine if differences in A3 expression could lead to differences in disease progression. There has been some disagreement in the literature on this subject. Jin *et al.,* showed an inverse relationship between A3G mRNA levels and viral load in HIV infected patients not on therapy (69). A positive relationship was observed between A3G mRNA level and CD4 count. These results were highly statistically significant. In fact, they found that long-term nonprogressors (infected individuals who show no signs of HIV-1 disease progression, without anti-retroviral therapy) had the most A3G in PBMC's, while uninfected subjects had an intermediate level, and progressors had the least amount of A3G. In 2009, Vazquez *et al.,* made very similar findings when examining A3G levels in uninfected HIV-1 exposed individuals. Upon exposure, these individuals expressed high levels of A3G (154). After removal of the exposure A3G levels decreased. This work suggested that HIV-1 may trigger A3G expression.

In 2006, Cho *et al.,* found a positive correlation in HIV-1 infected individuals between A3G and A3F mRNA levels and viral load (33). Specifically, infected patients had lower levels of A3G and A3F expression. There was no correlation found between A3G and A3F mRNA levels and CD4 count. In 2010, Reddy found no correlation between A3G expression and either viral load or CD4 T cell count (117). Ulenga *et al.,* in 2008 examining hypermutation in various regions of the virus found that higher levels of hypermutation did not correlate

with decreased viral load, suggesting that hypermutation is not the major mechanisms by which A3G restricts HIV-1 replication (150). Work still remains to determine the effect of A3 expression levels on disease progression.

Work from our lab led by Michael Vetter in 2009 showed variation in the amount of A3G expressed in various CD4 T helper lymphocyte subtypes (156). This difference led to differences in HIV-1 infectivity. Specifically, Th1cells contained higher levels of A3G and A3F RNA and protein, while Th2 cells had significantly less A3G and A3F expression. T cell activation increases A3G expression and this was seen in Th1 cells, but not in Th2 cells that already had low levels of A3G. Th1 cells produced viruses with more A3G and thus greatly reduced infectivity in contrast to Th2 cells, which produced virions with significantly higher infectivity. This showed that A3 expression changes with CD4 T cells differentiation and could account for higher infections in one subtype over another.

Research Objectives

The main objectives of this research project were (1) to determine if A3G complexes are necessary for A3G packaging into progeny virions (2) to determine if A3G complexes play a role in restricting HIV-1 in producer cells and (88) to examine the interaction between RNA granules with A3G complexes. Chapters II and III of this dissertation contains work that answers questions 1 and 2. In Chapter I, I showed that A3G complexes decrease HIV-1 production. In Chapter III I extend this knowledge and also showed that RCK/p54 knockdown

abrogates A3G complexes and this A3G-mediated restriction on HIV-1 production. This work was aided by use of a previously described mutant of A3G (C97A). Using this mutant, I show that A3G complexes are dispensable for A3G packaging into progeny virions. Further, I show that A3G complexes do play a role in an anti-HIV-1 response. I demonstrate that the presence of A3G complexes limits the production of HIV-1 from producer cells. My working model suggests that HIV-1 Gag is trapped in A3G complexes; away from the site of viral assembly. The Gag in A3G complexes is then targeted for degradation, resulting in decreased HIV-1 production. In Chapter III I examine the interplay between RNA granules and A3G complexes. I show that A3G likely resides in a granule that is only formed when A3G is present. This granule contains the processing body markers RCK/p54 and Dcp1, but little to no GW182. Most importantly, these A3G complexes are disrupted by siRNA against RCK/p54 and this disruption releases the A3G-mediated restriction on virus production, extending findings from Chapter II that A3G complexes restrict HIV-1 production.

Taken together, this work provides one of the first in-depth studies of A3G complexes. These structures were thought before to be inert, a belief likely held due to their absence of enzymatic activity. But, I show that A3G complexes are active against HIV-1 in the producer cell. Previously, A3G was thought to only act against HIV-1 in the target cell. This represents a novel anti-HIV restriction of A3G and could lead to the development of therapies that disrupt the Vif/A3G interaction and augment the transit of HIV-1 Gag to A3G complexes. It is

possible that this restriction is not only HIV-1 specific, but may affect other viruses restricted by A3G, such as Hepatitis B virus.

CHAPTER II

A3G Decreases Human Immunodeficiency Virus (HIV-1) Production

Introduction

Members of the A3 family of cytidine deaminases (A3B, A3D/E, A3F, A3G, and some variants of A3H) can restrict human immunodeficiency virus type 1 (HIV-1) replication in human lymphocytes (19, 30, 37, 86, 119, 180). The most studied and potent of these anti-viral enzymes is A3G (A3G) (91). HIV has a counter-measure to this host-defense, the virion infectivity factor (Vif) (105). Vif recruits a cullin-RING ubiquitin-ligase complex that marks A3G for proteasomal degradation, thereby precluding its packaging into virions (97, 175). In the absence of functional HIV-1 Vif, A3G is packaged into progeny virions via RNA-dependent interactions with the nucleocapsid (NC) domain of HIV Pr55 Gag to confer antiviral effects in the target cell (74, 177). Although some reports support the assumption that viral countermeasures, such as Vif, limit A3s' antiviral effects to only blocking *vif*-defective HIV-1 or retroviruses from other species, several *in vitro* and *in vivo* studies of HIV-1 indicate that there are some antiviral effects of A3G in *vif*-positive HIV-1 virions and HIV-1 target cells (68, 112, 155, 156). Similarly, murine A3 has been demonstrated to have activity *in vivo* against several exogenous mouse retroviruses (1, 59, 89, 108). Therefore, human A3's likely have physiological relevance for human retrovirus infections *in vivo*.

Previous studies of A3G's subcellular localization observed both diffuse cytoplasmic staining and localization to large, punctate cytoplasmic foci. Reports suggest that the cytoplasmic bodies may be RNA granules such as mRNA processing bodies (P-bodies), Staufen granules, or stress granules (54, 78, 163). High performance liquid chromatography (HPLC) has characterized the diffuse T cell A3G as being in a low molecular mass (LMM) form and the aggregated form in high molecular mass (HMM) complexes (32). An alternate method involving ultracentrifugation has also been validated to differentiate these two forms (116). The large HMM complexes have been identified as including A3G multimers, several pol III-transcribed RNAs, and a large number of other associated proteins, many found in more than one of the RNA granules listed above (32, 53, 54, 78). HMM complexes of A3G have also been implicated in restricting endogenous retrotransposons such as Alu (32, 63).

I examined the functional effects of cytoplasmic complexes of A3G on HIV-1 replication in HIV-1 producer cells. I called the cytoplasmic structures 'A3G complexes' here, because the earlier data implicated A3G co-localization with different RNA granules, the current models of these structures posit that some constituents dynamically exchange among different RNA granules, and my data also suggested dynamism of A3G (8, 73, 81, 147, 160, 176). A C97A A3G mutant was confirmed to have delayed A3G complex formation and then used in a comparison to wild-type A3G (109, 110). HIV-1 particle release was enhanced from cells lacking A3G complexes and having abundant LMM A3G. A p6-deleted HIV-1 Gag that is retained intracellularly decayed more slowly after protein

synthesis inhibition from cells lacking A3G complexes. Comparison of Vif-positive and Vif-negative HIV-1 strains which either did or did not deplete endogenous A3G complexes from producer T-cell lines, respectively, confirmed that this decrease in HIV-1 production is not an artifact of over-expression. I conclude that A3G complexes reduce HIV-1 production likely via a mechanism that increases Gag degradation. This work will lead to better understanding of the regulation and function of A3G complexes.

Materials and Methods

Cells, transfections, and HIV-1 p24 antigen ELISA

HeLa cells were maintained in DMEM supplemented with 10% fetal bovine serum (FBS, HyClone), penicillin (50 IU/ml), and streptomycin (50 µg/ml). CEM and CEM-SS cells were cultured in RPMI 1640 supplemented with 10% FBS, penicillin (50 IU/ml), and streptomycin (50 µg/ml). Transfections were performed by transient transfection using polyethylenimine (PEI) (118). Complete growth media was replaced 30 minutes prior to transfection. Transfections were carried out in 6-well plates and the reaction included 2 µg of DNA and 10 µg of PEI diluted in 250 µl of serum-free media, unless otherwise stated.

HIV-1 p24 antigen ELISA was carried out as previously described (156, 161). Virus-containing supernatant fluids were collected and filtered through a 0.45 µm syringe filter, prior to ultracentrifugation through a 20% sucrose cushion (detailed below). Cellular and viral lysates were prepared using ice cold lysis buffer [50 mM HEPES, pH 7.4, 125 mM NaCl, 0.2% NP-40 and 0.1 mM PMSF

and EDTA-free protease inhibitor cocktail (CalBiochem, San Diego, CA #539137)]. The percentage p24 release was calculated as culture supernatant ultracentrifugation pellet p24 antigen concentration divided by the total p24 antigen concentration (cell + culture supernatant ultracentrifuge pellet concentration). Others have previously used this method to determine changes in percent p24 antigen release (56, 152). The HIV-1 p24 antibody 183 detects Gag precursors polypeptides Pr55 and 41, as well as processed p24 capsid protein (CA), within the cell and processed p24 CA within the virion (151, 152).

Primary $CD4^+$ T lymphocytes were isolated from an uninfected donor using a protocol approved by the Vanderbilt IRB. $CD4^+$ T lymphocyte isolation was via a negative-selection (Stem Cell). Anti-CD3/CD28 beads (Dynal) were used for T cell activation at a ratio of 1:1 for 3 days. 2 million $CD4^+$ T lymphocytes were washed in cold PBS and lysed in 60 µl of ice cold lysis buffer (60 mM NaCl, 50 mM HEPES pH7.4, 0.2% NP-40, 0.1 mM PMSF and 1xEDTA-free protein inhibitor cocktail) by vortexing. Following 10 minute incubation on ice, lysates were clarified by low-speed spin at 18,000 x *g* for 10 minutes and used for immunoblotting for A3G.

A3G Mutant Construction

Plasmids expressing human A3G were constructed by PCR amplification from a construct obtained from Michael Malim (133). Primers containing the *Not*I and *Hind*III restriction sites and a single HA tag were used. The PCR product was TA cloned into pGEM T Easy Vector (Promega). The sequence was

validated and the plasmid (named *Not*I-hA3G-HA-*Hind*III) was used as a template for all site-directed mutagenesis. The QuikChange II Site-Directed Mutagenesis Kit (Stratagene #200523) was used according to manufacturer's protocol. The following forward and reverse primers were used for the construction of C-terminal HA-tagged A3G mutants. C97A A3G F–5'-CATATCCTGCCCCGCCACAAAGTGTACAAGG-3' and R–5'-CCTTGTACACTTTGTGGCGGGGCTCCAGGATATG-3'. Y124A A3G F–5'-CTTTGTTGCCCGCCTCGCCTACTTCTGGGACCCAG-3' and R–5'-CTGGGTCCCAGAAGTAGGCGCGGGCAACAAAG-3'. W127A A3G F–5-CGCCTCTACTACTTCGCGGACCCAGATTACCAG-3' and R–5'-CTGGTAATCTGG GTCCGCGAAGTAGTAGCG-3'. D128K A3G F–5'-CTACTACTTCTGGAAACCAGATTACCAGG-3' and R–5'-CCTCCTGGTAATCTGGTTTCCAGAAGTAGTAG-3'.

Immunostaining and confocal microscopy

Cells for imaging were grown on 22 mm cover slips in 6-well plates, and then fixed with 3.7% formaldehyde for 5 minutes at room temperature. Cells were permeabilized with 0.1% Triton X-100 for 5 minutes. Permeabilized cells were blocked in 5% BSA for 1 hour at room temperature. Nuclei were stained with 1:1000 dilution of To-Pro 3 in PBS for 20 minutes. For immunofluoresence experiments, primary antibodies were diluted in antibody dilution buffer (1% BSA, 0.05% NP-40, and 2% goat serum in PBS at a concentration of 1:500). Primary antibodies were incubated on cells for 1 hour and the cells washed 3 times with

wash buffer (1% BSA and 0.05% NP-40) for 5 minutes. A polyclonal anti-A3G antibody (NIH AIDS repository #9968) and HIV-1 anti-p24 mouse monoclonal antibody 183 were primary antibodies obtained from NIH AIDS Repository. Primary anti-goat antibodies directed against GW182, TIA-1, LAMP3 (CD63), and anti-rabbit HA antibody were used; all were obtained from Santa Cruz (Santa Cruz, CA). The Staufen anti-serum was a gift from Dr. Luc DesGroseillers, Universite de Montreal. Secondary antibodies used were anti-mouse Alexa Fluor 546, anti-goat Alexa Fluor 568, and anti-rabbit Alexa Fluor 488 from Molecular Probes (Eugene, OR). Secondary antibodies were diluted in antibody dilution buffer at a concentration of 1:1000. Arsenite treatment of cells to induce stress granules involved incubation in 1mM $NaAsO_2$ for 30 minutes. Images were acquired using a Carl Zeiss LSM 510 Meta confocal microscope. A3G expression plasmids (described above) were transfected into cells without endogenous A3G. An HIV-1 Gag construct expressing matrix (MA), spacer peptide 1 (Sp1), capsid (CA), nucleocapsid (NC), Sp2, and p6 open reading frames, with CFP fused to p6, was used; the construct is competent for pseudo-virion production (38). Quantitation of co-localization of A3G and Gag protein was performed by thresholding each channel of each image to eliminate nonspecific background and the co-localization function of Metamorph (Molecular Devices, Sunnyvale, CA) was used to derive percentages of co-localized pixels.

Biochemical separation of A3G forms

A previously validated ultracentifugation method was used to characterize the form of A3G in cell cytoplasm (116). This validation had correlated HPLC-defined HMM complexes of A3G with A3G in ultracentrifuge pellet fractions and the LMM form of A3G with A3G in supernatants after ultracentrifugation. HeLa cells were transfected with the indicated A3G expression plasmid by PEI. Confluent 100 mm plates of cells were rinsed with cold PBS, lysed with 500 µL cold lysis buffer, and vortexed for 10 minutes. Cell lysates were clarified at 17,900 x *g* for 10 minutes to remove nuclei. Clarified lysates were ultracentrifuged at 45,000 x *g* for 1 hour at 4°C. Supernatant fluid was carefully removed and the pellet was resuspended in lysis buffer at a volume equal to that of the supernatant fluid. Equal volumes of resuspended pellet and supernatant fluid were then subjected to western blot analysis. Proteins were resolved by 10% SDS-PAGE. Proteins were transferred to a nitrocellulose membrane and blocked overnight in 5% milk. The membrane was probed with a polyclonal anti-A3G antibody (NIH AIDS repository #9968) and washed with PBST (0.05% Tween 20).

Assessment of intracellular HIV-1 protein decay

A Gag expression plasmid that generates a myristoylated MA-CA-Sp1-NC Gag, lacking Sp2 and p6, was used (MACANC) (83). This deletes the late domain in p6 required for virus budding and allows all expressed Gag to be retained intracellularly. Eighteen hours post-transfection with this construct, HeLa

cells were either treated or not with 10 μg/ml of cycloheximide. Cells were lysed at 0, 6, 12, and 24 hours post-cycloheximide addition. Lysates were analyzed by western blot analysis using the Odyssey LI-COR system (LI-COR, Lincoln, Nebraska) to quantitate immunoreactive protein bands. Primary and secondary antibodies were incubated with the membrane for 1 hour. Nitrocellulose membranes were blocked overnight at 4° in Odyssey Blocking Buffer. Blots were washed 3 times for 5 minutes with Odyssey blocking buffer (0.05% Tween 20) before and after primary and secondary antibody incubation. HIV-1 Gag expression was normalized by β–tubulin for each time point. Secondary antibodies anti-mouse IRDye 800 and anti-rabbit Alexa Fluor 680 were used to quantitate HIV-1 Gag and β–tubulin respectively following primary antibody staining (polyclonal A3G antibody, NIH AIDS repository #9968, and anti-β-tubulin primary antibody sc-9104 from Santa Cruz; latter also used in immunoblots).

Viruses and infections

HIV-1 viral stocks were generated by PEI transfection of HeLa cells with 15 μg of the infectious (envelope +) molecular clones, pNL4.3, pNL4.3 *Δvif*, or pNL4.3 *vif null*. Similarly, Env- viruses were produced and pseudotyped by co-transfecting a vesicular stomatitis virus envelope glycoprotein G (VSV-G) expression plasmid with either pNL4.3 *(env-)* or pNL4.3 *Δvif (env-).* 3×10^6 cells/100 mm culture dish were plated 24 hour prior to transfection. pNL4.3 is a full length infectious clone, pNL4.3 *Δvif* contains a deletion in *vif*, pNL4.3 *Δvif (env-)* contains an additional deletion of env. These plasmids were provided by

Dr. Chris Aiken. Both pNL4.3 *Δvif (env+)* and pNL4.3 *Δvif (env-)* produce a truncated nonfunctional Vif peptide of 128 amino acids. pNL4.3 *vif null* contains tandem stop codons at positions 26 and 27 of the *vif* open reading frame. Finally, a HIV-1 viral construct Δ8.9 HIV-1 was also used. This virus contains HIV-1 *gag, pol, and rev* genes and lacks *env* and any accessory genes (182).

Viral supernatants were harvested 48 hours post-transfection. HIV-1 capsid protein content was determined using HIV-1 p24 ELISA. 1.5×10^6 CEM or CEM-SS cells were infected with 50 ng of p24 containing virus stock. Four hours later, cells were washed three times (to completely remove the input virus), resuspended in growth media, and cultured for an additional 24 hours. Washing at 30 minutes after inoculation prevented infection, and served as a control for adequacy of washing at 4 hours after inoculation to remove extracellular virions. In experiments with infectious (Env+) HIV-1, the non-nucleoside reserve transcriptase inhibitor efavirenz (EFV) was added at a concentration of 25 μM at 16 hours post-infection to limit subsequent rounds of infection. Viral supernatants were ultracentrifuged through a 20% sucrose cushion (125,000 x *g* at 4^oC for 45 min.), as previously described, prior to p24 antigen ELISA (41). Cellular and viral lysates were prepared and p24 antigen quantified by HIV-1 p24 antigen ELISA.

Results

A3G only partially co-localizes in HeLa cells with cellular markers for RNA granules

HeLa cells transfected with either A3G-YFP or A3G-HA expression vectors displayed both diffuse cytoplasmic staining and localization to large cytoplasmic puncta (Fig. 2-1A). Further analysis indicated that A3G-YFP partially co-localized with protein markers for several RNA granules including P-bodies (GW182) and Staufen granules (Staufen) (Fig. 2-1B). The number of P-bodies present in cells did not differ with and without A3G-YFP transfection. Fifty fields using the middle slices of confocal z-sections were chosen, using Dcp1 as a marker for P-bodies. From those 50 fields, 30 fields were randomly selected for quantitation. There were 5 ± 2 P-bodies per cell without A3G-YFP transfection and 6 ± 2 P-bodies per cell with A3G-YFP transfection. Stress granules were not seen in HeLa cells after A3G transfection; arsenite treatment was necessary to induce stress granules. A3G co-localized with TIA-1 in arsenite-induced stress granules (Fig. 2-1B). Potential dynamic transit among structures was also suggested by lack of co-localization of A3G with the late endosome marker CD63 at 16 hours and partial co-localization with that marker at 24 hours (Fig. 2-1C). Thus, A3G partially co-localizes with P-bodies and or Staufen granules, stress granules (if present after stress), and late endosomes. However, A3G complexes do not appear to be identical to any of these cytoplasmic structures. These complexes have been observed by many and are not dependent on overexpression of A3G (Fig. 2-2).

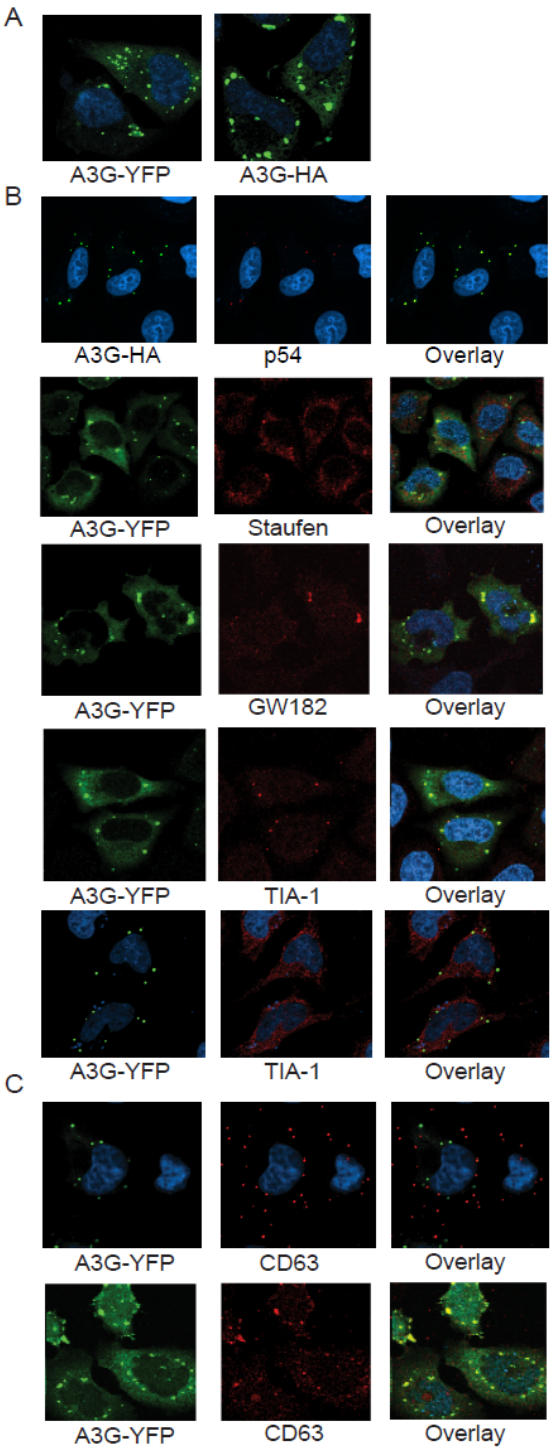

Figure 2-1. A3G only partially co-localizes in HeLa cells with cellular markers for RNA granules. **A.** shows confocal images of Hela cells transfected with A3G-YFP and A3G-HA. **B.** shows HeLa cells transfected with A3G-YFP and stained with antibodies for Staufen, GW182, and TIA-1 shown in red. **C.** HeLa cells transfected with A3G-YFP and stained with antibodies to the late endosome marker, CD63. The top row of Panel C are cells 16 hours post-transfection and the bottom row of Panel C are cells at 24 hours post-transfection. All nuclei are stained with To-Pro3.

HIV-1 Gag co-localizes with A3G complexes

To test whether these A3G complexes also co-localize with HIV-1 Gag, HeLa cells were co-transfected with HIV-1 Gag-CFP and A3G-YFP expression constructs. The Gag-CFP vector is competent for HIV-1 virus-like particle production (38). After 16 or 24 hours, cells were fixed and immunofluorescence images were taken (Fig. 2-3A). The 16 hour post-transfection time-point was selected because it maximizes intracellular Gag levels before large amounts of Gag are found at the plasma membrane. A3G and Gag co-localized at 16, but not 24, hours after co-transfection (Fig. 2-3A, top and middle rows). Gag localization was not affected by co-transfected A3G (Fig. 2-3A, comparing lower row with Gag transfected alone to top and middle rows with co-transfected Gag and A3G). HIV Gag is seen at the plasma membrane by 24 hours with or without A3G transfection, Fig. 2-3A. Areas of co-localization (yellow) were quantified in 30 randomly selected images using Metamorph software. Approximately 29% of A3G pixels overlap with those of Gag, while 31% of Gag pixels overlap with those of A3G. The CD63 late endosome marker that did not co-localize with A3G at 16 hours (as seen in Fig. 2-1C) was used as a negative control in Fig. 2-3B.

C97A A3G has delayed A3G complex formation

I studied several A3G mutants that varied in their ability to be packaged into the virion. I used confocal microscopy and biochemical fractionation to determine their subcellular localization. All A3Gs were HA-tagged. D128K and

C97A A3G are each packaged efficiently into virions (110, 130). D128K A3G alters species specificity for Vif, allowing degradation by SIV agm Vif but not HIV-1 Vif (18, 82, 130, 168). C97A A3G alters the first zinc-finger domain, is monomeric in biochemical assays, and maintains Vif-sensitive antiviral activity (109). Y124A and W127A A3G are each severely deficient in virion packaging (64).

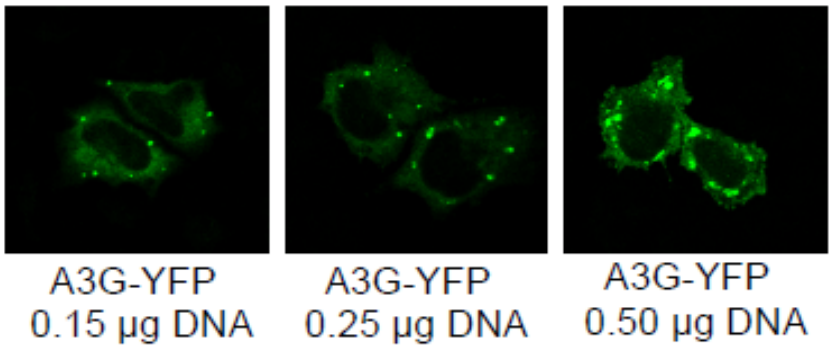

Figure 2-2. A3G complex formation. Confocal micrographs show HeLa cells transfected with varying amounts of A3G-YFP. 0.12, 0.25, and 0.50 µg of A3G-YFP plasmid DNA were transfected into HeLa cells. Cells were fixed and imaged 24 hours post-transfection for A3G-YFP (green). A3G complexes are observed in all conditions, indicating the ability of A3G complexes to form even when A3G is expressed at low levels.

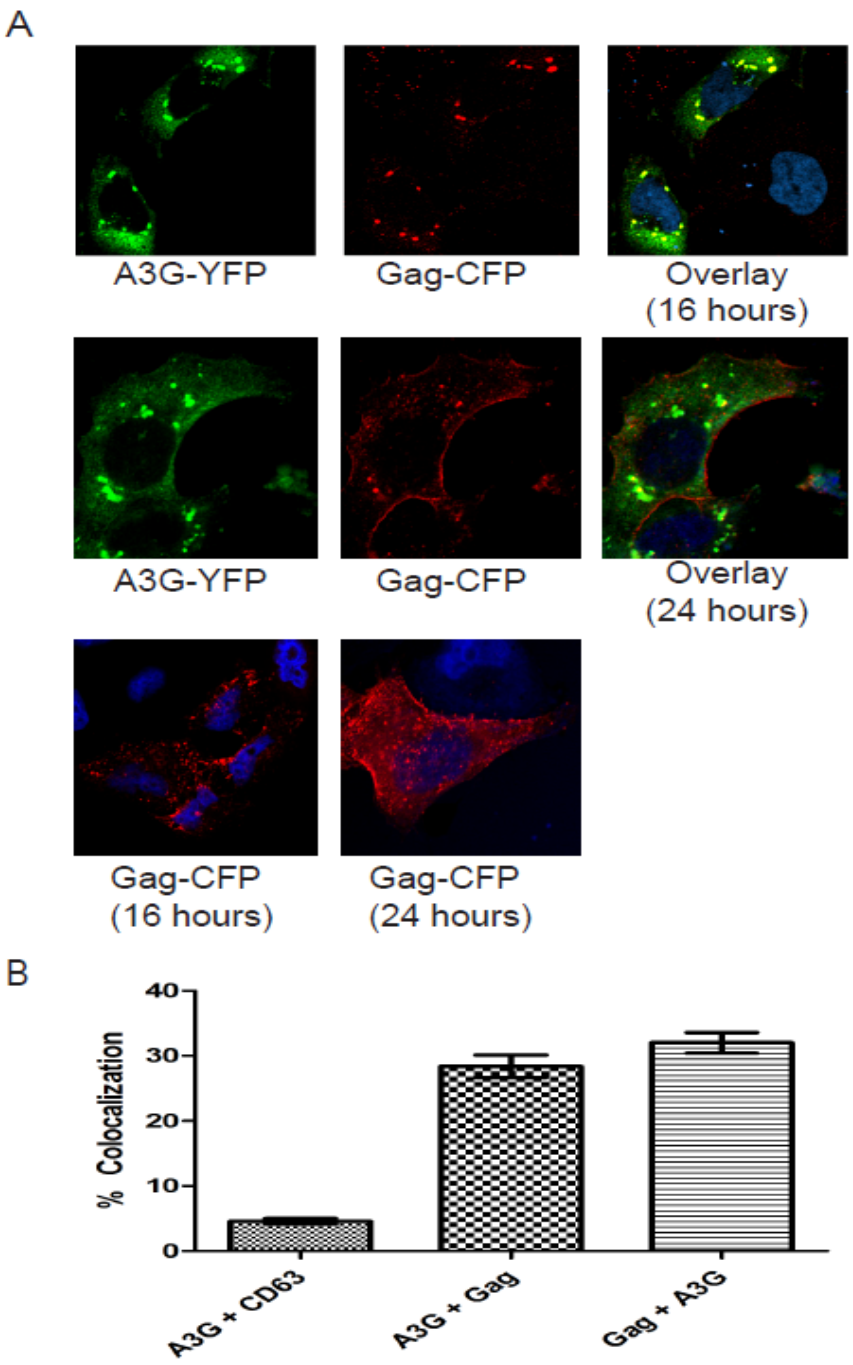

Figure 2-3. HIV-1 Gag Co-localizes with A3G-complexes. **A**. shows cells cotransfected with A3G-YFP (green) and HIV-1 Gag-CFP (125) or Gag-CFP alone in the bottom row at the indicated time point post-transfection. **B.** quantitates co-localization of A3G-YFP and Gag-CFP in cotransfected cells in 30 fields that were randomly selected from 50 fields for quantitation. As a control, cells transfected with A3G-YFP and stained with anti-CD63 antibody at 16 hours (before A3G co-localizes with CD63, Fig. 2-1, panel C) were also used. Error bars represent standard deviation.

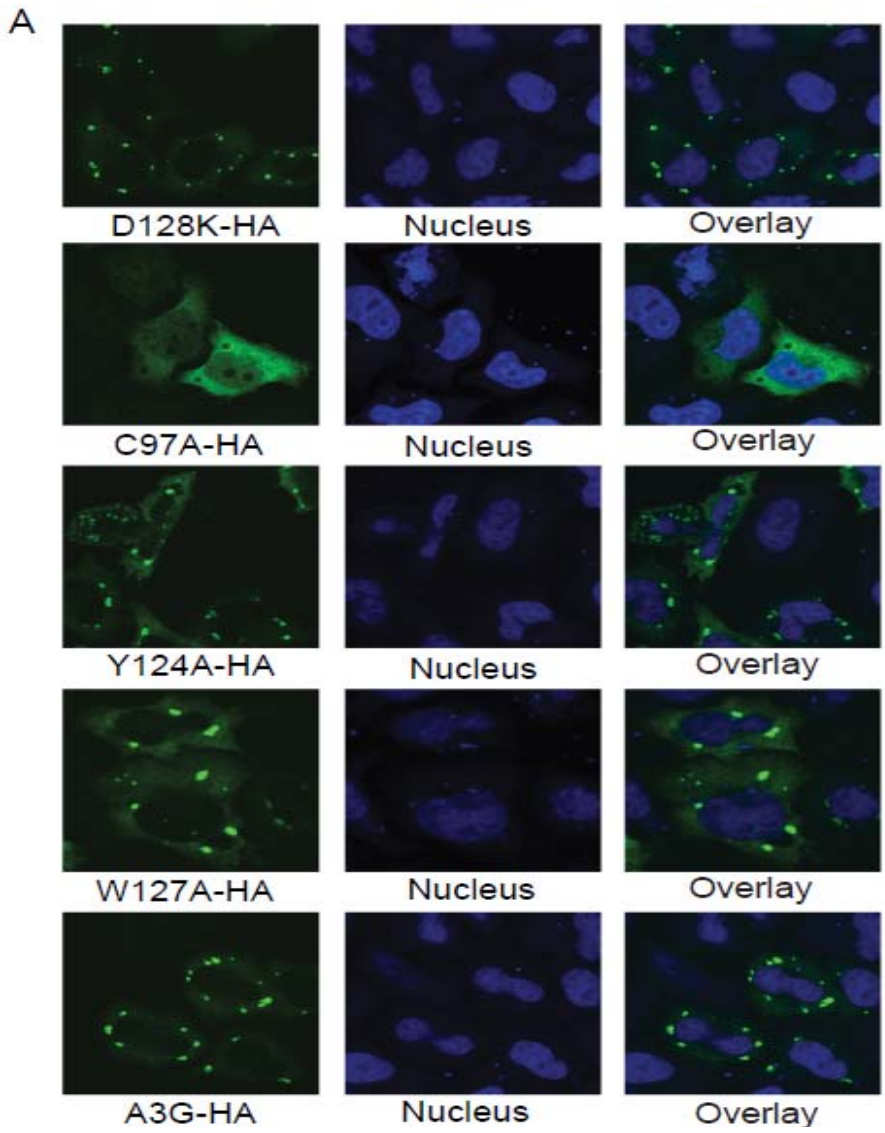

Figure 2-4A. C97A A3G fails to form complexes at 24 hours. A. HeLa cells were transfected with the indicated A3G-HA construct (either D128K, C97A, Y124A, Y127A or wild-type A3G-HA) and then imaged by staining with anti-HA antibody at 24 hours post-transfection.

B

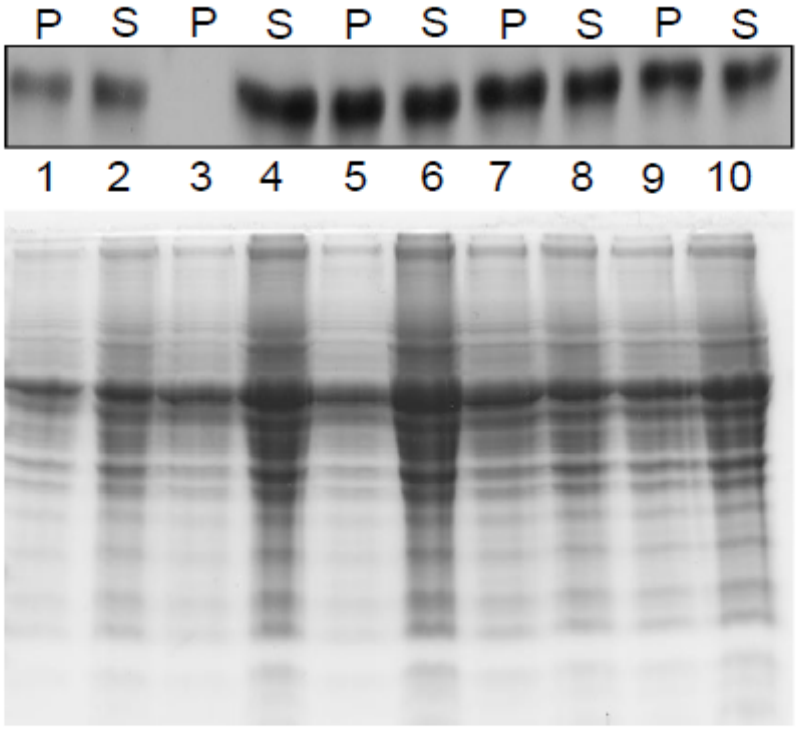

LANES	1	2	3	4	5	6	7	8	9	10
D128K-HA	+	+	-	-	-	-	-	-	-	-
C97A-HA	-	-	+	+	-	-	-	-	-	-
Y124A-HA	-	-	-	-	+	+	-	-	-	-
W127A-HA	-	-	-	-	-	-	+	+	-	-
A3G-HA	-	-	-	-	-	-	-	-	+	+

Figure 2-4B. C97A A3G fails to forms A3G complexes at 24 hours. B. Cell lysates of transfected cells from the same experiment as A. were subjected to ultracentrifugation at the same 24 hour time point after transfection. The pellet and supernatant were subjected to western blot analysis and the blot imaged by incubation with an anti- HA antibody. The amount of A3G in the pellet (P) and supernatant (S) of transfected cells are shown in the upper panel. The middle panel shows the same samples run on a SDS-PAGE gel and stained with coomassie as a loading control. The lower panel provides a key to indicate which A3G-HA construct is in each lane in the upper and middle panels.

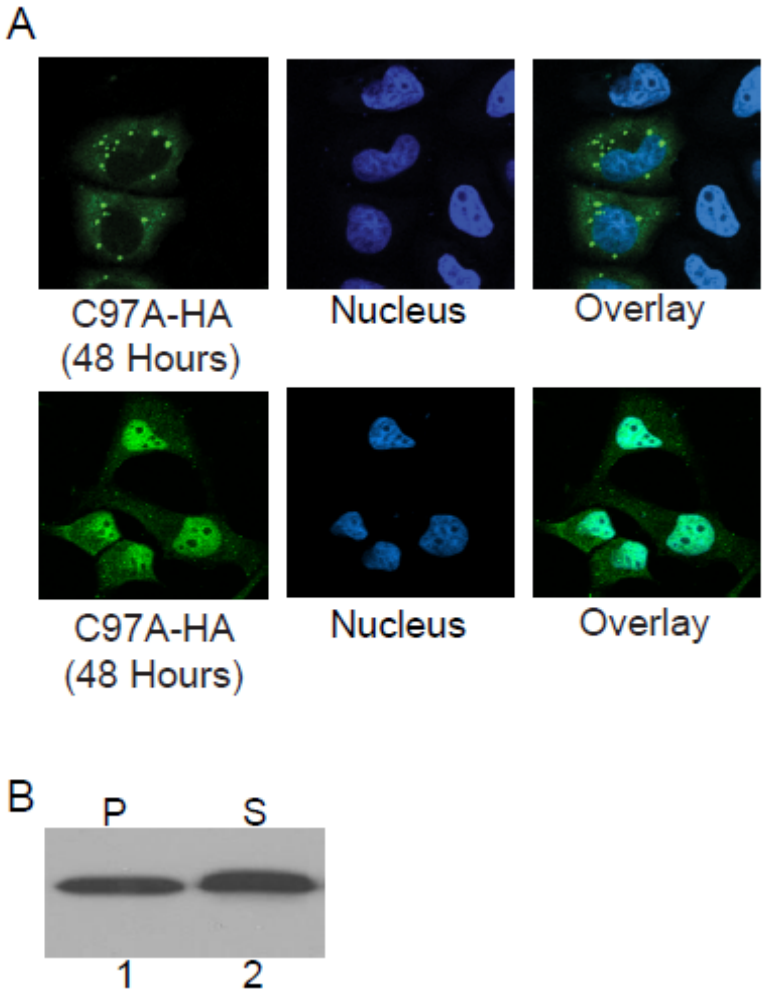

Figure 2-5. C97A A3G forms A3G complexes at 48 hours. HeLa cells were transfected with C97A A3G-HA and cells were either imaged or lysates generated and analyzed by ultracentrifugation. **A.** shows confocal images of HeLa cells transfected with C97A A3G -HA and visualized at 48 hours post-transfection. Two representative images are shown that indicate variation in complex formation at 48 hours post-transfection. **B.** shows lysates from C97A A3G-HA transfected HeLa cells 48 hours post-transfection. C97A A3G -HA is seen in both the pellet and supernatant fractions indicating the presence of A3G complexes at 48 hours.

Each of these C-terminal HA-tagged A3G constructs was transfected individually into HeLa cells to determine their ability to make A3G complexes. Cells were fixed at 24 hours post-transfection and stained with anti-HA antibodies to detect the various A3Gs. Fig. 2-4A shows that WT A3G-HA formed bodies at 24 hours. All A3G mutants formed bodies similar to that of wild-type, except C97A A3G-HA. C97A A3G-HA was more diffuse throughout the cytoplasm at 24 hours after transfection than the other A3Gs studied. C97A A3G-HA also displayed increased nuclear staining at that time, relative to the other A3Gs studied (Fig. 2-4A).

Ultracentrifugation of cytoplasmic lysates following removal of nuclei showed that D128K, Y124A, W127A, and WT A3G proteins each were present in both the pellet and the supernatant (Fig. 2-4B). In contrast, C97A A3G-HA was only detected in the supernatant (lanes 4, Fig. 2-4B) and not detected in the pellet (lane 3, Fig. 2-4B). This biochemically confirmed the absence of A3G complexes in C97A A3G-HA observed by confocal imaging at 24 hours (Fig. 2-4A). As a control for equivalent protein loading, the Coomassie blue-stained gel of the cytoplasmic lysate pellets shows similar protein amounts in the pellet of each mutant including C97A-HA (Fig. 2-4B, middle panel). The C97A mutant does form some complexes at 48 hours post-transfection, Fig. 2-5.

C97A A3G is packaged into virions at 24 hours

HeLa cells were transfected with the Δ8.9 HIV construct and constructs expressing wild-type A3G-HA, D128K, C97A, Y124A, or W127A. Twenty four

hours post-transfection clarified culture supernatant fluids were filtered and ultracentrifuged through a 20% sucrose cushion to concentrate pseudo-virions produced from the co-transfected cells. Both cell and pseudo-virion lysates were subjected to western blot analysis.

Cell lysates showed that equal amounts of A3G were produced in all transfected cells (Fig. 2-6B). The Y124A and W127A A3G mutants were not detected in pseudo-virion lysates, consistent with previous report (Fig. 2-6A) (64). At 24 hours post-transfection, the C97A A3G mutant was present in particles, as was WT A3G, and D128K A3G (Fig. 2-6A). These results confirm earlier reports of the packaging of C97A. These results are consistent with A3G complexes not being the source of packaged A3G as others have suggested based on different experimental strategies (109, 110, 145). Therefore, co-localization of Gag in A3G complexes does not suggest the complexes are involved in the process of virion assembly, as would be suggested if A3G was packaged from complexes.

Producer cell A3G complexes decrease HIV-1 pseudo-virus production and intracellular HIV-1 Gag half-life

I next sought to compare levels of HIV-1 production from cells with and without A3G complexes to test whether virus production was decreased in cells containing complexes. HeLa cells were co-transfected with Δ8.9 HIV-1 and either an empty vector control, WT A3G-HA, C97A A3G-HA or Y124A A3G-HA. After 24 hours, culture supernatant fluids and cellular lysates were collected and HIV-1 p24 antigen ELISA and western blots were performed. Culture

supernatant fluids were centrifuged at low speed to remove cellular debris, filtered, and ultracentrifuged through a 20% sucrose cushion to concentrate pseudo-virions containing CA. The concentration of p24 antigen in the pellet of the ultracentrifuged culture supernatant was divided by the sum of the amount of p24 antigen reactivity in the cell lysate plus the pellet of the ultracentrifuged culture

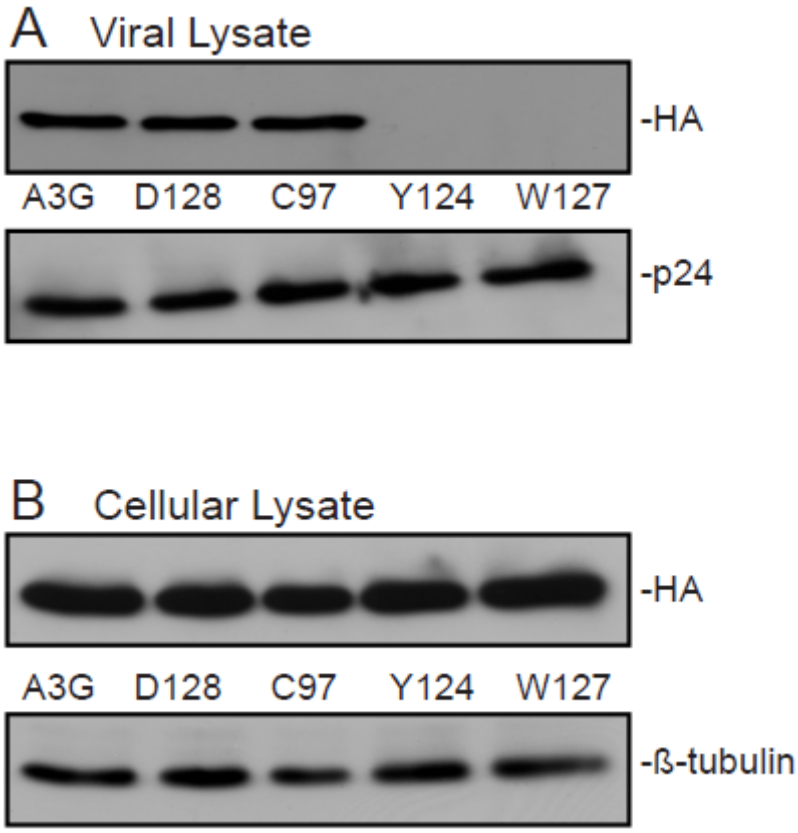

Figure 2-6. C97A A3G is packaged into virions at 24 hours. HeLa cells were transfected with the *env*-deleted 8.9 HIV-1 construct and the indicated A3G-HA DNA construct (WT, D128K, C97A, Y124A, Y127A). 24 hours post-transfection, cells and supernatants were harvested and cell lysates prepared. The supernatants were filtered and ultracentrifuged through a 20% sucrose cushion. The resulting pellet was resuspended in a volume equal to that of the cell lysate. **A.** shows western blots of the viral lysates. **B.** shows western blots of the cell lysates. Blots are visualized by staining with the antibodies shown at the right of each gel (anti-HA antibody, anti-HIV-1 p24 antibody, and anti-tubulin antibody).

supernatant to yield the percent p24 antigen produced. The amount of p24 antigen produced from HeLa cells co-transfected with HIV-1 and a control empty vector was comparable to similar experiments reported by others (49, 56, 152).

Cells co-transfected with the control plasmid not expressing A3G, as well as the plasmid expressing C97A A3G-HA that did not form A3G complexes at 24 hours, each released significantly more pseudo-virions than did cells co-transfected with WT A3G-HA or Y124A A3G-HA (Fig. 2-7A). Both A3G-HA and Y124A A3G-HA form A3G complexes at 24 hours, Fig. 2-4A. A3G levels in the cells containing each A3G variant were similar based on anti-HA staining, and anti-β–tubulin staining also controlled for similar loading of each specimen (Figure 2-7B). To determine whether the levels of A3G in transfected HeLa cells were within the range of endogenous A3G expression in T cells, cell lysates of CEM cells (which express endogenous A3G), WT A3G-HA-transfected HeLa cells (from the experiments depicted in Fig. 2-7 A & B), and activated primary $CD4^+$ T cells (derived from peripheral blood mononuclear cells of a donor not infected with HIV-1) were immunoblotted using an anti-A3G antibody (Fig. 2-7C). The level of exogenous A3G in the transfected HeLa cells was not higher than that of endogenous A3G in CEM cells and activated primary $CD4^+$ T cells (Fig. 2-7C, normalized for β-tubulin), indicating that there was not supra-physiologic over-expression of A3G.

Cells expressing either WT A3G-HA or Y124A-HA had 28% and 34% of the pseudo-virus output, respectively, compared to control cells lacking A3G (for each, $p<0.0079$, in both cases, Mann-Whitney U) (Fig. 2-7D). Cells containing

the C97A-HA mutant, that does not produce A3G complexes at 24 hours, did not differ from the A3G-negative control (Fig. 2-7D). The amount of intracellular HIV-1 p24 antigen did not differ between A3G-negative cells and WT A3G-HA- and C97A-HA-containing cells (Fig. 2-7D).

If A3G complexes were only blocking release of assembled pseudo-virions, an increase in intracellular p24 antigen would be expected to accompany decreased supernatant p24 from cells containing A3G complexes. The lack of such an increase in intracellular p24 suggested that A3G complexes may decrease intracellular HIV-1 levels rather than directly affecting only virion release. The rate of HIV-1 Gag degradation in HeLa cells was therefore studied after protein synthesis was blocked by cycloheximide. A Gag variant that is not released from cells because of a p6 late domain deletion was used for this experiment to avoid confounding differences in pseudo-virus release. Gag levels were compared over time in cells expressing p6-deleted Gag alone, p6-deleted Gag with WT A3G (forming complexes), and p6-deleted Gag with C97A A3G (not forming A3G complexes) (Fig. 2-7E). Cells were treated with 10 μg/ml of cycloheximide 18 hours post-transfection. Cells were collected and lysed at 0, 6, 12, and 24 hours following start of cycloheximide treatment. Gag protein level was normalized by β–tubulin immunoreactivity at each time point. There was no difference in Gag expression between cells with A3G and those without at time point 0 (Fig. 2-7E). β–tubulin expression did not change over time (not shown). Multiple linear regression showed Gag levels increased over time in cells left untreated as a control. Multiple linear regression also showed that HIV-1 Gag

A

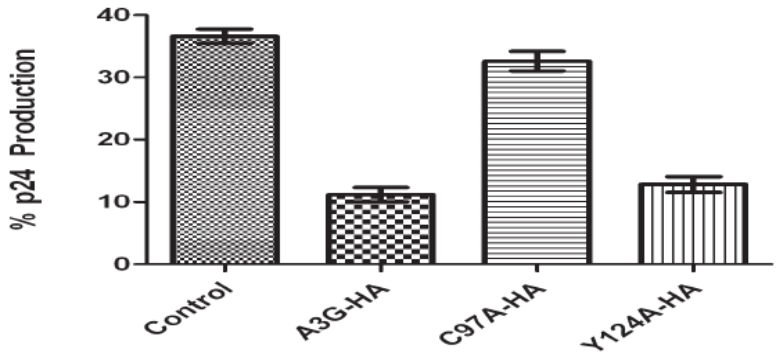

B

Δ8.9 HIV	Control	A3G	C97A	Y124A
Average p24 Cell (ng/ml)	40	42	43	40
Average p24 Sup (ng/ml)	23	5*	20	6*
Average Total p24	63	47*	63	46*
% p24 Production	100	28*	86	34*

C

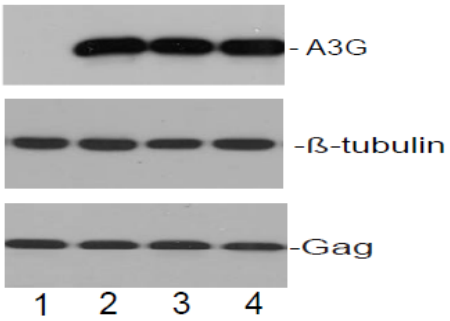

D

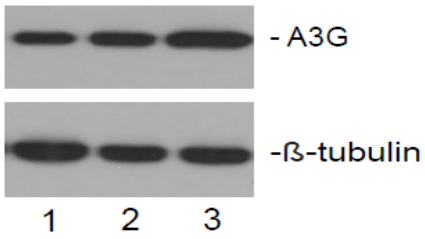

Figure 2-7A-D. Producer cell A3G complexes decrease HIV-1 pseudo-virus production and intracellular HIV-1 Gag half-life. **A.** The percentage of HIV-1 p24 antigen production 24 hours after HeLa cells were co-transfected with Δ8.9 HIV-1 and the indicated A3G expression plasmid construct (control = empty A3G expression vector) are shown. **B.** The table shows average p24 values from cell lysates and supernatants of the experiment in Fig. 5A. There is a significant difference in supernatant ($P = 0.0079$, in both cases, Mann-Whitney U) and total p24 levels ($P < 0.0079$, in both cases, Mann-Whitney U) between the no-A3G control and the A3G and Y124A conditions. Significant differences in percentage HIV-1 p24 antigen production from the no-A3G control are indicated by an asterisk ($P < 0.0079$ in each case, Mann Whitney U). **C.** Western blots of the cell lysates from Panel A are shown indicating equivalent amounts of: A3G for each variant (based on anti-HA staining, upper panel); HIV-1 Gag (middle-panel); and protein loading (based on anti-β-tubulin antibody staining, lower panel). Cells were co-transfected with Δ8.9 HIV-1 and: Lane 1. control empty-vector; Lane 2. A3G-HA; Lane 3. C97A A3G-HA; and Lane 4. Y124A A3G-HA. **D.** Western blot shows relative A3G levels in: Lane 1. CEM cells; Lane 2. A3G-transfected HeLa cells; and Lane 3. activated CD4 T cells.

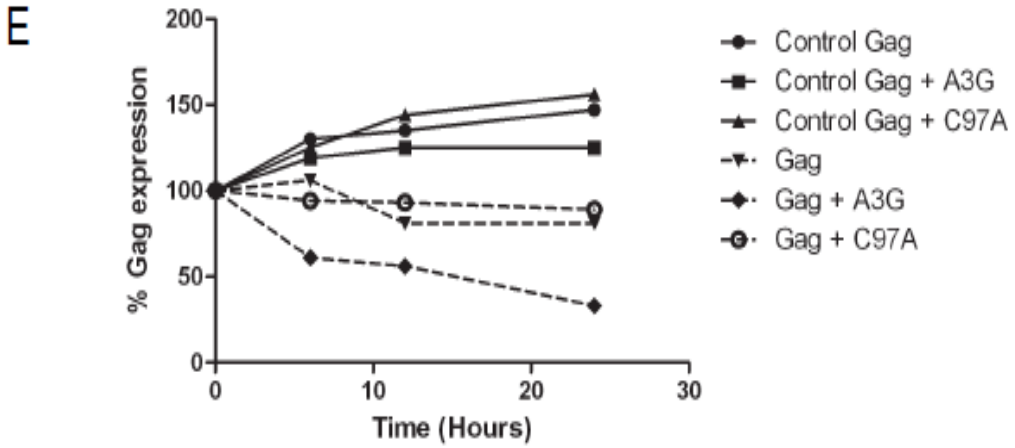

Figure 2-7E. Producer cell A3G complexes decrease supernatant HIV-1 pseudo-virus production and intracellular HIV-1 Gag half-life. **E.** Cycloheximide blocking experiment showing HIV-1 Gag half-life over 24 hours following 10 μg/ml treatment at 0 hours. Degradation of p24 was assessed by quantitative immunoblot after protein synthesis inhibition by cycloheximide, in the presence or absence of A3G complexes. Controls were treated similarly, but with no cycloheximide treatment. Cells were lysed at the indicated time point and subjected to western blot analysis and bands quantitated using Odessey Licor. HIV-1 Gag was normalized to β–tubulin. Multiple Linear Regression analysis showed that cells with wild-type A3G declined in their HIV-1 Gag expression more rapidly than cells with no A3G, $p = 0.009$. There was no difference in Gag levels between cells with no A3G versus those with C97A, $p= 0.8$. There was no statistical difference in Gag expression between cells with A3G and those without at time point 0, $p = 0.6$.

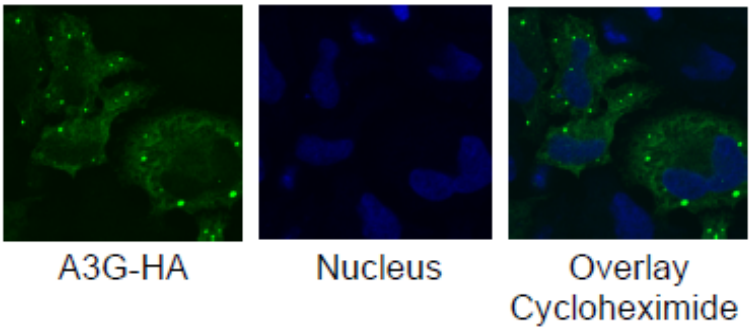

Figure 2-8. Cycloheximide does not inhibit A3G complex formation. The above images show HeLa cells transfected with A3G-HA and treated with 10 µg/ml of cycloheximide for 24 hours. After the 24 hour treatment, cells were fixed and stained for A3G using anti-HA antibody. A3G complexes are still observed following cycloheximide treatment.

levels decreased more rapidly after cycloheximide addition in cells with A3G complexes (WT A3G-transfected cells) than in cells with either no A3G or C97A A3G that does not form A3G complexes ($p = 0.009$). There was no difference between treated cells with C97A and those with no A3G. Cycloheximide treatment alone does not abrogate A3G complex formation, Fig. 2-8. Based on these data I hypothesize that A3G complexes shorten HIV-1 Gag protein half-life.

CEM cells depleted of endogenous A3G by Vif produce more HIV-1 virions than do A3G-containing CEM cells

I next sought to confirm that this effect of A3G complexes to decrease HIV-1 production was not an artifact of over-expression, exogenous expression, or virus transfection. I determined whether this A3G-mediated restriction would be seen in more physiological conditions: a single-replication cycle HIV-1 infection of a T cell line, CEM that expresses physiological levels of endogenous A3G (Fig. 2-9C). I hypothesized that Vif expressed from WT NL4.3 HIV-1 would degrade A3G both within and outside of A3G complexes, while cells infected with Vif-negative NL4.3 would have unaltered levels of A3G complexes. This allows a comparison of relative virus output from the same HIV-1- infected producer T cell type in the presence and absence of endogenous A3G, including A3G complexes. I limited virus replication to a single round to avoid possible confounding effects of multiple rounds of replication.

I first studied CEM cells infected with VSV-G envelope-pseudotyped HIV-1 that could not cause a spreading infection, and then assessed fully replication-

competent viruses with CXCR4-tropic HIV-1 envelopes. With both types of envelopes, HIV-1 replication was limited to a single round. EFV was added at 16 hours after infection with CXCR4-tropic HIV-1 envelope positive proviral clones to limit secondary rounds of replication in that experiment. A control experiment where 25 μM EFV was added at the time of infection confirmed that this concentration prevented viral replication, with no toxic effect on cell numbers or cell viability (data not shown). The VSV-G pseudotyped viruses were NL4.3 *env*-deleted strains, with either a wild-type or a deleted (*Δvif)* gene. In addition to wild-type, Vif-positive NL4.3, two different Vif-negative HIV-1 strains were used in the experiments with HIV-enveloped viruses: NL4.3 *Δvif* and NL4.3 *vif null*. NL4.3 *Δvif* is an isogenic clone of pNL4.3 with an in-frame deletion in *vif* resulting in a 128 amino acid protein that is inactive but incorporated into virions. NL4.3 *vif null* is an isogenic clone of pNL4.3 that contains tandem stop codons at residues 26 and 27 of the *vif* open reading frame. I also infected CEM-SS cells that lack any A3G protein, as another control to determine if results were specifically related to A3G (133). Culture supernatants were cleared of debris and virions ultracentrifuged through a 20% sucrose cushion before p24 antigen ELISA was done. As in the experiments in Fig. 2-7, the p24 content of the ultracentrifuged culture supernatant was divided by the sum of the amount of p24 antigen reactivity in the cell lysate plus the pellet of the ultracentrifuged culture supernatant to yield the percent p24 antigen release from the producer cell.

The percentage of p24 antigen production was decreased from CEM cells infected with a Vif-negative, VSV-G-pseudotyped NL4.3 compared to an

otherwise isogenic Vif-positive virus at 24 hours post-infection (Fig. 2-9A; two left bars; $p < 0.0022$, Mann-Whitney U). In addition, decreased HIV-1 production was observed from CEM cells infected with either of two CXCR4-tropic, HIV-enveloped Vif-negative viruses (*Δvif* and *vif null*), relative to a Vif-positive HIV-1 (Fig 2-9B; left three bars; $p = 0.005$ at each time point). A3G was detected only in the Vif-negative virus infections (lower panel in Fig. 2-9 A & B), with β–tubulin immunoreactivity indicating similar protein loading in each lane. A3G was present in cell lysate ultracentrifugation pellets indicating the presence of A3G complexes in CEM cell lysates transfected with NL4.3 *Δvif* and NL4.*3 vif null* (Fig. 2-9C). No A3G complexes, defined as A3G in ultracentrifugation pellets, were observed in CEM cells infected with Vif-positive NL4.3; no A3G was detected in cell lysate ultracentrifuge supernatants either (Fig 2-9C). A Coomassie blue-stained gel showed equivalent protein loading in all lanes of Fig. 2-9C (not shown). HIV-1 production from CEM-SS cells lacking any A3G did not differ at 24 hours after infection with Vif-positive versus Vif-negative viruses (Fig. 2-9 A & B, right hand bars). The amount of intracellular p24 detected in cell lysates was similar across all viruses and cells at 24 hours (Fig. 2-9D); amounts of HIV-1 p24 antigen were decreased in the pelleted supernatant, as seen previously in Fig. 2-7. This again is consistent with A3G complexes having an effect on intracellular levels of HIV-1 Gag protein, and not directly affecting release of virions from the cell. When percent production was calculated relative to wild-type, Vif-positive HIV-1, VSV-G pseudotyped NL4.3 *Δvif* produced 44% of the wild-type amount from CEM cells (Fig. 2-9D). Again no difference was observed in CEM-SS cells between VSV-G

pseudotyped viruses with or without HIV-1 Vif. The same effect was seen with Env+ viruses, as the Vif-deleted viruses produced 51% and 47% of the amount from CEM cells infected by WT, Vif-positive NL4-3 that were depleted of A3G ($p < 0.002$, Mann-Whitney U; Fig. 2-9D).

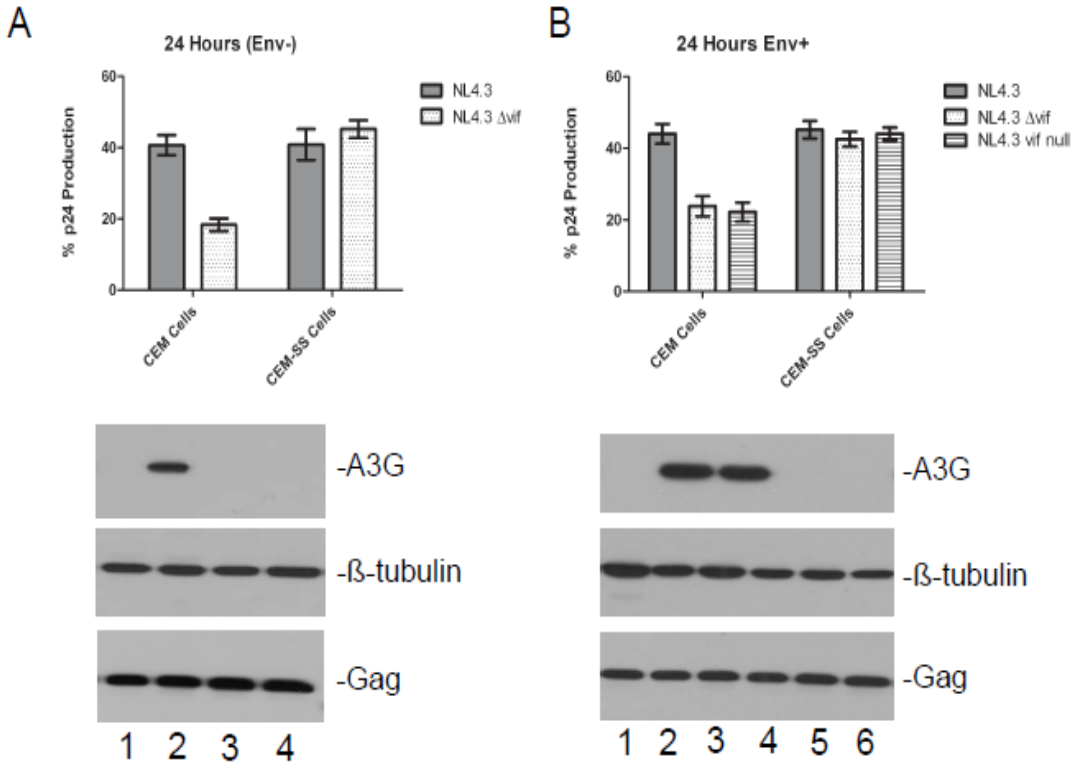

Figure 2-9 A-B. CEM cells depleted of endogenous A3G by Vif produce more HIV-1 virions than do A3G-containing CEM cells. **A.** shows single-round infections of Env- virus at 24 hours post-infection. Control is the VSV-G pseudotyped, vif-positive NL4.3-infected CEM cells that were washed at 30 minutes after infection. Lanes 1 and 3 are cellular lysates from CEM and CEM-SS cells infected with NL4.3 respectively. Lanes 2 and 4 are cellular lysates from CEM and CEM-SS cells infected with *Δvif* NL4.3 respectively. **B.** shows single-round infections of replication-competent CXCR4-tropic HIV-1 Env+ virus at 24 hours post-infection. The left bars represent percent virus production from CEM cells and the right bars represent percent virus production from CEM-SS cells. Lanes 1 and 4 are cellular lysates from CEM and CEM-SS cells infected with NL4.3 respectively. Lanes 2 and 5 are cellular lysates from CEM and CEM-SS cells infected with *Δvif* NL4.3 respectively. Lanes 3 and 6 are cellular lysates from CEM and CEM-SS cells infected with *vif null* NL4.3 respectively. Means of 6 replicates are presented in the graphs. Error bars represent standard deviation. The decrease in % p24 release from the *vif*-deleted virus, relative to the vif- positive viral control, in CEM cells was significant (A. P = 0.0022, Mann-Whitney U) (B. P = 0.005 in all cases, Mann-Whitney U). No difference in virus production between the *vif*-positive and *vif*-deleted virus constructs was seen in CEM-SS cells.

C

CEM Cells			
Env-	NL4.3	NL4.3 delta Vif	
Average p24 Cell (ng/ml)	40	37	
Average p24 Sup (ng/ml)	23	11*	
Average Total p24 (ng/ml)	63	48	
Percent p24 Production	100	44*	
Env+	NL4.3	NL4.3 delta Vif	NL4.3 Vif Null
Average p24 Cell (ng/ml)	44	40	43
Average p24 Sup (ng/ml)	28	13*	16*
Average Total p24 (ng/ml)	72	53	59
Percent p24 Production	100	51*	47*

D

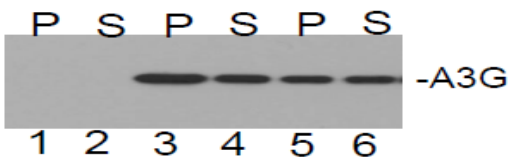

Figure 2-9C-D. CEM cells depleted of endogenous A3G by Vif produce more HIV-1 virions than do A3G-containing CEM cells. **C.** The table shows that the amount of HIV-1 p24 antigen in cell lysates infected with all viruses were similar at each time point; differences were seen only in supernatant p24 antigen amounts in CEM cells. Total p24 was lower in cells with A3G complexes. The CA-182 capsid monoclonal antibody recognizes both full length and processed forms of Capsid protein. There was no significant difference in HIV-1 p24 antigen production between vif positive and either vif defective virus at any time point in CEM-SS cells. Significant decreases in percentage HIV-1 p24 antigen production, compared to the vif-positive virus, are indicated by an asterisk. **D.** depicts ultracentrifugation of CEM cell lysates from the experiment in Panel B. and indicates that the vif-positive virus depleted A3G-complexes (found in the pellet, P) as well as the A3G found in the supernatant (S).

Discussion

My results demonstrated that cytoplasmic A3G complexes decrease HIV-1 virion production in a physiological system. Much of the cytoplasmic A3G in cell lines and activated primary T-lymphocytes is present in such complexes. I found that A3G only partially co-localizes with markers for RNA granules. A3G complexes also only partially associates with stress granules; indeed, stress granules were not present until after arsenite-induced cellular stress (32, 53, 54, 78, 94). Others have also found, as I did, that A3G expression does not induce P-bodies or stress granules (54). These findings, as well as the partial co-localization of A3G with the CD63 marker of late endosomes only at later time points after transfection, led us to conclude that A3G is dynamic and not exclusively localized to a single RNA granule / cytoplasmic compartment. Earlier reports also indicated that A3G's cytoplasmic location changes over time and that it traffics between compartments / RNA granules (25, 30, 45, 53, 73, 78, 94, 156). There is also consensus that there is a dynamic interaction among RNA granules in that they exchange many of their components (101, 147). My results are also consistent with the view that A3G complexes may not be identical with only one previously described type of RNA granule.

Because about 30% of HIV-1 Gag and A3G co-localized with each other (Fig. 2-3B), I speculated that A3G complexes may be the cytoplasmic source from which A3G gained access to assembling virions. An earlier report also suggested this (159).The hypothesis that A3G complexes may play a role in virion assembly is also consistent with data that P-bodies are required for

replication of Ty1 and Ty3 retrotransposons in yeast; indeed, human A3G has been localized to P-bodies when over-expressed in yeast (11, 45). Results presented here, however, are consistent with two prior lines of evidence indicating that the co-localization of A3G in cytoplasmic structures is not required for HIV-1 virion assembly and release. Opi, et al. previously reported, as I also observed, that C97A A3G did not form cytoplasmic bodies within 24 hours post-transfection and had greater nuclear localization than wild-type A3G (109, 110). Despite some differences in methodology, the concordance of results between the present study and Opi, et al. (109) conclusively indicate that C97A A3G is packaged into virions. Soros, et al. presented a separate line of evidence about the role of A3G complexes in virion packaging of A3G (138). Using pulse-chase radio-labeling, Soros, et al. showed that newly-synthesized A3G was packaged into virions, prior to the time required to observe complex formation. Their methodology did not allow exclusion of the possibility that virion packaging occurred from very recently assembled complexes. However, the present study indicates that C97A A3G packaging occurs in the absence of microscopically visible cytoplasmic bodies containing A3G.

A3G complexes have been implicated in A3G's inhibitory effects against retrotransposons (32, 63), leading us to explore if there was a functional effect of A3G complexes on HIV-1 replication. I started with a genetic analysis of A3G effects on pseudo-virion production and then used a more physiological approach to exclude that results were an epiphenomenon or artifact of A3G over-expression.

I compared HIV-1 production in the presence of wild-type A3G versus different mutant A3Gs, after confirming that C97A A3G had delayed A3G complex formation in HeLa cells (109, 110). HeLa cells that lack endogenous A3G were co-transfected with a non-infectious, *env*-deficient HIV-1 genome and a vector expressing either wild-type A3G, C97A A3G, Y124A A3G, or a control expression plasmid lacking A3G. HIV-1 virion production was reduced over three-fold in a single-round of replication from cells with wild-type A3G and Y124A A3G, which each form A3G complexes. In contrast, cells containing C97A A3G lacked biochemical evidence of A3G complexes at 24 hours, and released higher levels of HIV-1 p24 antigen; levels were similar to that seen from control-transfected cells lacking A3G (Fig. 2-7). While another difference between C97A A3G and the other A3G proteins studied that is unrelated to formation of A3G complexes in the cytoplasm cannot be excluded, the difference between the empty vector control and both wild-type A3G and Y124A A3G indicates that the observed reduction of particle production is A3G-specific.

One surprising aspect of the results in Fig. 2-7 was that intracellular HIV-1 Gag levels were not increased in the presence of A3G complexes, as would be expected if the complexes provided a direct block to virion release. This led us to test the hypothesis that intracellular HIV-1 Gag protein levels may be decreased in the presence of A3G complexes by following Gag protein levels after cycloheximide inhibition of protein synthesis. A late domain-deleted Gag that blocks Gag release by budding from membranes was used to limit analysis to study of intracellular Gag. Results showed that a more rapid decrease in

intracellular HIV-1 Gag levels following protein synthesis inhibition was associated with the presence of A3G complexes (Fig. 2-7E). This finding strongly suggests that the effect of A3G complexes to decrease HIV-1 production occurs at a step in replication prior to release of budding virus from the membrane.

I next sought to confirm that inhibitory effects of A3G complexes on HIV-1 production were not related to other effects of A3G mutations, exogenous A3G or A3G over-expression by using a different experimental strategy. I studied single-round infections of enveloped HIV-1 particles, with and without an intact *vif* open reading frame. This approach was intended to compare cells depleted of endogenous A3G by *vif*-positive infection with those retaining A3G, including complexes, after *vif*-defective virus replication. I tested viruses with VSV-G envelopes that were capable of only a single round of replication, as well as different viruses with CXCR4-tropic HIV envelopes. Inhibition of a second round of replication was achieved for the latter replication-competent viruses by adding a non-toxic, non-nucleoside reverse transcriptase inhibitor at 16 hours after infection. These experiments included two different types of *vif*-defective viruses. One *vif*-defective virus generates a truncated, non-functional Vif; the other *vif*-defective virus has tandem stop codons in the *vif* reading frame at positions 26 and 27. This therefore also allowed us to exclude that my results were not due only to lack of an HIV-1 envelope, or use of one particular *vif*-deleted HIV-1 variant.

CEM cells infected with either of the two strains of *vif*-defective HIV-1, whether pseudotyped by VSV-G or HIV-1 envelope, produced significantly less

HIV-1 p24 antigen into the supernatant than did CEM cells infected with the Vif-positive HIV-1 (Fig. 2-9). The wild-type Vif-positive virus degraded endogenous A3G that was diffuse in the cytoplasm as well as in A3G complexes in these CEM cells (Fig. 2-9C). CEM-SS cells contain no endogenous A3G; no difference in virion production was seen in the comparison of Vif-positive and Vif-defective HIV-1 from CEM-SS cells (Fig. 2-9 A & B). Vif-induced A3G degradation in CEM producer cells restored virus production to the higher levels that were seen in A3G-negative CEM-SS cells. Again, results indicate decreased HIV-1 production that is specific for the presence of A3G complexes.

In summary, I have identified that HIV-1 virion production is diminished from cells containing A3G complexes, and suggest that this is not due to an effect on release of budding virions from the plasma membrane. My results suggest that a mechanism for the decreased HIV-1 production observed here is that A3G complexes decrease the intracellular levels of HIV-1 Gag needed for virion assembly. This could be due to a process that moves A3G complexes and associated HIV-1 Gag into late endosomes, and then lysosomes for degradation. HIV-1 Gag has been shown by others to significantly co-localize with CD63 at times after 12 hours (42); A3G was identified here to have delayed partial co-localization with late endosomes. It is also possible that A3G complexes decrease the availability of HIV-1 mRNA for translation, as occurs in P-bodies (102). However, some evidence indicates that A3G has the opposite effect (e.g., shuttling of cellular mRNAs from P-bodies to polysomes), although HIV-1 mRNAs were not studied in that paper (78). Further experimentation will be needed to

define the cellular post-transcriptional mechanism underlying the more rapid decrease in Gag levels following protein synthesis inhibition seen here, however. The possibility that the antiviral effect of A3G complexes in the producer cell extends to other retroviruses also warrants study.

These results reveal a novel anti-HIV activity of A3G within the producer cell. Until now, it was thought that A3G only exerted its antiviral effect in the target cell following packaging into virions in the producer cell. The magnitude of this previously unrecognized anti-HIV activity of A3G in producer cells was modest. However, I performed only single-round replication experiments because this was the only way to isolate a potential effect of producer cell A3G from the effects of virion-packaged (and possibly target cell) A3G that would be seen in a spreading infection. The multiple rounds of infection that occur *in vivo* will likely enhance the effect of A3G complexes to decrease HIV-1 production. Another factor is that other A3s that are expressed in T-lymphocytes and present in cytoplasmic bodies, such as A3F (53), may have similar activity as that characterized here for A3G, and further decrease virion output from producer cells. Some cells that produce HIV-1 virions *in vivo* contain higher physiological levels of A3G, and A3F, than others (51, 52). In addition, NL4-3 Vif is relatively active in A3G degradation *in vitro*, compared to Vif from other HIV-1 strains including some derived from *in vivo* specimens (135). My results raise the possibility of increasing cellular A3G expression, and possibly that of other A3s, to reduce virion output from producer cells, as well as the previously described antiviral mechanisms that diminish virion infectivity and target cell infection. The

functional relevance of our observation would be enhanced if decreased virion production synergized with increased virion packaging of A3G. This investigation is underway and requires a different experimental approach than used here. In addition, the present work suggests that further characterization of the interactions of RNA granules and endosomes with A3G and Gag will illuminate both cellular and HIV-1 biology, particularly mechanisms of post-transcriptional control of HIV-1 expression that are not yet fully characterized.

CHAPTER III

Restriction of the Late Steps of HIV-1 Replication by A3G Complexes and mRNA Processing Bodies in Producer Cells

Introduction

In HIV-1 Vif-deficient strains, A3G (A3G) is incorporated into progeny virions (35, 84, 177). This results in the production of HIV-1 virions with significantly reduced infectivity because reverse transcription and integration are restricted in the target cell (61). HIV-1 Vif normally acts to target A3G for proteasomal degradation, thereby dramatically reducing cellular levels of A3G available for viral packaging (167, 175). A3G is found in two major forms in cells: the low molecular mass (LMM) form and high molecular mass (HMM) complexes (57, 79, 137). The LMM form is diffuse throughout the cytoplasm as seen by confocal microscopy and is the form packaged into virions. HMM complexes are observed as large cytoplasmic bodies called A3G complexes here.

A3G complexes contain many cellular proteins and RNAs; including motor proteins, ribosomal subunits, helicases, translation factors, and scaffold proteins (32, 159). These protein components resemble the constituents of cellular structures known as RNA granules (7, 73, 147, 164). Indeed, confocal microscopy confirms the colocalization of many protein markers RNA granules with A3G complexes (164). Others have used A3G as a marker for mRNA processing bodies (P-bodies) (102). P-bodies are cytoplasmic structures in

which RNA silencing occurs via microRNAs (miRNA) and other components of the RNA-induced silencing complexes (RISC). However, characterization of the proteins essential for structure and functions of RNA granules, including P-bodies, is ongoing.

Components of miRISC are proteins of the Argonaut family (Ago1 to Ago4) that are required for miRNA-mediated silencing. A key factor in this process is the GW182 protein that interacts directly with Ago proteins to orchestrate mRNA decapping. It also is thought to recruit RCK/p54 (DDX6) that regulates the activity of the 5' decapping enzymes DCP1/DCP2, and 3' mRNA deadenylation. mRNA decapping and deadenylation leads to mRNA decay through the action of XRN1, a 5'-3' exonuclease. RNAi effectors, including miRNAs and their target mRNAs, Ago proteins, GW182, RCK/p54, LSm-1 and DCP proteins co-localize in cytoplasmic structures called GW-bodies or P-bodies GW-bodies were recently proposed to be GW182-rich RNA granules associated with endosomes, and to be distinct from P-bodies with which they were previously grouped. P-bodies are now proposed to be a distinct GW182-poor pool of RNA granules It is unclear whether A3G complexes are distinct structures from RNA granules (136). In the cell, A3G complexes have been shown to restrict the retrotransposition of Alu (32, 63). Yet, they are required for the assembly of certain retroelements such as TY1 and TY3 (27, 45). Recent characterization of poliovirus disruption of P-bodies added to understanding of the scaffolding/formation of these structures, and also raised questions about whether GW182 was essential for P-body formation (43). Thus, I sought to

further investigate whether GW182 and RCK/p54 were each required for A3G complexes to form and function.

Until now, the role of these complexes in the HIV-1 viral lifecycle was not known. Recent reports suggest that P-bodies are necessary for formation of infectious HIV particles, based on the reduced virus production and infectivity seen with perturbation of a P-body component protein, Mov10.

There is even more evidence that RNA granules inhibit HIV-1 replication in the producer cell by affecting translation of HIV-1 RNA. HIV-1 has also been shown to actively suppress expression of a specific cellular miRNA cluster, thereby enhancing virus replication. Other specific cellular miRNAs were also shown to prevent HIV-1 mRNA translation by targeting the 3'UTR of HIV-1 RNA to transport the miRNA-bound viral RNA into RNA granules containing the RNA-induced silencing complex (RISC). Disruption of RNA granules or RISC by siRNA-mediated knockdown (of Drosha, Dicer, DGCR8, RCK/p54, GW182, LSm-1, or XRN1) relieved the restriction and enhanced HIV-1 p24 antigen levels in supernatants of cultures of infected cells that lack A3G. Knockdown of RCK/p54 shifted HIV-1 mRNA from the non-polysomal fraction to polysomes as compared to control siRNA transfected, A3G-negative cells. Other data indicate that miRNAs may also cause transcriptional gene silencing through epigenetic effects. In these earlier reports, the roles of RNA granules and miRNAs in HIV-1 replication have largely been studied without analysis of a contribution of A3G, although one did note that A3G decreased HIV-1 p24 in culture supernatant fluids both with, and without, knockdown of P-body proteins.

I also recently identified that these A3G complexes were involved in a novel anti-HIV-1 restriction. Cells containing A3G complexes produced significantly fewer virions than cells containing an A3G mutant (C97A A3G) that failed to form A3G complexes. Differences in Vif-negative versus Vif-positive HIV-1 production were only seen in the presence of A3G, indicating that A3 proteins degraded by Vif caused this inhibition. In the experiments described here, I aimed to verify, or refute, that A3G complexes, and not LMM A3G, were required for the decreased HIV-1 production I characterized as due to A3G. Also, NL4.3 Δvif replication was reduced in HeLa-A3G cells when compared to replication in HeLa cells, which contain no A3G. Recently, it was shown that P-bodies can prevent HIV-1 mRNA translation via a microRNA, miR-29A, which targets the 3'UTR of HIV-1 (2, 102). miRNA 29A transports viral RNA into P-bodies and decreases HIV-1 translation. Disruption of P-bodies by siRNA-mediated knockdown of RCK/p54 not only abrogated P-body formation but relieved the restriction by the miRNA and enhanced HIV-1 translation (102). RCK/p54 and GW182 were each knocked down to assess effects on A3G complexes because of their reported differential distribution in RNA granule sub-types.

Knockdown of RCK/p54 successfully abrogated formation of RNA granules in cells containing and lacking A3G. When cells containing A3G were infected after RCK/p54 knockdown, percent Vif-negative HIV-1 p24 antigen production was significantly increased compared to infected A3G complex-containing cells treated with the control shRNA vector. In contrast, GW182

knockdown abrogated RNA granules in cells lacking A3G, but did not affect formation of A3G complexes. The inhibition of Vif-negative HIV-1 production was not altered by GW182 knockdown, relative to control shRNA treatment. This adds to evidence that A3 proteins in complexes, and not just diffusely localized A3 proteins, are required for the inhibition in producer cells. Differences in the effects of GW182 versus RCK/p54 knockdown on HIV-1 production levels support the hypothesis that the mechanism of anti-HIV activity of A3G-containing RNA granules differs from that of RNA granules lacking A3G.

Materials and Methods

Cell culture, viral stocks, and infections

HeLa and HeLa-A3G cells were maintained in DMEM supplemented with 10% fetal bovine serum (FBS, HyClone), penicillin (50 IU/ml), and streptomycin (50 µg/ml). HIV-1 p24 antigen ELISA was carried out as previously described (156, 161). Virus-containing supernatant fluids were collected and filtered through a 0.45 µm syringe filter. The percentage p24 production was calculated as culture supernatant ultracentrifugation pellet p24 antigen concentration divided by the total p24 antigen concentration (cell + culture supernatant ultracentrifuge pellet concentration). Cellular and viral lysates were prepared using ice cold lysis buffer [50mM HEPES, pH 7.4, 125mM NaCl, 0.2% NP-40 and 0.1mM PMSF and EDTA-free protease inhibitor cocktail (CalBiochem, San Diego, CA #539137)].

RCK/p54 and GW182 shRNA-mediated knockdown

Knockdown of RCK/p54 and GW182 was performed using 100 nM of an shRNA-expressing construct, as described by others (85) (Dharmacon). HeLa or HeLa-A3G cells were seeded in a 6-well plate and grown overnight to 60% confluency. One day after plating, cells were transfected by Lipofectamine 2000 (Invitrogen) with non-specific scrambled, GW182, or RCK/p54-specific shRNA. On day two, cells were trypsinized, spun down and washed in PBS 5 times, and then replated. Four hours after trypsinization, cells were transfected a second time with either scrambled, GW182, or RCK/p54-specific siRNA. In experiments using HeLa cells, cells were co-transfected with A3G-HA during the second transfection. Cells were imaged by confocal microscopy performed after staining with anti-A3G antibody (polyclonal A3G antibody, NIH AIDS repository #9968) 24 hours after the second transfection. HeLa-A3G cells were used for HIV-1 infection experiments and an expression plasmid, CMX-44X (CD4), that expresses a tail-less CD4 that allows for high expression levels, was co-transfected with the shRNA vector during the first transfection (93, 181). CD4 protein levels were immunoblotting using rabbit anti-CD4 antibody (Sigma-Aldrich). Infection with HIV-1 virus stocks (either NL4.3 Δ*vif* or wild-type NL4.3) occurred on day 2 after trypsinization. Four hours after infection cells were washed 3 times to completely remove inocula, and virus production was assessed 24 hours after infection.

Immunofluoresence and Confocal Microscopy

Cells for imaging were grown in 6 well plates on 22mm cover slips, and then fixed with 3.7% formaldehyde for 5 minutes at room temperature. Cells were permeabilized with 0.1% Triton X-100 for 5 minutes. Permeabilized cells were blocked in 5% BSA for 1 hour at room temperature. Nuclei were stained with 1:1000 dilution of To-Pro 3 in PBS for 20 mins. Primary antibodies were diluted in antibody dilution buffer (1% BSA, 0.05% NP-40, and 2% goat serum in PBS at a concentration of 1:500) (and incubated on cells for 1 hour. Following 1 hour incubation cells were washed 3 times with wash buffer (1% BSA and 0.05% NP-40) for 5 minutes. Secondary antibodies anti-mouse Alexa Fluor 546, anti-goat Alexa Fluor 568, and anti-rabbit Alexa Fluor 488 Invitrogen (Eugene, Oregon) were diluted in antibody dilution buffer at a concentration of 1:1000. Primary antibodies directed against PABP (sc-18611), GW182 (sc-47036), Dcp1 (sc-100706), RCK/p54 (sc-51415), TIA-1 (sc-28237) and HA; all were obtained from Santa Cruz (Santa Cruz, CA). Images were acquired using a Carl Zeiss LSM 510 Meta confocal microscope. All images shown are the middle section of a z-series, to better show colocalization and decrease background.

Transfections for imaging were performed by transient transfection using polyethylenimine (PEI) (118). Complete growth media was replaced 30 minutes prior to transfection. The transfection reaction included 2ug of DNA and 10 µg of PEI diluted in 250 µl of serum-free media.

Biochemical fractionation of A3G

A previously validated ultracentifugation method was used to characterize the form of A3G in cell cytoplasm. HeLa-A3G-CD4 cells were infected. Confluent 100 mm plates of cells were rinsed with cold PBS, lysed with 500 µL cold lysis buffer, and vortexed for 10 minutes. Cell lysates were clarified at 17,900 x *g* for 10 minutes to remove nuclei. The supernatant was removed and the pellet was resuspended in lysis buffer at a volume equal to that of the supernatant fluid. Equal volumes of resuspended pellet and supernatant were then analyzed by western blot. Proteins were resolved by 10% SDS-PAGE. Proteins were transferred to a nitrocellulose membrane and blocked overnight in 5% milk. The membrane was probed with a polyclonal anti-A3G antibody (NIH AIDS repository #9968) and washed with PBST (0.05% Tween 20).

Results

A3G complexes co-localize with RNA granule markers

I studied if proteins associated with different RNA granule sub-types co-localized with A3G complexes. HeLa cells were transfected with A3G-HA. 24 hours post-transfection cells were fixed and stained for immunofluoresence using anti-p54, anti-GW182, or anti-Dcp1 antibodies and anti-HA to visualize A3G-HA. Fig. 3-1 shows colocalization of A3G-HA with p54 (top row), GW182 (middle row), and Dcp1 (bottom row). I found a high degree of co-localization with each marker. The number and shape of the bodies differed from cell to cell,

reminiscent of P-bodies. Panel B shows HeLa cells that stably express A3G. The staining pattern of this endogenous A3G is similar to that found in cells transfected with exogenous A3G-HA.

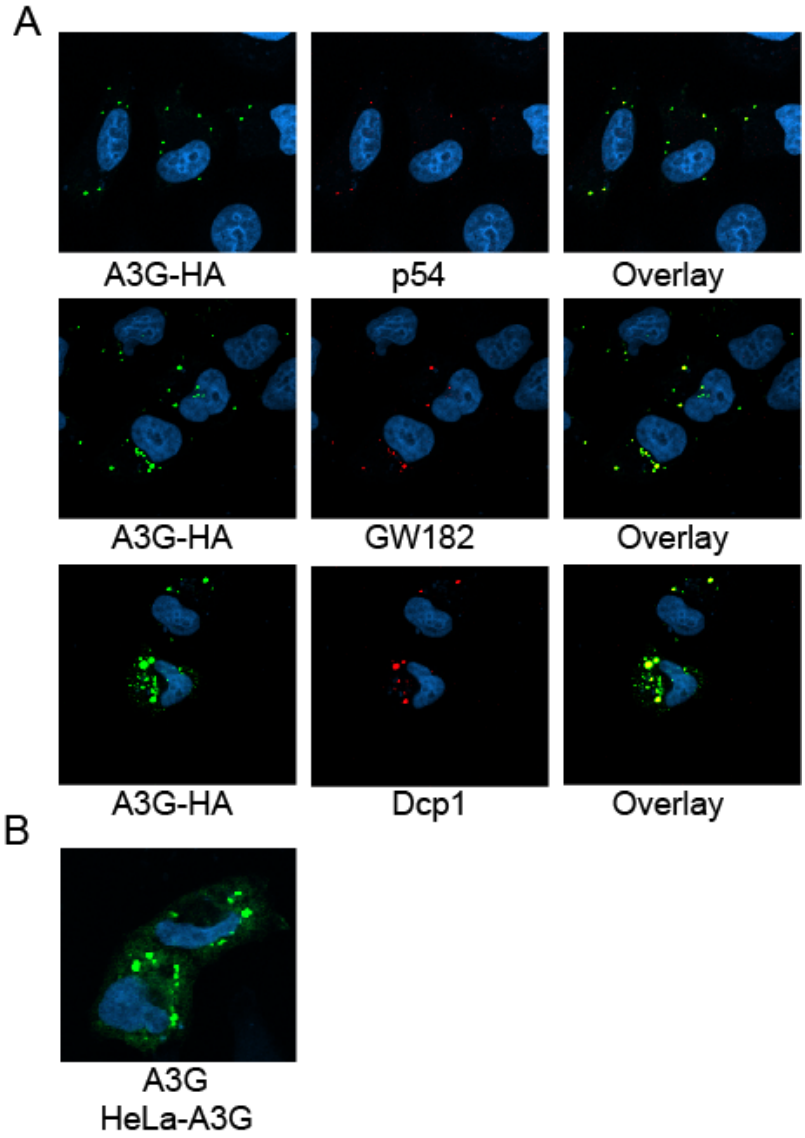

Figure 3-1. A3G complexes co-localize with RNA granule markers. **A.** Shown are confocal micrographs of HeLa cells transfected with A3G-HA. Cells have been stained with specific antibodies (see text) to visualize endogenous P-body marker proteins (125) and A3G (green), as well as incubated with To-Pro 3 to visualize the nucleus (blue). Areas of co-localization are seen as yellow in the last column (overlay). **B.** Shown is a confocal micrograph of a HeLa-CD4-A3G cell. Cells were stained with A3G-specific antibody to visualize endogenous A3G (green) and To-Pro 3 to visualize the nucleus (blue).

shRNA knockdown of RCK/p54 abrogates Dcp1 and A3G co-localization

Structural components of RNA granules have been shown to be critical to their stability. Knockdown of different protein components often abrogates granule formation. I used shRNA's directed against RCK/p54 to determine the effect on Dcp1 and RCK/p54 localization with and without A3G expression. Fig. 3-2A shows HeLa cells stained for the indicated markers. Cells in the bottom panel of Fig. 3-2A were co-transfected by PEI with an A3G-HA plasmid; cells in upper and middle panels are untransfected and stained for endogenous proteins. In the left column are cells transfected with scrambled control shRNA and the right column shows cells transfected with the p54-specific shRNA construct. The first row is stained for RCK/p54 and shows cells with and without p54 knockdown. No p54 is observed after knockdown. In the middle panel, Dcp1 is also shown before and after knockdown and the localization changes significantly, from localization to granules to being exclusively diffuse. The same is seen for A3G. Without p54 knockdown A3G is localized mainly to complexes. However, is observed exclusively as diffuse in the cytoplasm after p54 knockdown. These results suggest that RCK/p54 is a major structural component of granules containing both Dcp1 and A3G.

Fig. 3-2B shows western blots of cells HeLa after p54 knockdown. The top gel shows p54 after treatment with scrambled control versus p54-specific shRNA. The amount of p54 is significantly decreased by shRNA. The amount of β-actin in the lower panel is similar before and after knockdown. Fig. 3-2C is ultracentrifugation of cell lysates either transfected with scrambled control (left 2

lanes) or p54-specific shRNA (right 2 lanes). A3G is found in all lanes except the pellet fraction of the p54-specific shRNA-treated cell lysate, consistent with my confocal data. Fig. 3-2C shows cell lysates from cells used in Fig. 3A, bottom row. These HeLa cells were transfected with A3G-HA and either scrambled shRNA in lanes 1 and 2, or p54-specific shRNA in lanes 3 and 4. Lysates were then subjected to ultracentrifugation to separate the pellet and supernatant fractions. The immunoblot shows A3G in each fraction and the absence of A3G in the pellet fraction when cells were transfected with the p54-specific shRNA, lane 4.

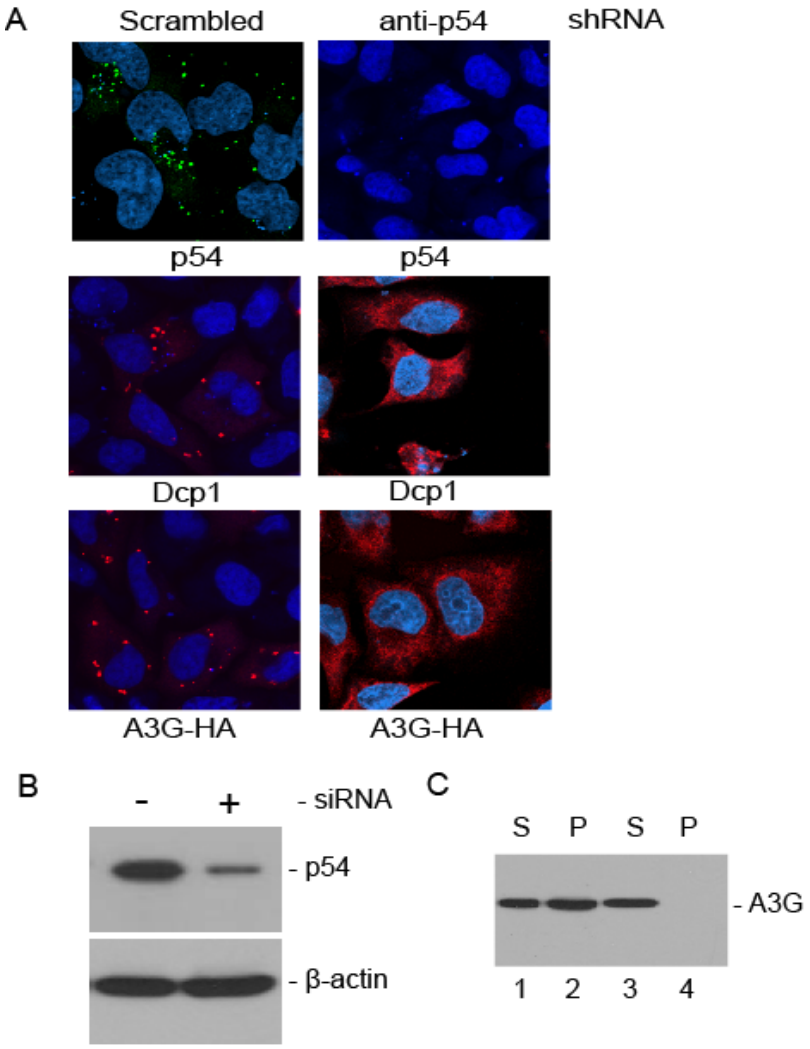

Figure 3-2. shRNA knockdown of RCK/p54 abrogates Dcp1 and A3G co-localization. **A.** HeLa cells were transfected with either scrambled (left column) or p54-specific (right column) shRNAs on days 1 and 2 after cells were plated. Nuclei were stained using To-Pro 3 (blue) in each panel. **B.** Cells used in A, upper panel, were lysed on day 1 after second shRNA transfection and subjected to western blot analysis to show degree of p54 knockdown. Cells transfected with scrambled shRNA are in the first lane and cells transfected with p54-specific shRNA in the second. β-actin staining is depicted in the lower panel as a loading control. **C.** Lysates from cells used in A, lower panel were subjected to ultracentrifugation to separate A3G complexes (pellet, P) from A3G not in complexes (supernatant, S) fractions. Fractions were immunoblotted with an anti-HA antibody. Ultracentrifuge fractions from cells co-transfected on day 2 with scrambled shRNA and A3G-HA are in lanes 1 and 2 and those from cells co-transfected on day 2 with p54-specific shRNA and A3G-HA are in lanes 3 and 4.

shRNA knockdown of GW182 abrogates Dcp1 but not A3G granule localization

I next determined the effects of GW182 knockdown on Dcp1 granule localization and A3G complex formation. Fig. 3-3A shows confocal images of HeLa cells that have been either transfected with a scrambled control shRNA (left column) or GW182-specific shRNA construct (right column). GW182 is localized to granules in the control, but granules are not detectable following knockdown. Dcp1 showed granule localization before knockdown, but following knockdown was only seen diffusely in the cytoplasm. A3G-HA was shown to localize to complexes before and after GW182 knockdown. This indicates that GW182 is not an essential component of all A3G-HA containing granules or that it is a component of only a small proportion of A3G complexes. This is consistent with the literature that RNA granules are dynamic structures and their protein components differ depending on function.

Western blots of HeLa cells with and without GW182 knockdown are shown in Fig. 3-3B. Fig. 3C shows HeLa cell lysates stained for A3G after ultracentrifugation from either cells transfected with scrambled (lanes 1 & 2) or GW182-specific shRNA (lanes 3 & 4). A3G is found in both the pellet and the supernatant with and without GW182 knockdown, indicating that GW182 has little to no effect on A3G complex localization.

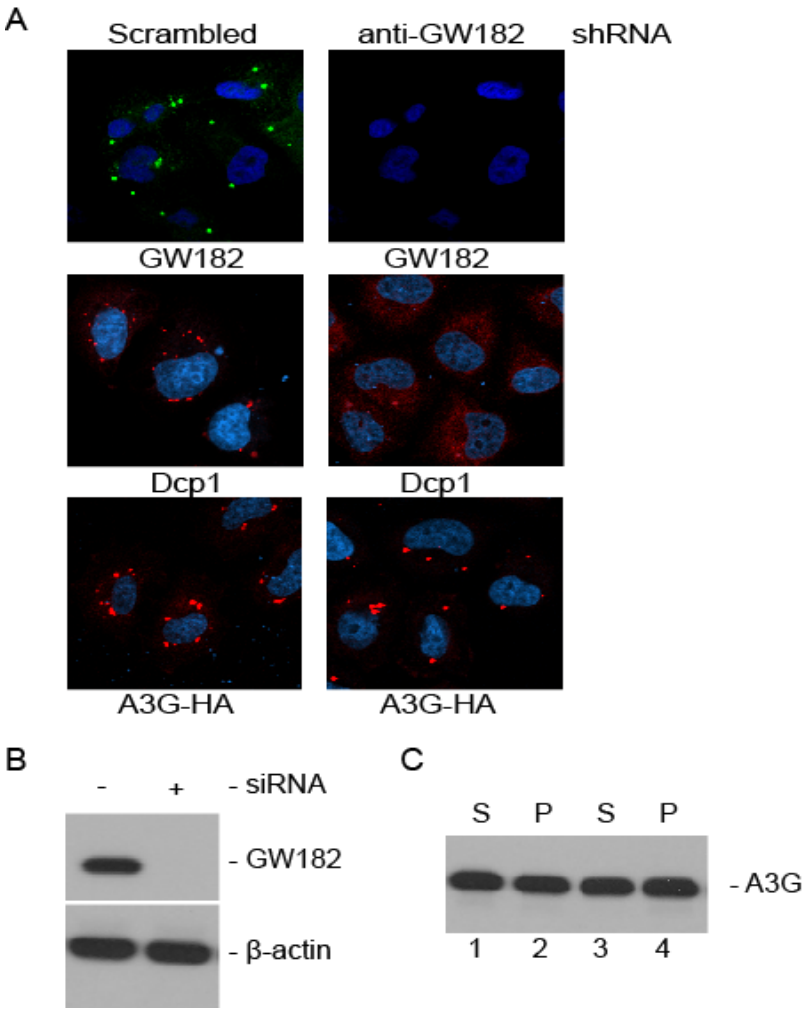

Figure 3-3. shRNA knockdown of GW182 abrogates Dcp1 but not A3G granule localization. **A.** HeLa cells were transfected with either scrambled (left column) or GW182-specific (right column) shRNAs on days 1 and 2 after plating. **B.** Cells used in A, upper panel, were lysed on day 1 after second shRNA transfection and subjected to western blot analysis to show degree of GW182 knockdown. Cells transfected with scrambled shRNA are in the first lane and cells transfected with GW182-specific shRNA in the second. β-actin staining is depicted in the lower panel as a loading control. **C.** Lysates from cells used in A, lower panel were subjected to ultracentrifugation to separate A3G complexes (pellet, P) from A3G not in complexes (supernatant, S) fractions. Fractions were immunoblotted with an anti-HA antibody. Ultracentrifuge fractions from cells co-transfected on day 2 with scrambled shRNA and A3G-HA are in lanes 1 and 2 and those from cells co-transfected on day 2 with GW182-specific shRNA and A3G-HA are in lanes 3 and 4.

A3G expression allows Dcp1 to retain its localization to granules in GW182 knockdown cells

Previously, I demonstrated that Dcp1 becomes diffuse and loses its localization in complexes following GW182 knockdown in the absence of A3G. However, transfected A3G remains localized to complexes following GW182 knockdown. Since A3G and Dcp1 co-localize under normal cellular conditions, I tested if Dcp1 would remain colocalized with A3G complexes after GW182 knockdown in cells containing A3G. HeLa cells were cotransfected with an A3G-HA expression plasmid and a GW182-specific shRNA construct. Cells were then stained to visualize A3G-HA, GW182, Dcp1, or RCK/p54. Confocal micrographs in Fig. 3-4 show that when A3G was co-expressed in GW182 deficient cells, Dcp1 could be found localized with A3G complexes. Therefore, A3G expression allows Dcp1 to retain its localization to A3G complexes, even in the absence of GW182.

Panel A shows that GW182 was effectively knocked down in these cells, but A3G complexes were found. Panel B shows that HeLa cells with GW182 knocked down and A3G expression retain co-localization of Dcp-1 to A3G complexes, in contrast to the diffuse localization of Dcp-1 seen with GW182 knockdown when A3G-HA is not expressed (Fig. 3-3A). Panel C shows that A3G-HA and p54 also colocalize in cells with GW182 knocked down.

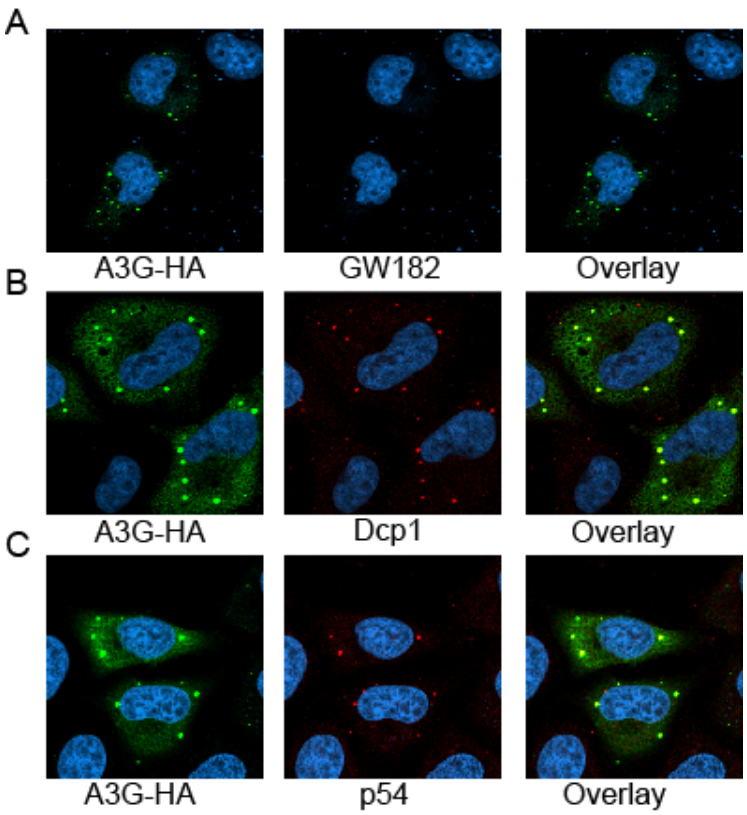

Figure 3-4. A3G expression allows Dcp1 to retain its localization to granules in GW182 knockdown cells. P-body markers were imaged after co-transfection of A3G-HA and GW182-specific shRNA. **A.** shows antibody staining for endogenous GW182 on day 1 after two GW182-specific shRNA transfections with co-transfection of A3G-HA along with the second GW182-specific shRNA transfection. **B.** shows antibody staining for endogenous Dcp1 on day 1 after two GW182-specific shRNA transfections with co-transfection of A3G-HA along with the second GW182-specific shRNA transfection. **C.** shows antibody staining for endogenous p54 on day 1 after two GW182-specific shRNA transfections with co-transfection of A3G-HA along with the second GW182-specific shRNA transfection.

Effect of RCK/p54 knockdown on HIV-1 replication

I next tested whether loss of A3G complex formation by knockdown of RCK/p54 would reverse the decreased HIV-1 production associated with A3G complexes. I infected Hela-A3G cells (HeLa cells that constitutively express A3G) with HIV-1 NL4.3 Δ*vif* after transfection with CD4 and either scrambled or RCK/p54-specific shRNAs. HeLa-A3G cells infected with NL4.3 Δ*vif* after RCK/p54 knockdown produced about 50% more virus than was produced from control scrambled shRNA-treated HeLa-A3G cells infected with NL4.3 Δ*vif* (Fig. 3-5A, two bars on the left; Mann-Whitney U, P = 0.0004. There was no difference in Vif-positive, HIV-1 NL4.3 virus production from HeLa-A3G cells transfected with the control versus RCK/p54-specific shRNAs (Fig. 3-5A, two bars on the right). The non-nucleoside reverse transcriptase inhibitor efavirenz (EFV) was used in all infections to limit infection to a single round.

Immunoblots of cell lysates showed that the HeLa-A3G cells infected with NL4.3 Δ*vif* and either transfected with scrambled (lane 1) or RCK/p54-specific (lane 2) shRNAs both contained A3G (Fig. 3-5A, upper panel below graph, lanes 1 and 2). However, A3G was not detected in Vif-positive, HIV-1 NL4.3 virus-infected cells transfected with either shRNA (Fig. 3-5A, upper panel below graph, lanes 3 and 4). RCK/p54 was decreased by the RCK/p54-specific, and not the scrambled, shRNA in cells infected with either virus (Fig. 3-5A, second panel below graph). Gag immunoreactivity was equivalent in each infection (Fig. 3-5A, third panel below graph). Anti-CD4 staining showed equivalent HIV-1 receptor protein levels in cells (Fig. 3-5A, fourth panel below graph). Anti-β-actin staining

indicated equivalent amounts of protein loading (Fig. 3-5A, bottom panel below graph). HIV-1 NL4.3 Δ*vif*-infected HeLa-A3G cells contained A3G in both pellet and supernatant ultracentrifuge fractions; the pellet fraction indicates the presence of A3G complexes (Fig. 3-5C, Lane 1, supernatant, and 2, pellet). No endogenous A3G was detected in either the ultracentrifuge pellet or supernatant fractions of HeLa-A3G cells infected by Vif-positive, wild type NL4.3 (Fig. 3-5C, lane 3, supernatant, and 4, pellet). In addition, transfection of RCK/p54-specific shRNA, and not scrambled shRNA, again led to diffuse staining of endogenous A3G throughout the cytoplasm in Hela-A3G cells and no evidence of A3G complexes on confocal microscopy (Fig. 3-5D).

Others have reported that A3G decreased absolute supernatant p24 levels whether RCK/p54 or Lsm-1 were knocked down or not. Similar results, and the finding that RCK/p54 knockdown increased supernatant p24 levels in the presence and absence of A3G, are noted here (Fig. 3-5B).

HeLa cells that contain no endogenous A3G were also transfected with CD4 and either of the two shRNAs prior to infection with NL4.3 or NL4.3 Δ*vif* to serve as an additional control. Production of Vif-positive and Vif-negative HIV-1 did not differ with RCK/p54 knockdown that causes loss of P-bodies in these cells that lack A3G expression (data not shown). This corroborates the Vif-positive HIV-1 infection of HeLa-A3G cells (Fig. 3-5A, right panel) as evidence that reversal of the decrease in HIV-1 NL4.3 Δ*vif* production by RCK/p54 knockdown was specific for the loss of A3G complexes.

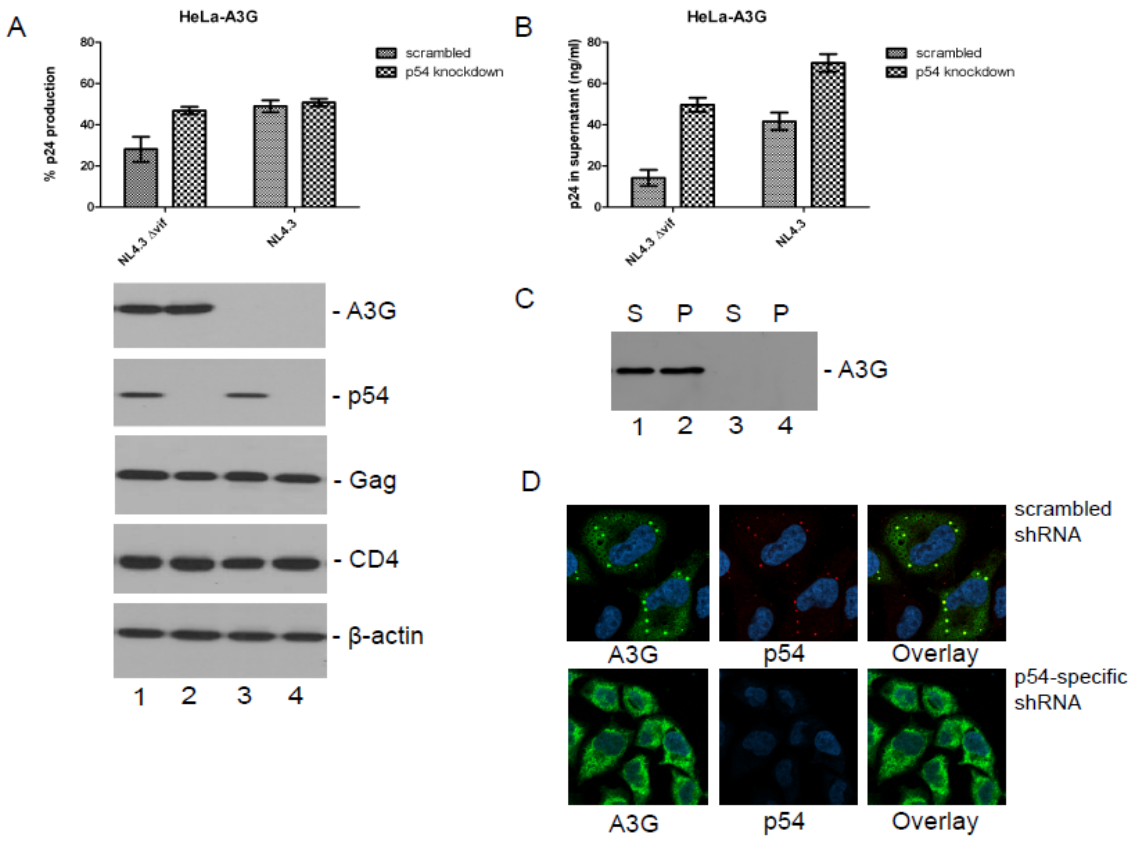

Figure 3-5. Effect of RCK/p54 knockdown on HIV-1 replication. **A.** HeLa-A3G cells were transfected with CD4 and either scrambled or p54-specific shRNA's. These transfected cells were then infected with wild-type NL4.3 or NL4.3 Δ*vif.* There was a significant difference in virus production between NL4.3 Δ*vif* infected cells transfected with scrambled and p54-specific shRNAs (Mann-Whitney, $p < 0.0004$). There was no significant difference among cells infected with wild-type NL4.3 that had different shRNAs. In the lower panel, cell lysates were analyzed by western blot. **B**. Supernatant p24 levels from the experiment in A. **C.** Cell lysates from CD4-expressing HeLa-A3G cells infected with either NL4.3 Δ*vif* or wild type NL4.3 were subjected to ultracentrifugation to separate the fraction containing A3G complexes (pellet, P) from the fraction containing non-complexed A3G (supernatant, S). Lanes 1 and 2 are cells infected with NL4.3 Δ*vif* and Lanes 3 and 4 are cells infected with wild type NL4.3 that contains an intact *vif* gene that is capable of degrading A3G. A3G was completely depleted from cells by Vif. A3G complexes were present in pellet in NL4.3 Δ*vif* infected cells. **D.** are images of HeLa-A3G cells transfected with either scrambled shRNA control (top row) or p54-specific shRNA (bottom row). Cells were fixed and stained for endogenous A3G and RCK/p54.

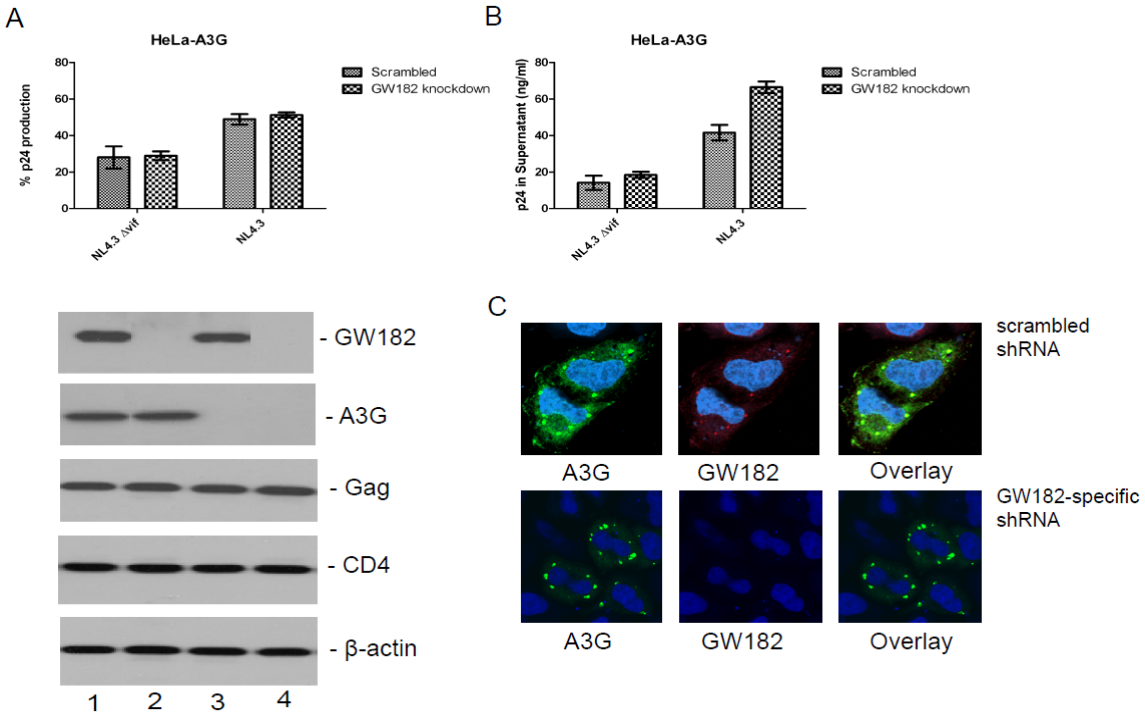

Figure 3-6. Effect of GW182 knockdown on HIV-1 replication. **A.** HeLa-A3G cells were transfected with CD4 and either scrambled or GW182-specific shRNA's. These transfected cells were then infected with wild-type NL4.3 HIV that degrades A3G or NL4.3 Δ*vif.* There were no significant differences in virus production. In the lower panel, cell lysates were analyzed by western blot. **B**. supernant p24 levels from the experiment in A. **C.** shows images of HeLa-A3G cells transfected with either scrambled shRNA control (top row) or GW182-specific shRNA (bottom row). Cells were fixed and stained for endogenous A3G and GW182.

Effect of GW182 knockdown on HIV-1 replication

I next tested whether knockdown of GW182 had an effect on HIV-1 production in the presence and the absence of A3G. Hela-A3G cells (that stably express A3G) were infected with either NL4.3 or NL4.3 Δ*vif* following transfections with the CD4 receptor for HIV and either scrambled, or GW182-specific, shRNAs (Fig. 3-6A). Transfection with GW182-specific shRNA had no effect on virus production when A3G was either present or depleted by Vif, although A3G depletion by Vif did increase virus production (Fig. 3-6A).

These results are consistent with p54 knockdown, and not GW182 knockdown, abrogating both A3G complexes and their functional effect to decrease HIV-1 production. HeLa-CD4 cells that contain no endogenous A3G served as a control (data not shown). Beneath graphs in panel A are western blots are of cell lysates from experiment in the graph above it. Westerns of GW182, Gag, CD4, and actin are shown. Equivalent levels of Gag, CD4, and actin show cells were equally infected and control for protein loading on the gel. The first two lanes are cells infected with NL4.3 Δ*vif* and either transfected with scrambled or GW182-specific shRNAs. A3G is present in equal amounts in all cases. However, in lanes 3-4 A3G is degraded by Vif in cells infected with wild type NL4.3. Transfection with shRNAs does not inhibit A3G degradation by Vif. In Fig. 3-6B, supernatant p24 levels are shown. There was no significant difference in p24 levels when HeLa-A3G cells were infected with NL4.3 Δ*vif.* There is a significant difference in supernatant p24 levels when cells were infected with wild-type virus. Fig. 3-6C, shows HeLa-A3G cells stained for A3G

and GW182. In the top row are cells transfected with control scrambled shRNA. The bottom row are cells transfected with GW182-specific shRNA.

RCK/p54 and GW182 knockdowns varying effects on HIV-1 release

Other results supported the conclusion that knockdown of RNA granules containing A3G had different effects on HIV replication than did knockdown of granules not containing A3G. This is in addition to the results in Fig. 3-5 that A3G decreased absolute supernatant p24 levels whether RCK/p54 was knocked down or not and that RCK/p54 knockdown increased supernatant p24 levels in the presence and absence of A3G. The complete data from controls, as well as RCK/p54 and GW182 knockdowns are depicted in Table 3-1. Kruskal-Wallis analysis was significant for differences, and individual comparisons of mean p24 values from each knockdown to controls were therefore tested by Mann-Whitney U tests. Because there were 32 different comparisons, a Bonferroni correction for the level of significance was applied (0.05/32=0.015). Asterisks in the table indicate a significance level <0.015.

shRNA	Control	RCK/p54	GW182	Control	RCK/p54	GW182
Cell type	HeLa-A3G					
	NL4.3 Δvif			NL4.3		
Average p24 Cell (ng/ml)	36	57*	46	44	68*	63*
Average p24 Sup (ng/ml)	14	50*	18	42	70*	67*
Average Total p24	50	107*	64	86	138*	130*
Percent p24 Production	28	47*	29	49	51	51
Cell type	HeLa					
	NL4.3 Δvif			NL4.3		
Average p24 Cell (ng/ml)	42	59*	57*	44	63*	53*
Average p24 Sup (ng/ml)	32	46*	42*	39	52*	45*
Average Total p24	74	105*	99*	83	115*	98*
Percent p24 Production	43	44	42	47	45	46

Table 3-1. RCK/p54 and GW182 knockdowns varying effects on HIV-1 release. The table shows HIV p24 antigen levels from the experiments in Fig. 3-5 and 3-6. The table details levels in the cell lysate, the ultracentrifuged supernatant, the total (sum of cell and supernatant), and the percent p24 production (supernatant / cell + supernatant). Percent p24 production does not change with Rck/p54 or GW182 knockdown in HeLa-A3G cells infected with Vif-positive virus (which degrades A3G) or in HeLa cells (lacking A3G) infected with either vif-negative or –positive virus. Asterisks indicate a significant difference, $p < 0.015$, when compared to the matched control.

Discussion

Another group showed that knockdown of RCK/p54, Lsm1, or Ago2 in 293T cells (not containing A3G) disrupted P-body formation and that subsequent transfection of an A3G expression vector led to A3G being seen only diffusely throughout the cytoplasm without localization to RNA granules (26). I sought out to understand the nature of the relationship between A3G and RNA granules. Like others I see that A3G complexes colocalize with various markers for RNA granules (Fig 3-1). Work is increasingly showing that RNA granules are highly dynamic structures (8, 73, 81, 147, 160, 176). The complexity of their arrangement is immense. These structures assemble the necessary proteins to mediate a certain function and can readily disassemble after that function is completed. The dynamic nature of A3G complexes has yet to be studied in depth, but will likely line up with the new knowledge of RNA granules, that they are highly dynamic structures whose protein and RNA components can change rapidly depending on the state of the cell (176).

I chose two known P-body components RCK/p54 and GW182 to study the interaction of A3G complexes and RNA granules (47, 48, 72, 85, 131, 148, 171, 172). The knockdown of GW182 has been shown in several species to lead to abrogation of granules rich in GW182 (88, 120). In cells in which I knocked down RCK/p54, Dcp1 and A3G granule localization was abrogated. This is in line with work by Rana and colleagues that found RCK/p54 knockdown caused A3G to lose its localization to complexes (102). My data demonstrated that RCK/p54 was likely enriched in granules containing dcp1 and A3G. This may give clues

as to the cellular function of A3G granules, as RCK/p54 is a DEAD box protein and as such acts as an RNA helicase (4, 95, 100). Indeed, A3G complexes have been shown to sequester the RNA of Alu retrotransposons and RCK/p54 could function to initiate steps of RNA degradation (32, 63).

I next knocked down GW182 and found that like with p54 knockdown Dcp1 granule localization was abrogated. However, A3G complexes were still observed (Fig 3-3A). These results lead us to hypothesis that A3G complexes were low in GW182, while Dcp1 localizes to various granules some that are GW182 high and some GW182 low. Recent discoveries have shown that indeed some RNA granules are rich in GW182 whereas others seem to be completely devoid of GW182 (23, 55, 153). Clear evidence that "P-bodies" are not a single entity, but that groups of proteins come together in an orchestrated manner to perform a function, mostly related to mRNA metabolism. GW182 and RCK/p54 are critical for miRNA-mediated silencing of mRNA (34, 39, 46, 144). These results could indicate that these granules colocalize with A3G complexes, but may be separate entities and that A3G may play little to no role in miRNA function.

Given my results on the difference in the response of Dcp1 and A3G to GW182 knockdown, I looked to determine if A3G expression during GW182 knockdown would allow a portion of Dcp1 to remain in granules. HeLa cells were co-transfected with A3G-HA and GW182-specific shRNAs and 24 hours post-transfection stained for endogenous Dcp1 or A3G-HA. Knockdown was confirmed by western blot. Fig. 3-4 shows that with A3G-HA expression Dcp1

still retains some granule localization at A3G complexes. This is unlike what I found in the absence of A3G in Fig. 3-3A. These results indicate that Dcp1 is likely a component of the A3G complex. Dcp1 role as a decapping enzyme suggests this process is important in the function of A3G complexes and may be a mechanism by which A3G complexes restrict Alu retrotransposition (21, 126, 169).

Finally, I sought to extend finding I recently discovered that show that A3G complexes can restrict HIV-1 Gag release from infected cells. Since p54 knockdown abrogated A3G granule localization, I wanted to determine if these cells were relieved of the A3G-mediated restriction on HIV-1 release. HeLa cells expressing both CD4 and A3G were infected with NL4.3 or NL4.3 Δvif. Cells were either transfected with a scrambled shRNA, p54-, or GW182-specific shRNA. Results show that at 24 hours post-transfection cells transfected with the p54-secific shRNA were relieved of the A3G restriction on HIV-1 release. While cells transfected with scrambled or GW182 shRNAs were not. I also determined if any of the knockdowns had an effect on HIV-1 release in the absence of A3G, using wild-type NL4.3, in which Vif was able to degrade endogenous A3G. Whether the A3G-deleted cells were transfected with scrambled, p54-, or GW182-specific shRNAs there were no difference on the amount of virus released. In all cases, these cells released amounts of virus similar to that released by cells with p54 knockdown and infected with Vif-deficient NL4.3, suggesting that the lack of A3G, allowed normal levels of HIV-1 release. RCK/p54 knockdown does result in increased total p24 levels. This

effect of RCK/p54 knockdown is separate from the A3G-mediated restriction on HIV-1 production.

An independent consequence of RCK/p54 and GW182 knockdown is increased cellular and supernatant levels of p24, Table 3-1. These increases are modest, but highly reproducible and are in line with published reports (26, 102). The mechanism that has been put forth by others is that micro RNAs normally target HIV-1 RNA for storage in P-bodies. Upon abrogation of P-bodies, HIV-1 RNA is released and translated at higher levels, resulting in increased virus production. I agree with these earlier findings and show that this effect of P-body knockdown is independent of the A3G-mediated restriction, due to the fact that in all cases P-body knockdown resulted in higher cellular and supernatant p24 levels, but percent p24 production was only decreased when A3G complexes were absent Fig. 3-5A.

RNA granules are highly dynamic structures and the study of their role in the HIV-1 lifecycle is of high importance (7, 147). I show here that A3G may form a granule or complex along with RCK/p54 or GW182 that has distinct functions from a p54 or GW182-containing granule lacking A3G. A3G complex formation is dependent on the presence of RCK/p54. The fact that Dcp1 remains localized to granules in the absence of GW182 only when A3G is present indicates a separate structure. This A3G complex is likely formed of many RNA binding proteins and RNAs. It appears now that A3G complexes can restrict endogenous and exogenous retroviruses. A3G complexes seem to be multifunctional structures whose presence inhibits the replication of HIV-1.

CHAPTER IV

Conclusions and Future Directions

Conclusions

This work has focused on the High Molecular Mass complex (HMM) form of A3G, a cytidine deaminase found within cells. This large ribonucleoprotein complex, called the A3G complex here, was not known to play a role in any anti-viral response prior to this work. Previously, it had been shown that the A3G complex is enzymatically inactive for cytidine deaminase activity. The major cellular role for the A3G complex was shown to be in restricting exogenous retroviruses, namely retroelements. This work for the first time extends the role of the A3G complex to include an anti-HIV response.

I showed that A3G complexes are responsible for limiting the production of HIV in infected cells at a late step in replication. I demonstrated that HIV Gag, the major polyprotein that drives HIV assembly colocalizes with the A3G complex. Nearly, 30% of HIV Gag can be found at A3G complexes at a given time point. The restriction of A3G complexes on virus production can lead to up to a 70% reduction in virion production following a single-round of infection. This reduction was highly significant and highly reproducible. This work was aided by the observation that a mutant of A3G, C97A fails to form complexes by 24 hours. I hypothesize that producer cell A3G complexes trap HIV Gag, thereby making it unavailable for assembly at the plasma membrane. I found that HIV Gag in cells

containing A3G complexes had a shorter half-life than Gag in cells lacking A3G complexes. This suggested that A3G complexes lead to increased HIV Gag turnover.

I also showed that A3G complexes are not necessary for the packaging of A3G within virions. The other mechanism for A3G viral restriction is carried out in the target cell and thus it is essential for A3G to be packaged into progeny virions. Using the C97A mutant of A3G, I demonstrated that the LMM form of A3G is packaged at levels near that of WT A3G. This extended previous findings by others that newly synthesized A3G is packaged within the virus.

Finally, using RNAi I showed that RCK/p54 knockdown, but not GW182 knockdown abrogates A3G complexes. Both p54 and GW182 are markers for RNA granules; my results suggested that they represent two different cellular structures. A3G may form a unique RNA granule that is only present when A3G is expressed in cells. These A3G complexes contain both Dcp1 and p54. A3G complexes likely contain little to no GW182. These results indicate A3G complexes may form a unique RNA granule structure. In cells with A3G complexes, a portion of Gag gets trapped within A3G complexes. This leaves a smaller amount of Gag available for virus production. Gag trapped in A3G complexes is likely targeted for degradation via an unknown mechanism. I hypothesized that this mechanism for A3G complex effects on HIV-1 replication in the producer cell differs from effects of RNA granules lacking A3G on HIV-1 replication. In the latter case, the model predicts a different effect on HIV-1

replication, such as blocking translation of, or degrading, some Gag mRNAs A schematic of this model is presented in Fig. 4-1.

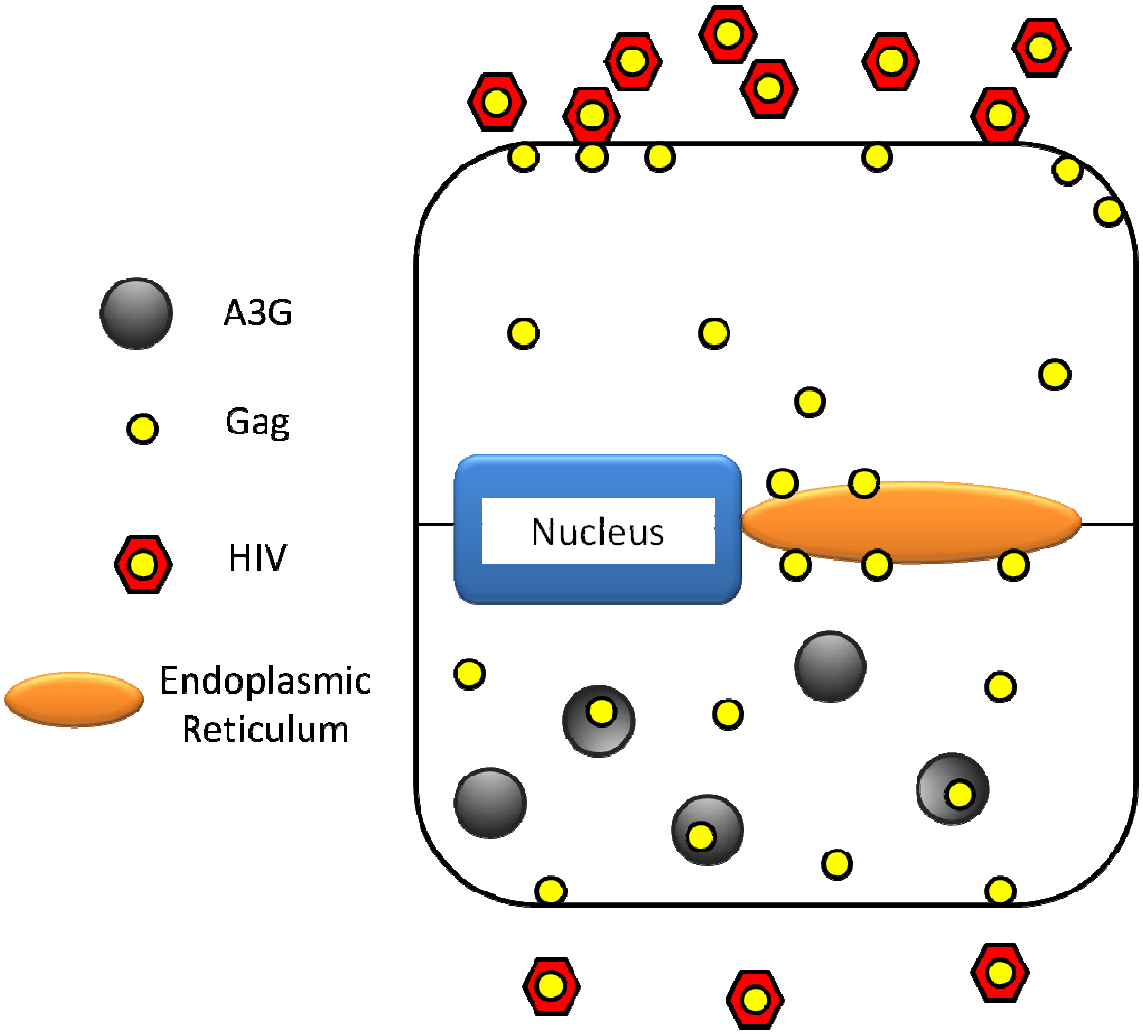

Figure 4-1. Predicted model of A3G-mediated restriction of HIV-1 production. The above schematic shows a typical cell with nucleus and endoplasmic reticulum in the middle. Above the center line is the typical late stages of HIV-1 assembly. Gag is made on ribosomes bound to the endoplasmic reticulum and then transits to the plasma membrane for budding and release. Where large numbers of viruses are produced in the absence of A3G complexes. Below the line is what I predict occurs in cells with A3G complexes. Gag is still made on bound ribosomes, however, a portion of Gag gets trapped within A3G complexes. This leaves a smaller amount of Gag available for virus production. Gag trapped in A3G complexes is likely targeted for degradation via an unknown mechanism that may involve late endosomes.

Significance

In summary, I have shown that APOBEC3G has the ability to limit the production of HIV-1 in producer cells at a late (post-integration) step of viral replication if A3G is not degraded by Vif, that this antiviral effect is due to cytoplasmic complexes of A3G, and that these complexes are not identical to P-bodies. A3G complexes may be as dynamic as other RNA granules now appear to be. The mechanism of their effect on late steps of HIV-1 replication is different and distinct from the effect of RNA granules that are abolished by GW182 knockdown (now called GW-bodies), and also different and distinct from the effect of RNA granules abolished by RCK/p54 knockdown (likely P-bodies). The different mechanisms of anti-HIV effect of these different RNA granules were apparent in the presence of absence of A3G. Some data that requires extension suggests that A3G complexes may sequester/degrade HIV-1 p24 protein, and that GW-bodies and P-bodies may decrease the translation or stability of HIV-1 mRNA. Thus, I suggest that the effect of GW- and P-bodies cannot be reversed, unless A3G complex effects are also reversed.

These results have significant implications for understanding the biology of RNA granules that are critical components of cells, as well as of HIV-1 replication. This is the most important and basic aspect of my work's significance, as increasing fundamental understanding of these important biological processes may have broad implications. There is also the potential for this work to lead to novel therapeutics for HIV-infected patients. Manipulation of A3G complex

formation for therapeutic purposes by a small molecule would potentially allow for the production of fewer viruses and/or less infectious viruses.

Disrupting the interaction of A3G and Vif could potentially lead to a new class of anti-retrovirals. HIV-1 would theoretically have very limited chances to evade drugs that target the human A3G, rather than a viral protein, through development of drug resistant mutations. Understanding the A3G complex may play a vital role in future development of therapies based on my findings. I show that Vif can degrade A3G both in the LMM form and in A3G complexes. The interactions of A3G with Vif may change depending on if A3G exists as a monomer in the cytoplasm than when A3G is complexed with RNAs and proteins in complexes. Protecting both A3G in the cytoplasm and within complexes would be an important consideration for future development of a Vif-A3G inhibitor, as now it is clear that the A3G complexes are not inactive against HIV-1 as previously thought.

APOBEC3 proteins evolved long ago and have undergone little change. This indicates they play a major role in human survival. The discovery that A3G has the ability to bind and sequester Gag away from the site of viral assembly could be extended to other viruses. A3G is known to restrict several other viruses, and it is conceivable that A3G is able to sequester other viral molecules as well. And even if A3G is not packaged into virions, maybe this producer cell effect of limiting virus production may contribute to reducing viral spread throughout the body.

The amount of A3G within patient lymphocytes may not be the only factor that influences disease progression. My results suggest that the ratio of LMM:HMM A3G also may play a critical role. It would be expected that patients with higher levels of HMM A3G may produce less virus. On the other hand, patients with higher amounts of LMM A3G, will likely package more A3G into progeny virions to block replication in the target cell. Thus, this work suggests seeking an optimum ration that will maximize restriction of HIV-1 replication in the producer and the target cell. The ratio of A3G complexes to the LMM form may also be studied further to determine utility to predict disease outcome, viral or immunological markers of disease progression, or effectiveness of HAART.

Future Directions

This works sheds light on the role of A3G complexes during HIV-1 infection. I showed that the complex is not involved in the packaging of A3G into virions. I then extended those findings to show that the A3G complex is involved in an anti-viral response that restricts the amount of HIV-1 produced from cells. There are many possible next steps. I will outline some important experiments that I prioritize to further extend these results to lead to the potential significance described above.

Characterize the nature of the interaction between A3G complexes and HIV-1 Gag

I have shown by confocal microscopy that a significant portion of HIV-1 Gag colocalizes with A3G complexes. I show some evidence that this interaction leads to the restriction of HIV-1 release, and also that A3G complexes are not identical to other RNA granules. However, the characterization of this interaction, and the complexity of RNA granules, can be greatly enhanced by the use of live cell imaging.

Live cell imaging would allow us a glimpse at the dynamic nature of A3G complexes. To date, no study has examined the half-life of A3G complexes and this knowledge would help us to understand the role of A3G complexes in cells. It has been shown that A3G complexes can form within 30 minutes of A3G synthesis, but it is unclear how dynamic they are. Live cell imaging would give us clues as to proteins transiting through A3G complexes. These experiments would allow a next step to see if Gag is eventually released, or more likely degraded by the lysosome or proteasome. I, and others have shown that A3G complexes can be found in close proximity to late endosomes and this may indicate that some of the constituents of A3G complexes may be turned over by the endosomal pathway. Of note, GW-bodies also are now thought to play a role in directing miRISC components to these degradative compartments. A3G complexes may share similar protein markers with other RNA granules, but may in fact be distinct structures. RNA granules are known for their ability to store or

degrade RNA's, but maybe A3G complexes also lead to the degradation of specific proteins.

Infectivity of wild-type NL4.3 and NL4.3 Δvif viruses produced from cells with or without A3G complexes

I have shown experiments that highlight the effect of A3G complexes on virus production. However, we don't know if virions produced in the presence or absence of A3G complexes have the same or different infectivities. A3G complexes may affect the ability of other positive or negative factors on virus replication to be packaged into virions. Further, the varying amount of A3G packaged could play a major role in virion infectivity.

This experiment would allow us to understand any difference in infectivity of viruses produced in the absence or presence of A3G complexes. I could utilize two approaches to studying the impact of no A3G complexes on viral infectivity. I could compare cells transfected with wild-type A3G to cells transfected with the C97A mutant. This would allow us to compare cells all with A3G, but only one condition having A3G complexes. Further, I could use knockdown of RCK/p54 to abrogate A3G complexes and compare to cells transfected with a control-scrambled shRNA. I know that A3G packaging does not require A3G complexes. However, detailed analysis on the amount of A3G packaged in cells with or without A3G complexes has not been performed. The virion content of A3G and virion infectivity would be determined.

There potentially could be great differences in the amount of A3G packaged when only LMM is present in the cell. Since evidence points to LMM being the source of A3G within virions, increasing LMM in the cell would lead to much higher levels of A3G packaging. This would likely lead to the production of virions with greatly reduced infectivity. There is potential for this strategy to contribute to a "functional cure" if ongoing replenishment of the reservoir occurs from virus replication during therapy.

Enzymatically inactive C97A and WT A3G

All experiments I have presented have used A3G proteins that are enzymatically active. Therefore, we do not know if enzymatic activity of A3G plays a role in the restriction on virus production by A3G complexes.

In these experiments I would make use of mutants of A3G; the E259A mutant, that is known not to posses enzymatic activity. The exact contribution of enzymatic activity to the target cell effect of A3G is still unclear. Enzymatic activity likely plays a smaller role in A3G restricting the early stages of the viral lifecycle in the target cell than originally believed, but I have not addressed the need for enzymatic activity in the producer cell effect of A3G.

To extend my findings that A3G complexes are restricting HIV-1 release, it is necessary to understand the mechanism of this restriction. I hypothesis that Gag localized within these complexes is not available for assembly at the plasma membrane and rapidly degraded. If this is the case, I need to determine the fate of Gag that is sequestered in these complexes. It is unlikely that this restriction

requires enzymatic activity, since the HMM complex of A3G is enzymatically inactive, but to rule out the role of cytidine deamination by A3G in restricting the release of HIV-1 Gag, this experiment is highly important.

The role of protein degradation in A3G complex HIV-1 restriction

The role that protein degradation plays in the A3G-mediated restriction of HIV-1 release has only been minimally investigated. I have found that A3G complexes colocalize with late endosomes about 24 hours after formation. This colocalization may give us clues as to a role that A3G complexes play in protein turnover.

I also did an experiment in which translation in cells was blocked using cycloheximide. I then followed the fate of HIV Gag in cells transfected with no A3G, wild-type A3G, or C97A A3G. I found that HIV Gag in treated cells transfected with wild-type A3G was degraded much more rapidly than in cells with no A3G or C97A mutant that is severely delayed in A3G complex formation.

A3G complexes contain many proteins associated with processing bodies. A subset of these bodies, GW-Bodies are known to colocalize with late endosomes and multivesicular bodies or MVBs and play a role in turnover of the RISC complex associated with siRNA and miRNA. Processing bodies have not been found to overlap with late endosomes and are thought of as distinct structures. The fact that A3G complexes colocalize strongly with late endosomes, raises the possibility that they may be involved in protein turnover.

Additional experiments can be done where cells are co-transfected with WT A3G or C97A and HIV-1 Gag. The amount of Gag found within lysosomes and exosome structures can be assessed by first subcellular fractionation and western blotting. If the amount of HIV-1 Gag is higher in cells with A3G complexes it would suggest lysosomal degradation plays a role in A3G-mediated restriction of HIV-1 release. Additionally, these experiments can be done in the presence or absence of lysosomal function, to determine if blocking the lysosomal degradation pathway leads to increased HIV-1 release in cells with A3G complexes, further implicating lysosomal degradation of HIV Gag as the reason for decreased HIV production in cells with A3G complexes.

Spreading Infections of WT NL4.3 and NL4.3 Δvif in CEM and CEM-SS cells

I have shown that A3G complexes greatly restrict the release of HIV-1 from cells in a single-round of infection. However, it will become important to understand the level of this restriction over the course of a spreading infection. These experiments would more reflect a natural infection.

In order to perform the following experiment, I would first have to separate the producer cell restriction on HIV-1 described here from the target cell effect of A3G. This likely can be accomplished using mutants. The discovery of an A3G mutant that lacks either the target cell or producer cell effect would greatly advance the field and aid in further studies of the long-term effects of these restrictions.

Another means by which the target cell and producer cell effect could be separated is by using CEM and CEM-SS cells that contain no RCK/p54. These cells would not allow A3G to form A3G complexes. I could compare virus spread in sister cells with and without RCK/p54 expression to determine the effect of knocking out the producer cell effect. An important control would be to make sure that RCK/p54 knockdown has no influence on the target cell effect of A3G.

Once, a system is established that separates the target cell and producer cell restrictions of A3G, the following experiment could be performed. In these spreading infection experiments both CEM and CEM-SS cells would be infected with either Vif-positive or Vif-negative HIV. I have previously shown that HIV-1 Vif is able to rid cells of both LMM and HMM A3G. I have also shown that LMM A3G does not restrict HIV-1 production. So, depleting cells of both LMM and HMM A3G should be an accurate reflection of the contribution of A3G complexes to HIV-1 production. Virus would be collected over the course of weeks and the difference in NL4.3 and NL4.3Δvif should be observed in CEM cells, which posses A3G and CEM cells with RCK/p54 knocked down. CEM-SS cells would be used as a negative control, since they do not contain A3G.

This experiment would more closely reflect what happens within patients. This experiment is complicated by the fact that virus output would be a result of the combined effects of the producer cell and target cell restrictions of A3G. However, during the experiment the amount of Gag and A3G association could be monitored by ultracentrifugation followed by western blots to visualize A3G and Gag.

Determine how A3G complex formation is regulated

I know that A3G complexes contain many proteins and RNA's. However, there are likely still roles that A3G complexes play that are unknown. An important step toward understanding the role of A3G complexes understands what signals govern their formation.

It does seem that T cell activation plays a role in A3G complex formation. Resting T cells posses higher levels of LMM compared to HMM A3G. However, upon T cell activation, a majority of LMM A3G is converted to A3G complexes. Using resting and activated T cells as a model may be a way to tease apart the steps necessary for A3G complex formation. Mutant cell lines that don't readily shift their A3G into complexes after T cell activation would be useful in identify the factors necessary. Also, cytokines may play a role and taking a closer look at those pathways, may yield important clues. It is known that extracellular signals can influence the formation of HMM A3G, without cell activation. Understanding how A3G complexes are formed will lead to a better understanding of their cellular functions.

In conclusion, this work demonstrates that A3G complexes play an important role in an anti-HIV response in the producer cell. This anti-viral role of A3G complexes was previously unknown, but likely plays an important role *in vivo*. Making use of a mutant of A3G that was delayed in A3G complex formation was the initial finding that led to further investigation. I first demonstrated that the

presence of A3G complexes was not necessary for A3G packaging into virions. Also, this mutant, C97A, allowed us to demonstrate that A3G complexes were linked to decreased levels of virus output. Depletion of A3G complexes by HIV-1 Vif and knockdown of p54 relieves this A3G-mediated restriction. This work identified a new antiviral function of the cytidine deaminase A3G. Further work on A3G complexes, will yield important clues as to any additional functions of A3G complexes and may lead to the development of therapies that will decrease the amount of virus output in patients.

BIBLIOGRAPHY

1. **Abudu, A., A. Takaori-Kondo, T. Izumi, K. Shirakawa, M. Kobayashi, A. Sasada, K. Fukunaga, and T. Uchiyama.** 2006. Murine retrovirus escapes from murine APOBEC3 via two distinct novel mechanisms. Curr Biol **16:**1565-1570.

2. **Ahluwalia, J. K., S. Z. Khan, K. Soni, P. Rawat, A. Gupta, M. Hariharan, V. Scaria, M. Lalwani, B. Pillai, D. Mitra, and S. K. Brahmachari.** 2008. Human cellular microRNA hsa-miR-29a interferes with viral nef protein expression and HIV-1 replication. Retrovirology **5:**117.

3. **Alce, T. M., and W. Popik.** 2004. APOBEC3G is incorporated into virus-like particles by a direct interaction with HIV-1 Gag nucleocapsid protein. J Biol Chem **279:**34083-34086.

4. **Alves-Rodrigues, I., A. Mas, and J. Diez.** 2007. Xenopus Xp54 and human RCK/p54 helicases functionally replace yeast Dhh1p in brome mosaic virus RNA replication. Journal of virology **81:**4378-4380.

5. **Anderson, J. L., and T. J. Hope.** 2004. HIV accessory proteins and surviving the host cell. Curr HIV/AIDS Rep **1:**47-53.

6. **Anderson, J. L., and T. J. Hope.** 2003. Recent Insights into HIV Accessory Proteins. Curr Infect Dis Rep **5:**439-450.

7. **Anderson, P., and N. Kedersha.** 2009. RNA granules: post-transcriptional and epigenetic modulators of gene expression. Nat Rev Mol Cell Biol **10:**430-436.

8. **Anderson, P., and N. Kedersha.** 2008. Stress granules: the Tao of RNA triage. Trends in biochemical sciences **33:**141-150.

9. **Armitage, A. E., A. Katzourakis, T. de Oliveira, J. J. Welch, R. Belshaw, K. N. Bishop, B. Kramer, A. J. McMichael, A. Rambaut, and A. K. Iversen.** 2008. Conserved footprints of APOBEC3G on Hypermutated human immunodeficiency virus type 1 and human endogenous retrovirus HERV-K(HML2) sequences. J Virol **82:**8743-8761.

10. **Bach, D., S. Peddi, B. Mangeat, A. Lakkaraju, K. Strub, and D. Trono.** 2008. Characterization of APOBEC3G binding to 7SL RNA. Retrovirology **5:**54.

11. **Beliakova-Bethell, N., C. Beckham, T. H. Giddings, Jr., M. Winey, R. Parker, and S. Sandmeyer.** 2006. Virus-like particles of the Ty3 retrotransposon assemble in association with P-body components. Rna **12:**94-101.

12. **Bennett, R. P., J. D. Salter, X. Liu, J. E. Wedekind, and H. C. Smith.** 2008. APOBEC3G subunits self-associate via the C-terminal deaminase domain. J Biol Chem **283:**33329-33336.

13. **Bergeron, J. R., H. Huthoff, D. A. Veselkov, R. L. Beavil, P. J. Simpson, S. J. Matthews, M. H. Malim, and M. R. Sanderson.** 2010. The SOCS-box of HIV-1 Vif interacts with ElonginBC by induced-folding to recruit its Cul5-containing ubiquitin ligase complex. PLoS Pathog **6:**e1000925.

14. **Bieniasz, P. D.** 2004. Intrinsic immunity: a front-line defense against viral attack. Nature immunology **5:**1109-1115.

15. **Bishop, K. N., R. K. Holmes, and M. H. Malim.** 2006. Antiviral potency of APOBEC proteins does not correlate with cytidine deamination. J Virol **80:**8450-8458.

16. **Bishop, K. N., R. K. Holmes, A. M. Sheehy, and M. H. Malim.** 2004. APOBEC-mediated editing of viral RNA. Science **305:**645.

17. **Bishop, K. N., M. Verma, E. Y. Kim, S. M. Wolinsky, and M. H. Malim.** 2008. APOBEC3G inhibits elongation of HIV-1 reverse transcripts. PLoS Pathog **4:**e1000231.

18. **Bogerd, H. P., B. P. Doehle, H. L. Wiegand, and B. R. Cullen.** 2004. A single amino acid difference in the host APOBEC3G protein controls the primate species specificity of HIV type 1 virion infectivity factor. Proc Natl Acad Sci U S A **101:**3770-3774.

19. **Bogerd, H. P., H. L. Wiegand, B. P. Doehle, and B. R. Cullen.** 2007. The intrinsic antiretroviral factor APOBEC3B contains two enzymatically active cytidine deaminase domains. Virology **364:**486-493.

20. **Bogerd, H. P., H. L. Wiegand, B. P. Doehle, K. K. Lueders, and B. R. Cullen.** 2006. APOBEC3A and APOBEC3B are potent inhibitors of LTR-retrotransposon function in human cells. Nucleic Acids Res **34:**89-95.

21. **Borja, M. S., K. Piotukh, C. Freund, and J. D. Gross.** 2011. Dcp1 links coactivators of mRNA decapping to Dcp2 by proline recognition. RNA **17:**278-290.

22. **Brengues, M., D. Teixeira, and R. Parker.** 2005. Movement of eukaryotic mRNAs between polysomes and cytoplasmic processing bodies. Science **310:**486-489.

23. **Buchet-Poyau, K., J. Courchet, H. Le Hir, B. Seraphin, J. Y. Scoazec, L. Duret, C. Domon-Dell, J. N. Freund, and M. Billaud.** 2007. Identification and characterization of human Mex-3 proteins, a novel family of evolutionarily conserved RNA-binding proteins differentially localized to processing bodies. Nucleic acids research **35:**1289-1300.

24. **Burdick, R., J. L. Smith, C. Chaipan, Y. Friew, J. Chen, N. J. Venkatachari, K. A. Delviks-Frankenberry, W. S. Hu, and V. K. Pathak.** 2010. P body-associated protein Mov10 inhibits HIV-1 replication at multiple stages. J Virol **84:**10241-10253.

25. **Burnett, A., and P. Spearman.** 2007. APOBEC3G multimers are recruited to the plasma membrane for packaging into human immunodeficiency virus type 1 virus-like particles in an RNA-dependent process requiring the NC basic linker. J Virol **81:**5000-5013.

26. **Chable-Bessia, C., O. Meziane, D. Latreille, R. Triboulet, A. Zamborlini, A. Wagschal, J. M. Jacquet, J. Reynes, Y. Levy, A. Saib, Y. Bennasser, and M. Benkirane.** 2009. Suppression of HIV-1 replication by microRNA effectors. Retrovirology **6:**26.

27. **Checkley, M. A., K. Nagashima, S. J. Lockett, K. M. Nyswaner, and D. J. Garfinkel.** 2010. P-body components are required for Ty1 retrotransposition during assembly of retrotransposition-competent virus-like particles. Mol Cell Biol **30:**382-398.

28. **Chelico, L., P. Pham, P. Calabrese, and M. F. Goodman.** 2006. APOBEC3G DNA deaminase acts processively 3' --> 5' on single-stranded DNA. Nat Struct Mol Biol **13:**392-399.

29. **Chen, M. Y., F. Maldarelli, M. K. Karczewski, R. L. Willey, and K. Strebel.** 1993. Human immunodeficiency virus type 1 Vpu protein induces degradation of CD4 in vitro: the cytoplasmic domain of CD4 contributes to Vpu sensitivity. Journal of virology **67:**3877-3884.

30. **Chiu, Y. L., and W. C. Greene.** 2008. The APOBEC3 cytidine deaminases: an innate defensive network opposing exogenous retroviruses and endogenous retroelements. Annu Rev Immunol **26:**317-353.

31. **Chiu, Y. L., V. B. Soros, J. F. Kreisberg, K. Stopak, W. Yonemoto, and W. C. Greene.** 2005. Cellular APOBEC3G restricts HIV-1 infection in resting CD4+ T cells. Nature **435:**108-114.

32. **Chiu, Y. L., H. E. Witkowska, S. C. Hall, M. Santiago, V. B. Soros, C. Esnault, T. Heidmann, and W. C. Greene.** 2006. High-molecular-mass APOBEC3G complexes restrict Alu retrotransposition. Proc Natl Acad Sci U S A **103:**15588-15593.

33. **Cho, S. J., H. Drechsler, R. C. Burke, M. Q. Arens, W. Powderly, and N. O. Davidson.** 2006. APOBEC3F and APOBEC3G mRNA levels do not correlate with human immunodeficiency virus type 1 plasma viremia or CD4+ T-cell count. J Virol **80:**2069-2072.

34. **Chu, C. Y., and T. M. Rana.** 2006. Translation repression in human cells by microRNA-induced gene silencing requires RCK/p54. PLoS biology **4:**e210.

35. **Conticello, S. G., R. S. Harris, and M. S. Neuberger.** 2003. The Vif protein of HIV triggers degradation of the human antiretroviral DNA deaminase APOBEC3G. Curr Biol **13:**2009-2013.

36. **Cullen, B. R.** 2006. Role and mechanism of action of the APOBEC3 family of antiretroviral resistance factors. Journal of virology **80:**1067-1076.

37. **Dang, Y., X. Wang, W. J. Esselman, and Y. H. Zheng.** 2006. Identification of APOBEC3DE as another antiretroviral factor from the human APOBEC family. J Virol **80:**10522-10533.

38. **Derdowski, A., L. Ding, and P. Spearman.** 2004. A novel fluorescence resonance energy transfer assay demonstrates that the human immunodeficiency virus type 1 Pr55Gag I domain mediates Gag-Gag interactions. J Virol **78:**1230-1242.

39. **Ding, L., and M. Han.** 2007. GW182 family proteins are crucial for microRNA-mediated gene silencing. Trends Cell Biol **17:**411-416.

40. **Doehle, B. P., A. Schafer, and B. R. Cullen.** 2005. Human APOBEC3B is a potent inhibitor of HIV-1 infectivity and is resistant to HIV-1 Vif. Virology **339:**281-288.

41. **Donahue, J. P., M. L. Vetter, N. A. Mukhtar, and R. T. D'Aquila.** 2008. The HIV-1 Vif PPLP motif is necessary for human APOBEC3G binding and degradation. Virology **377:**49-53.

42. **Dong, X., H. Li, A. Derdowski, L. Ding, A. Burnett, X. Chen, T. R. Peters, T. S. Dermody, E. Woodruff, J. J. Wang, and P. Spearman.** 2005. AP-3 directs the intracellular trafficking of HIV-1 Gag and plays a key role in particle assembly. Cell **120:**663-674.

43. **Dougherty, J. D., J. P. White, and R. E. Lloyd.** 2011. Poliovirus-mediated disruption of cytoplasmic processing bodies. Journal of virology **85:**64-75.

44. **Douville, R. N., and J. Hiscott.** 2010. The interface between the innate interferon response and expression of host retroviral restriction factors. Cytokine **52:**108-115.

45. **Dutko, J. A., A. E. Kenny, E. R. Gamache, and M. J. Curcio.** 2010. 5' to 3' mRNA decay factors colocalize with Ty1 gag and human APOBEC3G and promote Ty1 retrotransposition. J Virol **84:**5052-5066.

46. **Eulalio, A., E. Huntzinger, and E. Izaurralde.** 2008. GW182 interaction with Argonaute is essential for miRNA-mediated translational repression and mRNA decay. Nature structural & molecular biology **15:**346-353.

47. **Eulalio, A., F. Tritschler, and E. Izaurralde.** 2009. The GW182 protein family in animal cells: new insights into domains required for miRNA-mediated gene silencing. Rna **15:**1433-1442.

48. **Eystathioy, T., A. Jakymiw, E. K. Chan, B. Seraphin, N. Cougot, and M. J. Fritzler.** 2003. The GW182 protein colocalizes with mRNA degradation associated proteins hDcp1 and hLSm4 in cytoplasmic GW bodies. RNA **9:**1171-1173.

49. **Fitzpatrick, K., M. Skasko, T. J. Deerinck, J. Crum, M. H. Ellisman, and J. Guatelli.** 2010. Direct restriction of virus release and incorporation of the interferon-induced protein BST-2 into HIV-1 particles. PLoS pathogens **6:**e1000701.

50. **Furtak, V., A. Mulky, S. A. Rawlings, L. Kozhaya, K. Lee, V. N. Kewalramani, and D. Unutmaz.** 2010. Perturbation of the P-body component Mov10 inhibits HIV-1 infectivity. PLoS One **5:**e9081.

51. **Furukawa, A., T. Nagata, A. Matsugami, Y. Habu, R. Sugiyama, F. Hayashi, N. Kobayashi, S. Yokoyama, H. Takaku, and M. Katahira.** 2009. Structure and real-time monitoring of the enzymatic reaction of APOBEC3G which is involved in anti-HIV activity. Nucleic Acids Symp Ser (Oxf)**:**87-88.

52. **Gallo, C. M., E. Munro, D. Rasoloson, C. Merritt, and G. Seydoux.** 2008. Processing bodies and germ granules are distinct RNA granules that interact in C. elegans embryos. Dev Biol **323:**76-87.

53. **Gallois-Montbrun, S., R. K. Holmes, C. M. Swanson, M. Fernandez-Ocana, H. L. Byers, M. A. Ward, and M. H. Malim.** 2008. Comparison of cellular ribonucleoprotein complexes associated with the APOBEC3F and APOBEC3G antiviral proteins. J Virol **82:**5636-5642.

54. **Gallois-Montbrun, S., B. Kramer, C. M. Swanson, H. Byers, S. Lynham, M. Ward, and M. H. Malim.** 2007. Antiviral protein APOBEC3G localizes to ribonucleoprotein complexes found in P bodies and stress granules. J Virol **81:**2165-2178.

55. **Gibbings, D. J., C. Ciaudo, M. Erhardt, and O. Voinnet.** 2009. Multivesicular bodies associate with components of miRNA effector complexes and modulate miRNA activity. Nat Cell Biol **11:**1143-1149.

56. **Goffinet, C., S. Schmidt, C. Kern, L. Oberbremer, and O. T. Keppler.** 2010. Endogenous CD317/Tetherin limits replication of HIV-1 and murine leukemia virus in rodent cells and is resistant to antagonists from primate viruses. Journal of virology **84:**11374-11384.

57. **Goila-Gaur, R., M. A. Khan, E. Miyagi, S. Kao, S. Opi, H. Takeuchi, and K. Strebel.** 2008. HIV-1 Vif promotes the formation of high molecular mass APOBEC3G complexes. Virology **372:**136-146.

58. **Goncalves, J., and M. Santa-Marta.** 2004. HIV-1 Vif and APOBEC3G: multiple roads to one goal. Retrovirology **1:**28.

59. **Groom, H. C., M. W. Yap, R. P. Galao, S. J. Neil, and K. N. Bishop.** 2010. Susceptibility of xenotropic murine leukemia virus-related virus (XMRV) to retroviral restriction factors. Proc Natl Acad Sci U S A **107:**5166-5171.

60. **Hache, G., M. T. Liddament, and R. S. Harris.** 2005. The retroviral hypermutation specificity of APOBEC3F and APOBEC3G is governed by the C-terminal DNA cytosine deaminase domain. J Biol Chem **280:**10920-10924.

61. **Harris, R. S., and M. T. Liddament.** 2004. Retroviral restriction by APOBEC proteins. Nat Rev Immunol **4:**868-877.

62. **Holden, L. G., C. Prochnow, Y. P. Chang, R. Bransteitter, L. Chelico, U. Sen, R. C. Stevens, M. F. Goodman, and X. S. Chen.** 2008. Crystal structure of the anti-viral APOBEC3G catalytic domain and functional implications. Nature **456:**121-124.

63. **Hulme, A. E., H. P. Bogerd, B. R. Cullen, and J. V. Moran.** 2007. Selective inhibition of Alu retrotransposition by APOBEC3G. Gene **390:**199-205.

64. **Huthoff, H., and M. H. Malim.** 2007. Identification of amino acid residues in APOBEC3G required for regulation by human immunodeficiency virus type 1 Vif and Virion encapsidation. J Virol **81:**3807-3815.

65. **Iwatani, Y., D. S. Chan, L. Liu, H. Yoshii, J. Shibata, N. Yamamoto, J. G. Levin, A. M. Gronenborn, and W. Sugiura.** 2009. HIV-1 Vif-mediated

ubiquitination/degradation of APOBEC3G involves four critical lysine residues in its C-terminal domain. Proc Natl Acad Sci U S A **106:**19539-19544.

66. **Jarmuz, A., A. Chester, J. Bayliss, J. Gisbourne, I. Dunham, J. Scott, and N. Navaratnam.** 2002. An anthropoid-specific locus of orphan C to U RNA-editing enzymes on chromosome 22. Genomics **79:**285-296.

67. **Jern, P., R. A. Russell, V. K. Pathak, and J. M. Coffin.** 2009. Likely role of APOBEC3G-mediated G-to-A mutations in HIV-1 evolution and drug resistance. PLoS Pathog **5:**e1000367.

68. **Jin, X., A. Brooks, H. Chen, R. Bennett, R. Reichman, and H. Smith.** 2005. APOBEC3G/CEM15 (hA3G) mRNA levels associate inversely with human immunodeficiency virus viremia. J Virol **79:**11513-11516.

69. **Jin, X., H. Wu, and H. Smith.** 2007. APOBEC3G levels predict rates of progression to AIDS. Retrovirology **4:**20.

70. **Kamata, M., Y. Nagaoka, and I. S. Chen.** 2009. Reassessing the role of APOBEC3G in human immunodeficiency virus type 1 infection of quiescent CD4+ T-cells. PLoS Pathog **5:**e1000342.

71. **Karczewski, M. K., and K. Strebel.** 1996. Cytoskeleton association and virion incorporation of the human immunodeficiency virus type 1 Vif protein. J Virol **70:**494-507.

72. **Kedersha, N., and P. Anderson.** 2007. Mammalian stress granules and processing bodies. Methods Enzymol **431:**61-81.

73. **Kedersha, N., G. Stoecklin, M. Ayodele, P. Yacono, J. Lykke-Andersen, M. J. Fritzler, D. Scheuner, R. J. Kaufman, D. E. Golan, and P. Anderson.** 2005. Stress granules and processing bodies are dynamically linked sites of mRNP remodeling. J Cell Biol **169:**871-884.

74. **Khan, M. A., S. Kao, E. Miyagi, H. Takeuchi, R. Goila-Gaur, S. Opi, C. L. Gipson, T. G. Parslow, H. Ly, and K. Strebel.** 2005. Viral RNA is required for the association of APOBEC3G with human immunodeficiency virus type 1 nucleoprotein complexes. J Virol **79:**5870-5874.

75. **Kiebler, M. A., and G. J. Bassell.** 2006. Neuronal RNA granules: movers and makers. Neuron **51:**685-690.

76. **Knoepfel, S. A., F. Di Giallonardo, M. Daumer, A. Thielen, and K. J. Metzner.** 2011. In-depth analysis of G-to-A hypermutation rate in HIV-1 env DNA induced by endogenous APOBEC3 proteins using massively parallel sequencing. J Virol Methods **171:**329-338.

77. **Kobayashi, M., A. Takaori-Kondo, Y. Miyauchi, K. Iwai, and T. Uchiyama.** 2005. Ubiquitination of APOBEC3G by an HIV-1 Vif-Cullin5-Elongin B-Elongin C complex is essential for Vif function. J Biol Chem **280:**18573-18578.

78. **Kozak, S. L., M. Marin, K. M. Rose, C. Bystrom, and D. Kabat.** 2006. The anti-HIV-1 editing enzyme APOBEC3G binds HIV-1 RNA and messenger RNAs that shuttle between polysomes and stress granules. J Biol Chem **281:**29105-29119.

79. **Kreisberg, J. F., W. Yonemoto, and W. C. Greene.** 2006. Endogenous factors enhance HIV infection of tissue naive CD4 T cells by stimulating high molecular mass APOBEC3G complex formation. J Exp Med **203:**865-870.

80. **Kremer, M., and B. S. Schnierle.** 2005. HIV-1 Vif: HIV's weapon against the cellular defense factor APOBEC3G. Curr HIV Res **3:**339-344.

81. **Kulkarni, M., S. Ozgur, and G. Stoecklin.** 2010. On track with P-bodies. Biochem Soc Trans **38:**242-251.

82. **Kuroishi, A., K. Bozek, T. Shioda, and E. E. Nakayama.** 2010. A single amino acid substitution of the human immunodeficiency virus type 1 capsid protein affects viral sensitivity to TRIM5 alpha. Retrovirology **7:**58.

83. **Li, H., J. Dou, L. Ding, and P. Spearman.** 2007. Myristoylation is required for human immunodeficiency virus type 1 Gag-Gag multimerization in mammalian cells. J Virol **81:**12899-12910.

84. **Li, X. Y., F. Guo, L. Zhang, L. Kleiman, and S. Cen.** 2007. APOBEC3G inhibits DNA strand transfer during HIV-1 reverse transcription. J Biol Chem **282:**32065-32074.

85. **Lian, S., M. J. Fritzler, J. Katz, T. Hamazaki, N. Terada, M. Satoh, and E. K. Chan.** 2007. Small interfering RNA-mediated silencing induces target-dependent assembly of GW/P bodies. Mol Biol Cell **18:**3375-3387.

86. **Liddament, M. T., W. L. Brown, A. J. Schumacher, and R. S. Harris.** 2004. APOBEC3F properties and hypermutation preferences indicate activity against HIV-1 in vivo. Curr Biol **14:**1385-1391.

87. **Liu, B., P. T. Sarkis, K. Luo, Y. Yu, and X. F. Yu.** 2005. Regulation of Apobec3F and human immunodeficiency virus type 1 Vif by Vif-Cul5-ElonB/C E3 ubiquitin ligase. J Virol **79:**9579-9587.

88. **Liu, J., F. V. Rivas, J. Wohlschlegel, J. R. Yates, 3rd, R. Parker, and G. J. Hannon.** 2005. A role for the P-body component GW182 in microRNA function. Nat Cell Biol **7:**1261-1266.

89. **Low, A., C. M. Okeoma, N. Lovsin, M. de las Heras, T. H. Taylor, B. M. Peterlin, S. R. Ross, and H. Fan.** 2009. Enhanced replication and pathogenesis of Moloney murine leukemia virus in mice defective in the murine APOBEC3 gene. Virology **385:**455-463.

90. **Luo, K., B. Liu, Z. Xiao, Y. Yu, X. Yu, R. Gorelick, and X. F. Yu.** 2004. Amino-terminal region of the human immunodeficiency virus type 1 nucleocapsid is required for human APOBEC3G packaging. J Virol **78:**11841-11852.

91. **Luo, K., T. Wang, B. Liu, C. Tian, Z. Xiao, J. Kappes, and X. F. Yu.** 2007. Cytidine deaminases APOBEC3G and APOBEC3F interact with human immunodeficiency virus type 1 integrase and inhibit proviral DNA formation. J Virol **81:**7238-7248.

92. **Madani, N., and D. Kabat.** 1998. An endogenous inhibitor of human immunodeficiency virus in human lymphocytes is overcome by the viral Vif protein. J Virol **72:**10251-10255.

93. **Mangasarian, A., M. Foti, C. Aiken, D. Chin, J. L. Carpentier, and D. Trono.** 1997. The HIV-1 Nef protein acts as a connector with sorting pathways in the Golgi and at the plasma membrane. Immunity **6:**67-77.

94. **Marin, M., S. Golem, K. M. Rose, S. L. Kozak, and D. Kabat.** 2008. Human immunodeficiency virus type 1 Vif functionally interacts with diverse APOBEC3 cytidine deaminases and moves with them between cytoplasmic sites of mRNA metabolism. J Virol **82:**987-998.

95. **Matsumoto, K., O. Y. Kwon, H. Kim, and Y. Akao.** 2005. Expression of rck/p54, a DEAD-box RNA helicase, in gametogenesis and early embryogenesis of mice. Dev Dyn **233:**1149-1156.

96. **Mehle, A., J. Goncalves, M. Santa-Marta, M. McPike, and D. Gabuzda.** 2004. Phosphorylation of a novel SOCS-box regulates assembly of the HIV-1 Vif-Cul5 complex that promotes APOBEC3G degradation. Genes Dev **18:**2861-2866.

97. **Mehle, A., B. Strack, P. Ancuta, C. Zhang, M. McPike, and D. Gabuzda.** 2004. Vif overcomes the innate antiviral activity of APOBEC3G by promoting its degradation in the ubiquitin-proteasome pathway. J Biol Chem **279:**7792-7798.

98. **Mehle, A., E. R. Thomas, K. S. Rajendran, and D. Gabuzda.** 2006. A zinc-binding region in Vif binds Cul5 and determines cullin selection. J Biol Chem **281:**17259-17265.

99. **Miller, J. H., V. Presnyak, and H. C. Smith.** 2007. The dimerization domain of HIV-1 viral infectivity factor Vif is required to block virion incorporation of APOBEC3G. Retrovirology **4:**81.

100. **Minshall, N., M. Kress, D. Weil, and N. Standart.** 2009. Role of p54 RNA helicase activity and its C-terminal domain in translational repression, P-body localization and assembly. Molecular biology of the cell **20:**2464-2472.

101. **Moser, J. J., and M. J. Fritzler.** 2010. Cytoplasmic ribonucleoprotein (RNP) bodies and their relationship to GW/P bodies. Int J Biochem Cell Biol **42:**828-843.

102. **Nathans, R., C. Y. Chu, A. K. Serquina, C. C. Lu, H. Cao, and T. M. Rana.** 2009. Cellular microRNA and P bodies modulate host-HIV-1 interactions. Mol Cell **34:**696-709.

103. **Neil, S. J., T. Zang, and P. D. Bieniasz.** 2008. Tetherin inhibits retrovirus release and is antagonized by HIV-1 Vpu. Nature **451:**425-430.

104. **Newman, E. N., R. K. Holmes, H. M. Craig, K. C. Klein, J. R. Lingappa, M. H. Malim, and A. M. Sheehy.** 2005. Antiviral function of APOBEC3G can be dissociated from cytidine deaminase activity. Curr Biol **15:**166-170.

105. **Niewiadomska, A. M., and X. F. Yu.** 2009. Host restriction of HIV-1 by APOBEC3 and viral evasion through Vif. Curr Top Microbiol Immunol **339:**1-25.

106. **Nowarski, R., E. Britan-Rosich, T. Shiloach, and M. Kotler.** 2008. Hypermutation by intersegmental transfer of APOBEC3G cytidine deaminase. Nat Struct Mol Biol **15:**1059-1066.

107. **Ochsenbauer, C., T. Wilk, and V. Bosch.** 1997. Analysis of vif-defective human immunodeficiency virus type 1 (HIV-1) virions synthesized in 'non-permissive' T lymphoid cells stably infected with selectable HIV-1. The Journal of general virology **78 (Pt 3):**627-635.

108. **Okeoma, C. M., J. Petersen, and S. R. Ross.** 2009. Expression of murine APOBEC3 alleles in different mouse strains and their effect on mouse mammary tumor virus infection. J Virol **83:**3029-3038.

109. **Opi, S., S. Kao, R. Goila-Gaur, M. A. Khan, E. Miyagi, H. Takeuchi, and K. Strebel.** 2007. Human immunodeficiency virus type 1 Vif inhibits packaging and antiviral activity of a degradation-resistant APOBEC3G variant. J Virol **81:**8236-8246.

110. **Opi, S., H. Takeuchi, S. Kao, M. A. Khan, E. Miyagi, R. Goila-Gaur, Y. Iwatani, J. G. Levin, and K. Strebel.** 2006. Monomeric APOBEC3G is catalytically active and has antiviral activity. J Virol **80:**4673-4682.

111. **Overbaugh, J., S. M. Jackson, M. D. Papenhausen, and L. M. Rudensey.** 1996. Lentiviral genomes with G-to-A hypermutation may result from Taq polymerase errors during polymerase chain reaction. AIDS research and human retroviruses **12:**1605-1613.

112. **Pace, C., J. Keller, D. Nolan, I. James, S. Gaudieri, C. Moore, and S. Mallal.** 2006. Population level analysis of human immunodeficiency virus

type 1 hypermutation and its relationship with APOBEC3G and vif genetic variation. J Virol **80:**9259-9269.

113. **Paul, I., J. Cui, and E. L. Maynard.** 2006. Zinc binding to the HCCH motif of HIV-1 virion infectivity factor induces a conformational change that mediates protein-protein interactions. Proc Natl Acad Sci U S A **103:**18475-18480.

114. **Perron, M. J., M. Stremlau, B. Song, W. Ulm, R. C. Mulligan, and J. Sodroski.** 2004. TRIM5alpha mediates the postentry block to N-tropic murine leukemia viruses in human cells. Proceedings of the National Academy of Sciences of the United States of America **101:**11827-11832.

115. **Pillai, S. K., J. K. Wong, and J. D. Barbour.** 2008. Turning up the volume on mutational pressure: is more of a good thing always better? (A case study of HIV-1 Vif and APOBEC3). Retrovirology **5:**26.

116. **Pion, M., A. Granelli-Piperno, B. Mangeat, R. Stalder, R. Correa, R. M. Steinman, and V. Piguet.** 2006. APOBEC3G/3F mediates intrinsic resistance of monocyte-derived dendritic cells to HIV-1 infection. J Exp Med **203:**2887-2893.

117. **Reddy, K., C. A. Winkler, L. Werner, K. Mlisana, S. S. Abdool Karim, and T. Ndung'u.** 2010. APOBEC3G expression is dysregulated in primary HIV-1 infection and polymorphic variants influence CD4+ T-cell counts and plasma viral load. AIDS **24:**195-204.

118. **Reed, S. E., E. M. Staley, J. P. Mayginnes, D. J. Pintel, and G. E. Tullis.** 2006. Transfection of mammalian cells using linear polyethylenimine is a simple and effective means of producing recombinant adeno-associated virus vectors. J Virol Methods **138:**85-98.

119. **Refsland, E. W., M. D. Stenglein, K. Shindo, J. S. Albin, W. L. Brown, and R. S. Harris.** 2010. Quantitative profiling of the full APOBEC3 mRNA repertoire in lymphocytes and tissues: implications for HIV-1 restriction. Nucleic Acids Res **38:**4274-4284.

120. **Rehwinkel, J., I. Behm-Ansmant, D. Gatfield, and E. Izaurralde.** 2005. A crucial role for GW182 and the DCP1:DCP2 decapping complex in miRNA-mediated gene silencing. RNA **11:**1640-1647.

121. **Rose, K. M., M. Marin, S. L. Kozak, and D. Kabat.** 2005. Regulated production and anti-HIV type 1 activities of cytidine deaminases APOBEC3B, 3F, and 3G. AIDS Res Hum Retroviruses **21:**611-619.

122. **Russell, R. A., M. D. Moore, W. S. Hu, and V. K. Pathak.** 2009. APOBEC3G induces a hypermutation gradient: purifying selection at multiple steps during HIV-1 replication results in levels of G-to-A mutations that are high in DNA, intermediate in cellular viral RNA, and low in virion RNA. Retrovirology **6:**16.

123. **Russell, R. A., and V. K. Pathak.** 2007. Identification of two distinct human immunodeficiency virus type 1 Vif determinants critical for interactions with human APOBEC3G and APOBEC3F. J Virol **81:**8201-8210.

124. **Russell, R. A., J. Smith, R. Barr, D. Bhattacharyya, and V. K. Pathak.** 2009. Distinct domains within APOBEC3G and APOBEC3F interact with separate regions of human immunodeficiency virus type 1 Vif. J Virol **83:**1992-2003.

125. **Sacha, J. B., M. B. Buechler, L. P. Newman, J. Reed, L. T. Wallace, J. T. Loffredo, N. A. Wilson, and D. I. Watkins.** 2010. SIV-specific CD8+ T cells recognize Vpr- and Rev-derived epitopes early after infection. J Virol.

126. **Sakuno, T., Y. Araki, Y. Ohya, S. Kofuji, S. Takahashi, S. Hoshino, and T. Katada.** 2004. Decapping reaction of mRNA requires Dcp1 in fission yeast: its characterization in different species from yeast to human. J Biochem **136:**805-812.

127. **Santoni de Sio, F. R., and D. Trono.** 2009. APOBEC3G-depleted resting CD4+ T cells remain refractory to HIV1 infection. PLoS One **4:**e6571.

128. **Schafer, A., H. P. Bogerd, and B. R. Cullen.** 2004. Specific packaging of APOBEC3G into HIV-1 virions is mediated by the nucleocapsid domain of the gag polyprotein precursor. Virology **328:**163-168.

129. **Schmidt, S., J. V. Fritz, J. Bitzegeio, O. T. Fackler, and O. T. Keppler.** 2011. HIV-1 Vpu Blocks Recycling and Biosynthetic Transport of the Intrinsic Immunity Factor CD317/Tetherin To Overcome the Virion Release Restriction. MBio **2**.

130. **Schrofelbauer, B., D. Chen, and N. R. Landau.** 2004. A single amino acid of APOBEC3G controls its species-specific interaction with virion infectivity factor (Vif). Proc Natl Acad Sci U S A **101:**3927-3932.

131. **Serman, A., F. Le Roy, C. Aigueperse, M. Kress, F. Dautry, and D. Weil.** 2007. GW body disassembly triggered by siRNAs independently of their silencing activity. Nucleic Acids Res **35:**4715-4727.

132. **Shandilya, S. M., M. N. Nalam, E. A. Nalivaika, P. J. Gross, J. C. Valesano, K. Shindo, M. Li, M. Munson, W. E. Royer, E. Harjes, T. Kono, H. Matsuo, R. S. Harris, M. Somasundaran, and C. A. Schiffer.** 2010. Crystal structure of the APOBEC3G catalytic domain reveals potential oligomerization interfaces. Structure **18:**28-38.

133. **Sheehy, A. M., N. C. Gaddis, J. D. Choi, and M. H. Malim.** 2002. Isolation of a human gene that inhibits HIV-1 infection and is suppressed by the viral Vif protein. Nature **418:**646-650.

134. **Simon, J. H., D. L. Miller, R. A. Fouchier, M. A. Soares, K. W. Peden, and M. H. Malim.** 1998. The regulation of primate immunodeficiency virus infectivity by Vif is cell species restricted: a role for Vif in determining virus host range and cross-species transmission. The EMBO journal **17:**1259-1267.

135. **Simon, V., V. Zennou, D. Murray, Y. Huang, D. D. Ho, and P. D. Bieniasz.** 2005. Natural variation in Vif: differential impact on APOBEC3G/3F and a potential role in HIV-1 diversification. PLoS Pathog **1:**e6.

136. **Siomi, H., and M. C. Siomi.** 2009. RISC hitches onto endosome trafficking. Nat Cell Biol **11:**1049-1051.

137. **Soros, V. B., and W. C. Greene.** 2007. APOBEC3G and HIV-1: strike and counterstrike. Curr HIV/AIDS Rep **4:**3-9.

138. **Soros, V. B., W. Yonemoto, and W. C. Greene.** 2007. Newly synthesized APOBEC3G is incorporated into HIV virions, inhibited by HIV RNA, and subsequently activated by RNase H. PLoS Pathog **3:**e15.

139. **Souza, A. W., D. Mesquita Junior, J. A. Araujo, T. T. Catelan, W. D. Cruvinel, L. E. Andrade, and N. P. Silva.** 2010. [Immune system: part III. The delicate balance of the immune system between tolerance and autoimmunity.]. Rev Bras Reumatol **50:**665-679.

140. **Strebel, K.** 2007. HIV accessory genes Vif and Vpu. Adv Pharmacol **55:**199-232.

141. **Strebel, K., D. Daugherty, K. Clouse, D. Cohen, T. Folks, and M. A. Martin.** 1987. The HIV 'A' (sor) gene product is essential for virus infectivity. Nature **328:**728-730.

142. **Suspene, R., C. Rusniok, J. P. Vartanian, and S. Wain-Hobson.** 2006. Twin gradients in APOBEC3 edited HIV-1 DNA reflect the dynamics of lentiviral replication. Nucleic Acids Res **34:**4677-4684.

143. **Suspene, R., P. Sommer, M. Henry, S. Ferris, D. Guetard, S. Pochet, A. Chester, N. Navaratnam, S. Wain-Hobson, and J. P. Vartanian.** 2004. APOBEC3G is a single-stranded DNA cytidine deaminase and functions independently of HIV reverse transcriptase. Nucleic Acids Res **32:**2421-2429.

144. **Takimoto, K., M. Wakiyama, and S. Yokoyama.** 2009. Mammalian GW182 contains multiple Argonaute-binding sites and functions in microRNA-mediated translational repression. RNA **15:**1078-1089.

145. **Tavassoli, A., Q. Lu, J. Gam, H. Pan, S. J. Benkovic, and S. N. Cohen.** 2008. Inhibition of HIV budding by a genetically selected cyclic peptide targeting the Gag-TSG101 interaction. ACS Chem Biol **3:**757-764.

146. **Teixeira, D., U. Sheth, M. A. Valencia-Sanchez, M. Brengues, and R. Parker.** 2005. Processing bodies require RNA for assembly and contain nontranslating mRNAs. Rna **11:**371-382.

147. **Thomas, M. G., M. Loschi, M. A. Desbats, and G. L. Boccaccio.** 2011. RNA granules: the good, the bad and the ugly. Cellular signalling **23:**324-334.

148. **Tritschler, F., E. Huntzinger, and E. Izaurralde.** 2010. Role of GW182 proteins and PABPC1 in the miRNA pathway: a sense of deja vu. Nat Rev Mol Cell Biol **11:**379-384.

149. **Turelli, P., B. Mangeat, S. Jost, S. Vianin, and D. Trono.** 2004. Inhibition of hepatitis B virus replication by APOBEC3G. Science **303:**1829.

150. **Ulenga, N. K., A. D. Sarr, D. Hamel, J. L. Sankale, S. Mboup, and P. J. Kanki.** 2008. The level of APOBEC3G (hA3G)-related G-to-A mutations does not correlate with viral load in HIV type 1-infected individuals. AIDS Res Hum Retroviruses **24:**1285-1290.

151. **Varthakavi, V., R. M. Smith, S. P. Bour, K. Strebel, and P. Spearman.** 2003. Viral protein U counteracts a human host cell restriction that inhibits HIV-1 particle production. Proc Natl Acad Sci U S A **100:**15154-15159.

152. **Varthakavi, V., R. M. Smith, K. L. Martin, A. Derdowski, L. A. Lapierre, J. R. Goldenring, and P. Spearman.** 2006. The pericentriolar recycling endosome plays a key role in Vpu-mediated enhancement of HIV-1 particle release. Traffic **7:**298-307.

153. **Vasudevan, S., Y. Tong, and J. A. Steitz.** 2008. Cell-cycle control of microRNA-mediated translation regulation. Cell Cycle **7:**1545-1549.

154. **Vazquez-Perez, J. A., C. E. Ormsby, R. Hernandez-Juan, K. J. Torres, and G. Reyes-Teran.** 2009. APOBEC3G mRNA expression in exposed seronegative and early stage HIV infected individuals decreases with removal of exposure and with disease progression. Retrovirology **6:**23.

155. **Vetter, M. L., and R. T. D'Aquila.** 2009. Cytoplasmic APOBEC3G restricts incoming Vif-positive human immunodeficiency virus type 1 and increases two-long terminal repeat circle formation in activated T-helper-subtype cells. J Virol **83:**8646-8654.

156. **Vetter, M. L., M. E. Johnson, A. K. Antons, D. Unutmaz, and R. T. D'Aquila.** 2009. Differences in APOBEC3G expression in CD4+ T helper lymphocyte subtypes modulate HIV-1 infectivity. PLoS Pathog **5:**e1000292.

157. **Vivier, E., D. H. Raulet, A. Moretta, M. A. Caligiuri, L. Zitvogel, L. L. Lanier, W. M. Yokoyama, and S. Ugolini.** 2011. Innate or adaptive immunity? The example of natural killer cells. Science **331:**44-49.

158. **Wang, T., C. Tian, W. Zhang, K. Luo, P. T. Sarkis, L. Yu, B. Liu, Y. Yu, and X. F. Yu.** 2007. 7SL RNA mediates virion packaging of the antiviral cytidine deaminase APOBEC3G. J Virol **81:**13112-13124.

159. **Wang, X., P. T. Dolan, Y. Dang, and Y. H. Zheng.** 2007. Biochemical differentiation of APOBEC3F and APOBEC3G proteins associated with HIV-1 life cycle. J Biol Chem **282:**1585-1594.

160. **Wasserman, T., K. Katsenelson, S. Daniliuc, T. Hasin, M. Choder, and A. Aronheim.** 2010. A novel c-Jun N-terminal kinase (JNK)-binding protein WDR62 is recruited to stress granules and mediates a nonclassical JNK activation. Molecular biology of the cell **21:**117-130.

161. **Wehrly, K., and B. Chesebro.** 1997. p24 antigen capture assay for quantification of human immunodeficiency virus using readily available inexpensive reagents. Methods **12:**288-293.

162. **Weil, D.** 2007. [GW bodies and stress granules, two cytoplasmic structures for mRNA degradation and storage in mammalian cells]. J Soc Biol **201:**349-358.

163. **Wichroski, M. J., K. Ichiyama, and T. M. Rana.** 2005. Analysis of HIV-1 viral infectivity factor-mediated proteasome-dependent depletion of APOBEC3G: correlating function and subcellular localization. J Biol Chem **280:**8387-8396.

164. **Wichroski, M. J., G. B. Robb, and T. M. Rana.** 2006. Human retroviral host restriction factors APOBEC3G and APOBEC3F localize to mRNA processing bodies. PLoS Pathog **2:**e41.

165. **Wiegand, H. L., B. P. Doehle, H. P. Bogerd, and B. R. Cullen.** 2004. A second human antiretroviral factor, APOBEC3F, is suppressed by the HIV-1 and HIV-2 Vif proteins. Embo J **23:**2451-2458.

166. **Xiao, Z., E. Ehrlich, K. Luo, Y. Xiong, and X. F. Yu.** 2007. Zinc chelation inhibits HIV Vif activity and liberates antiviral function of the cytidine deaminase APOBEC3G. Faseb J **21:**217-222.

167. **Xiao, Z., E. Ehrlich, Y. Yu, K. Luo, T. Wang, C. Tian, and X. F. Yu.** 2006. Assembly of HIV-1 Vif-Cul5 E3 ubiquitin ligase through a novel zinc-binding domain-stabilized hydrophobic interface in Vif. Virology **349:**290-299.

168. **Xu, H., E. S. Svarovskaia, R. Barr, Y. Zhang, M. A. Khan, K. Strebel, and V. K. Pathak.** 2004. A single amino acid substitution in human APOBEC3G antiretroviral enzyme confers resistance to HIV-1 virion infectivity factor-induced depletion. Proc Natl Acad Sci U S A **101:**5652-5657.

169. **Xu, J., J. Y. Yang, Q. W. Niu, and N. H. Chua.** 2006. Arabidopsis DCP2, DCP1, and VARICOSE form a decapping complex required for postembryonic development. The Plant cell **18:**3386-3398.

170. **Yamashita, T., K. Kamada, K. Hatcho, A. Adachi, and M. Nomaguchi.** 2008. Identification of amino acid residues in HIV-1 Vif critical for binding and exclusion of APOBEC3G/F. Microbes Infect **10:**1142-1149.

171. **Yang, Z., A. Jakymiw, M. R. Wood, T. Eystathioy, R. L. Rubin, M. J. Fritzler, and E. K. Chan.** 2004. GW182 is critical for the stability of GW bodies expressed during the cell cycle and cell proliferation. J Cell Sci **117:**5567-5578.

172. **Yao, B., S. Li, H. M. Jung, S. L. Lian, G. X. Abadal, F. Han, M. J. Fritzler, and E. K. Chan.** 2010. Divergent GW182 functional domains in the regulation of translational silencing. Nucleic acids research.

173. **Yap, M. W., S. Nisole, C. Lynch, and J. P. Stoye.** 2004. Trim5alpha protein restricts both HIV-1 and murine leukemia virus. Proceedings of the National Academy of Sciences of the United States of America **101:**10786-10791.

174. **Yu, Q., R. Konig, S. Pillai, K. Chiles, M. Kearney, S. Palmer, D. Richman, J. M. Coffin, and N. R. Landau.** 2004. Single-strand specificity of APOBEC3G accounts for minus-strand deamination of the HIV genome. Nat Struct Mol Biol **11:**435-442.

175. **Yu, Y., Z. Xiao, E. S. Ehrlich, X. Yu, and X. F. Yu.** 2004. Selective assembly of HIV-1 Vif-Cul5-ElonginB-ElonginC E3 ubiquitin ligase complex through a novel SOCS box and upstream cysteines. Genes Dev **18:**2867-2872.

176. **Zeitelhofer, M., P. Macchi, and R. Dahm.** 2008. Perplexing bodies: The putative roles of P-bodies in neurons. RNA biology **5:**244-248.

177. **Zennou, V., D. Perez-Caballero, H. Gottlinger, and P. D. Bieniasz.** 2004. APOBEC3G incorporation into human immunodeficiency virus type 1 particles. J Virol **78:**12058-12061.

178. **Zhang, K. L., B. Mangeat, M. Ortiz, V. Zoete, D. Trono, A. Telenti, and O. Michielin.** 2007. Model structure of human APOBEC3G. PLoS One **2:**e378.

179. **Zhang, W., G. Chen, A. M. Niewiadomska, R. Xu, and X. F. Yu.** 2008. Distinct determinants in HIV-1 Vif and human APOBEC3 proteins are required for the suppression of diverse host anti-viral proteins. PLoS One **3:**e3963.

180. **Zheng, Y. H., D. Irwin, T. Kurosu, K. Tokunaga, T. Sata, and B. M. Peterlin.** 2004. Human APOBEC3F is another host factor that blocks human immunodeficiency virus type 1 replication. J Virol **78:**6073-6076.

181. **Zhou, J., and C. Aiken.** 2001. Nef enhances human immunodeficiency virus type 1 infectivity resulting from intervirion fusion: evidence supporting a role for Nef at the virion envelope. Journal of virology **75:**5851-5859.

182. **Zufferey, R., D. Nagy, R. J. Mandel, L. Naldini, and D. Trono.** 1997. Multiply attenuated lentiviral vector achieves efficient gene delivery in vivo. Nat Biotechnol **15:**871-875.